UNIVERSIDADE DA BEIRA INTERIOR
Ciências

Iminosugar-steroid conjugates as potential α-glycosidase inhibitors and antiproliferative agents

Sara Cristina Nobre Garcia

Dissertação para obtenção do Grau de Mestre em
Química Medicinal
(2º ciclo de estudos)

Orientador: Prof. Doutor Samuel Martins Silvestre
Co-orientador: Prof. Doutor Carmen Ortiz Mellet

Covilhã, junho de 2016

À minha irmã, a minha versão mais velha,
mas o (meu) modelo a seguir.

Agradecimentos/Acknowledgements

Em primeiro lugar gostaria de agradecer ao Professor Doutor Samuel Silvestre por ter possibilitado o desenvolvimento deste projeto, e ainda toda a orientação, paciência, confiança e disponibilidade ao longo de todo o ano.

Also, I want to thank to Cathedratic Professor Carmen Ortiz Mellet for allowing to carry out the organic synthesis of this project in her investigation group on Departamento de Quimica Organica of Universidad de Sevilla, and to Doctor Elena Sáchez-Fernández for the assisting and help during the whole period. I am grateful for the reception and mutual aid that I found in the group. Especially, I want to thank to Doctor Rita Pereira who always was present from the first year of my bachelor until this moment, even more in the course of this project, helping me as much as possible.

Agradeço a todas as minhas colegas de laboratório no Centro de Investigação em Ciências da Saúde-UBI, principalmente à Mariana Matias, Sandrina Maçãs, Elisabete Alves, Mafalda Catarro, Ângela Gonçalves e Vanessa de Brito por tudo o que ensinaram e auxiliaram e claro, pelos bons momentos passados.

Agradeço aos meus pais, avó e irmãos que tornaram todo este caminho possível, e ainda a todos os outros familiares e amigos que me apoiaram durante todo o meu percurso académico.

Resumo alargado

A conjugação de esteroides com produtos naturais como as pirimidinas, purinas alcaloides, hidratos de carbono (açúcares) ou poliaminas permitem obter compostos nomeadamente com diferentes atividades biológicas, agentes complexantes ou gelificantes. Todos estes tipos de compostos são classificados como conjugados de esteroides. De facto, estes compostos são atualmente usados em várias áreas da química, designadamente supramolecular e medicinal, e bioquímica, sendo alvos de interesse no desenho e síntese de novos compostos. Há diversas aplicações destes compostos na química medicinal, como sistemas de entrega de fármacos, agentes complexantes de fármacos ou mesmo como fármaco em si.

Nesta área, uma das principais classes de conjugados são os esteroides glicosilados, surgindo através da combinação de um esteroide com hidratos de carbono. Esta classe inclui moléculas muito variadas em termos estruturais e de ação biológica, sintéticas ou de origem natural.

Tendo em conta a variedade de fármacos atualmente existentes, considera-se que uma parte significativa são compostos glicosilados (glicósidos ou glicosídeos), incluindo alguns esteroides glisosilados. Embora os açúcares não estejam habitualmente associados a uma atividade terapêutica concreta, está bastante claro que a sua presença em estruturas naturais ou dos seus miméticos têm um efeito muito pronunciado nas propriedades físicas, químicas e biológicas das moléculas. Ainda pouca investigação tem sido dedicada ao papel biológico e farmacológico dos açúcares, contudo, sabe-se que, na maioria dos casos, apenas a aglícona não é ativa só por si.

As principais possíveis aplicações biomédicas baseadas na glicobiologia têm sido relacionadas com a área dos glicoconjugados, nomeadamente dos esteroides glicosilados. Curiosamente, de entre o grande número de gliconconjugados utilizados na medicina tradicional chinesa, os esteroides glicosilados foram os principais componentes identificados. Deste modo, este tipo de compostos tem recebido muita atenção devido às suas atividades fisiológicas e farmacológicas.

Os conjugados de esteroides e alcaloides têm revelado ser também um grupo importante de conjugados de esteroides. Alguns alcaloides polhidroxilados são igualmente glicomiméticos, como por exemplo alguns iminoaçúcares. Estes alcaloides, naturais e sintéticos, apresentam poder de inibir glicosidases e por isso têm sido alvo de diversos estudos, utilizados como ferramentas biológicas para ensaios que envolvem a função e turnover dos glicoconjugados, bem como potenciais agentes terapêuticos para o tratamento de infeções,

doenças cancerígenas e metabólicas como a diabetes *mellitus* (DM) tipo II. Por exemplo, a inibição seletiva de glucosidases pode levar a uma intervenção na glicosilação aberrante de glicoproteínas e glicolípidos, o que parece estar presente em vários passos patofisiológicos na progressão de tumores. A maioria dos compostos mais interessantes do ponto vista biológico desta classe são os referidos iminoaçúcares (também denominados azaçúcares) derivados da castanospermina, um alcaloide glicomimético, e da nojirimicina ou da 1-desoxinojirimicina. Entre estes, o iminoaçúcar nojirimicina mimetiza perfeitamente a estereoquímica da *D*-glucose, apresentando apenas a substituição do oxigénio endocíclico original por um átomo de azoto. No entanto, estes compostos carecem ainda de seletividade entre as glicosidases inibidas, uma vez que a inibição de vários tipos de enzimas pode levar a vários efeitos secundários indesejados. Nomeadamente, é necessária uma seletividade anomérica, por exemplo entre α- e ß-glucosidases, uma vez que há ainda a possibilidade de existir alguns efeitos colaterais.

Deste modo, para melhorar a seletividade anomérica foi desenvolvida uma nova família de glicomiméticos com um azoto endocíclico incorporado numa estrutura carbâmica que promove um alto caracter de hibridação sp^2 (iminoaçúcares sp^2). O controlo da configuração α pseudoanomérica na redução dos iminoaçúcares sp^2 pode ser obtida pela exploração do efeito anomérico generalizado, o que se traduz em seletividades anoméricas muito altas para a inibição das glicosidases. Os compostos resultantes têm revelado possuir seletividade demarcada para as isoformas da α-glucosidase, com preferência pela isoforma neutra. Para além deste facto, foi ainda verificado que a incorporação de substituintes axialmente orientados na posição pseudoanomérica pode ser um fator importante na modulação baseada na aglícona da atividade inibidora e na permeabilidade através das membranas celulares, dada a elevada hidrofilicidade das moléculas iniciais. Assim, aliando estruturas esteroides a este tipo de composto é possível criar uma nova classe de conjugados de esteroides com potencial atividade biológica.

Nesta dissertação são apresentados os resultados da síntese de novos conjugados de esteroides conhecidos e comerciais (colesterol, colestanol, pregnenolona, desidroepiandrosterona (DHEA), estigmasterol e diosgenina) e um iminoaçúcar sp^2 derivado da nojirimicina conhecido pela sua ação inibitória de glicosidases e com potencial efeito antiproliferativo em células humanas. Neste sentido, os compostos finais preparados foram avaliados como inibidores de um painel de glicosidases bem como a análise do seu efeito na proliferação celular em várias linhas celulares humanas.

O processo para a obtenção dos compostos desejados iniciou-se pela preparação do iminoaçúcar sp^2 derivado da nojirimicina **1**, através de vários passos sintéticos relevantes. Para que ocorresse glicosidação do iminoaçúcar foi necessária a preparação de um derivado fluorado que aumentou a nucleofilicidade do grupo álcool dos esteróis. Através desta estratégia conseguiu-se obter os seis conjugados com rendimentos variáveis.

O ensaio enzimático *in vitro* demonstrou que os compostos sintetizados apresentam seletividade para as glucosidases, especialmente para as α-glucosidades com a excepção do composto derivado do 5*α*-cholestanol (**19**) que tem preferência pela ß-glucosidase. Este estudo revelou ainda que, dos seis compostos, dois (compostos **20** e **21**) apresentam K_i bastante inferiores aos de outras moléculas, para além de se distinguirem pelo seu mecanismo de inibição misto, ao contrário da inibição competitiva apresentada pelos outros compostos (**18**, **19**, **22** and **23**).

A avaliação dos efeitos antiproliferativos das moléculas obtidas foi realizado através do método colorimétrico do brometo de 3-(4,5-dimetiltiazol-2-il)-2,5-difeniltetrazolio após a cultura celular de 3 diferentes linhas celulares, do cancro da próstata (LNCaP) e da mama (T-47D) hormono-dependentes e uma linha celular de fibroblastos normais da derme (NHDF). Os resultados revelaram que aparentemente não existe uma vantagem clara na junção do esterol com o referido iminoaçúcar em termos de efeitos antiproliferativos, uma vez que, de uma forma geral, o efeito foi inferior ao dos compostos esteróides. O composto **23**, derivado da diosgenina, foi o único que mostrou em estudos preliminares ação pronunciada comparável à apresentada pelo seu precursor nas três linhas celulares. Os efeitos destes compostos foram também avaliados através de uma curva de concentração-resposta com a qual se obteve os valores de IC_{50}. Este estudo revelou que apesar o composto **23** apresenta valores de IC_{50} superiores ao controlo positivo, 5-fluorouracilo (5-FU), considerando-se menos potente. Ainda assim, verificou-se que, nas células NHDF, o composto **23** não atingia uma ação to demarcada quanto nas células cancerígenas, o que poderá significar alguma seletividade para estas células. Os resultados dos estudos revelaram também que parece não existir uma relação direta entre a inibição da enzima α-glucosidase e a ação antiproliferativa destes compostos, uma vez que os compostos que apresentam maior potência enquanto inibidores da α-glucosidase não são aqueles que apresentam maior efeito na proliferação celular.

Dada a potencialidade do composto **23**, prosseguiu-se à avaliação da sua ação preliminar na viabilidade celular através da técnica da citometria de fluxo, comparando-se com o controlo positivo 5-FU e o precursor diosgenina. Este estudo revelou uma elevada semelhança entre o comportamento do fármaco 5-FU e do composto **23.**

No decorrer deste projeto constatou-se uma relação entre a DM tipo II e a doença de Alzheimer (AD). Aparentemente, a AD, tal como a DM tipo II, está também associada a uma desregulação ao nível da ação da insulina. Quando a sua atividade está aumentada, a acetilcolinesterase (AcCHE), um importante alvo terapêutico na AD, leva à resistência à insulina. Assim, inibindo a α-glucosidase, que controla a absorção da glucose, e a AcCHE pode se obter resultados benéficos nas duas doenças, pelo que a obtenção de inibidores duais pode ser de grande interesse terapêutico. Deste modo, verificado o potencial dos compostos sintetizados como inibidores da α-glucosidase, resolveu proceder-se a um estudo de *docking* molecular no local ativo da AcCHE afim de se verificar qual o potencial destes compostos como

inibidores também da AcCHE. A simulação revelou que os compostos em estudo apresentam alta afinidade para a enzima no local ativo em comparação com um inibidor conhecido. Tal indica que poderia ser interessante, no futuro, a realização de um estudo experimental da ação inibitória dos compostos sintetizados na AcCHE.

Palavras-chave

Esteróis, iminoaçúcar sp^2, esteroides glicosilados, inibidores da α-glucosidase, efeitos antiproliferativos.

Abstract

Steroidal conjugates are actually used in biological, medicinal or supramolecular chemistry, being a target of interest in the design and synthesis of new compounds. A large class of these conjugates are the steroidal glycosides, which includes structurally and biologically diverse semi-synthetic and natural molecules, isolated from a wide variety of both plant and animal species. Another important group of steroid conjugates is formed by steroids and alkaloids. Interestingly, several alkaloids are also glycomimetics, and includes iminosugars such as 1-deoxynojirimycin, and castanospermine. These polyhydroxylated natural and synthetic alkaloids present ability to inhibit glycosidases and have high interest, once they can be used as biological tools in studies concerning glycoconjugates function, targeting and turnover, and as potential therapeutic agents in the treatment of infections, cancer, and metabolic diseases, such as type II diabetes mellitus (DM). Among these, nojirimycin is a *D*-glucose mimetic and is a selective glucosidase inhibitor, however lacks anomeric selectivity for one type of glucosidases (α or β). To improve this feature one family of glycomimetics with an endocyclic nitrogen with higher sp^2 hybridation character (sp^2 iminosugars) was developed based on 1-desoxynojirimycin structure, which has high selectivity for α-glucosidases. Furthermore, it was proposed that the incorporation of axially orientated substituents on pseudoanomeric position can be an important factor in aglycon-based modulation of inhibitory activity and in permeability through biologic membranes. In this context, several new sp^2-iminosugar-steroid conjugates were successfully synthesised by the hybridization of a sp^2-derivative of 1-desoxynojirimycin and a sterol moiety. These compounds were tested as glycosidase inhibitors, revealing a general high selectivity for α-glucosidases. In addition, a cell proliferation assay through the colorimetric 3-(4,5-dimethylthiazol-2-yl)-2,5-diphenyltetrazolium bromide method revealed that, in general, the combination of the two molecules did not lead to an improved cytotoxic effect in comparison with the isolated mother compounds.

In addition, it was performed molecular docking studies in order to predict the binding energies and possible interactions with acetylcholinesterase (AcCHE), once it was noticed that dual *α*-glucosidase and AcCHE inhibitors can be very useful agents on the treatment of type II DM and Alzheimer Disease. The study revealed these compounds can aslo be potential AcCHE inhibition.

Keywords

Sterols, sp^2-iminosugar, steroidal glycosides, α-glucosidase inhibitors, antiproliferative effects.

Index

Figures Index

Schemes Index

Graphics Index

Tables Index

Acronyms Index

17OH-PREG	17α-Hydropregnenolone
17OH-PROG	17α-Hydroprogesterone
3α,5α-THDOC	Tetrahydrodeoxyxorticosterone
5α-DHDOC	Dihydrodeoxycorticosterone
Ac	Acetyl
AcCHE	Acetylcholinesterase
AD	Alzheimer disease
ATP	Adenine triphospate
Bcl-2	B-cell limphoma 2 family
CYP	Cytochrome P 450
DCM	Dichloromethane
DHEA	Dehydroepiandrosterone
DHEA-S	Dehydroepiandrosterone sulphate
DHP	3,4-Dihydro-2*H*-pyran
DIPEA	Diisopropylethylamine
DM	Diabetes *Mellitus*
DMF	Dimethylformamide
DMSO	Dimethylsulfoxide
Et	Ethyl
EtOAc	Ethyl Acetate
EtOH	Ethanol
GAE	Generalized anomeric effect
HDL	High-density lipoprotein
HF-Pyr	Poly(hydrogen fluoride)pyrimidinium complex
HIV	Human immunodeficiency virus
LDL	Low-density lipoprotein
Me	Methyl
MTT	3-(4,5-Dimethylthiazol-2-yl)-2,5-diphenyltetrazolium bromide
NHDF	Normal Human Dermal Fibroblasts
NMR	Nuclear Magnetic Resonance
PARP	Poly(ADP-ribose)polymerase
PI	Propidium Iodide
PPTS	Piridinium *p*-toluenesulfonate
PREG	Pregnenolone
PREG-S	Pregnenolone Sulfate
PROG	Progesterone
p-TsOH	*p*-Toluenosulphonic acid
Py	Pyridine
r.t.	Room temperature
SAR	Structure-activity relationship
TFA	Trifluoroacetic acid
THF	Tetrahydrofurane
THP	Tetrahydropirane
TLC	Thin Layer Chromatography
VEGF-A	Vascular endotelial growth factor A

1. Introduction

1.1. Carbohydrates

Carbohydrates family, a group of compounds also known as sugars or glycans, is present in all living organisms as part of the essential constituents, being the most abundant and widespread in nature. Also, this class is the most important (in volume and availability) of non-nitrogenous compounds of chiral pool, and are particularly important in chiral synthesis[1].

The carbohydrate term was initially applied to all organic compounds possessing the empirical formula $C_n(H_2O)_n$, possessing an oxygen atom attached to each carbon atom. Nowadays, it is extended to many other compounds, including, for example, the deoxy sugars. In general, the monomers of this class are polyhydroxylated structures containing 3 to 9 carbons typically very functionalized[2]. Carbohydrates embrace polyhydroxy aldehydes, ketones, and acids, together with linear and cyclic polyols, constituting a diversified class of compounds due to their wide range of stereoisomers[1]. The most common type of structures are aldoses, linear carbon chains with an aldehyde (CHO) group at C-1, a varying number of secondary alcohols (-CHOH) (which offer a variable number of chiral centres), and a primary alcohol at the end of the chain. The simplest one is glyceraldehyde with 3 carbons, but in general they can also display 4 (tetrose), 5 (pentose), 6 (hexose) or even 7 (heptose) carbon atoms. Ketoses such as fructose, which have a primary alcohol at both ends and a ketone in the chain, exists too, however are much less abundant than aldoses[2]. Once carbohydrates have both carbonyl and hydroxyl functions, they are able to form intramolecular hemiacetals, also known as lactols. Moreover, the equilibrium of this reaction is displaced to the formation of the cyclic hemiacetal, becoming the amount linear sugar almost negligible, in both solution and solid form.

Simple carbohydrates, also known as saccharides, can be organized according the number of the basic units that the compound is formed by. To these units we call monosaccharides, the simplest carbohydrates which cannot be hydrolysable in other carbohydrates. Furthermore, there are disaccharides composed by two molecules of monosaccharides, trisaccharides consisting in three molecules of monosaccharides and so on (compounds with 3 to 10 monosaccharides molecules can also be called by oligosaccharides). Polysaccharides is a class of compounds formed by more than ten basic units, such starch or cellulose, both polymers of the hexose D-glucose[3]. The difference between these two polymers aside the number of units of D-glucoses, relies on the way units bind, since this type of compounds can make glycosidic bonds in different positions, resulting in diverse branched-chain or linear sugars[4]. Moreover, glycosidic bonds can form deoxy compounds, when a hydroxyl function is replaced or dehydro compounds, when a C-bonded hydrogen is substituted. In general, cyclic carbohydrates are represented by Haworth formulae, but representations as planar ring representation (Millis formula) and chair convention are also encountered (Figure 1)[1].

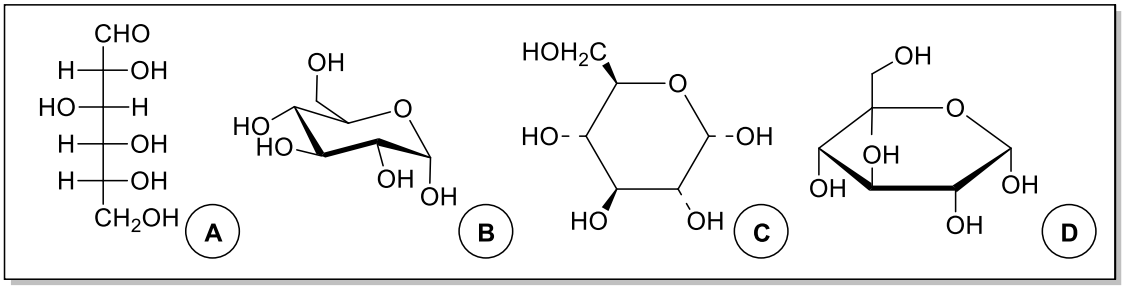

Figure 1 | Structure of *D*-glucose in Fisher (A), chair (B), Harworth (C) and Millis (D) representations. Adaptated[1].

1.1.1. Carbohydrates in nature

Carbohydrates are the most abundant biomolecules in the world[4], however only five, D-glucose, D-frutose, D-galactose, D-mannose and L-arabinose, naturally occur in free state of the thirty six possible steroisomeric pentoses, pentuloses, hexoxes, and hexuloses. Of those five sugars just D-glucose and D-fructose are found in significant amounts. If we consider the compounds resulting from the modification of the 36 fundamental sugars, the number of natural sugars surprisingly increases. As an example of natural modified compounds of the initial pool there are amino-, thio-, deoxy, branched chain and higher sugars, and yet various alditols, cyclitols and sugar acids (Figure 2)[1].

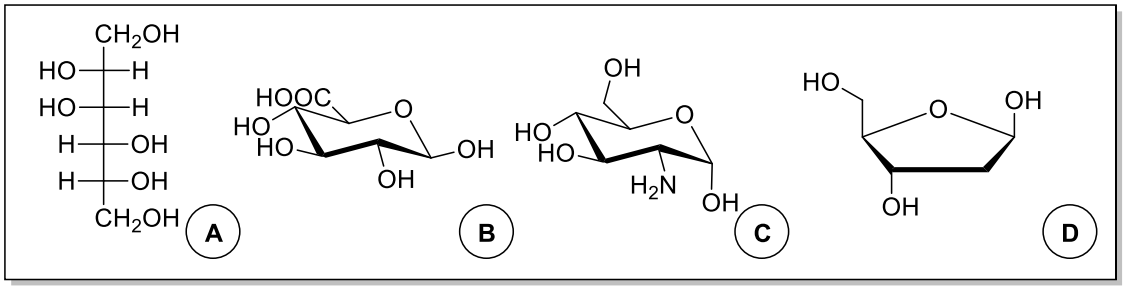

Figure 2 | Structures of mannitol (A), an alditol, glucuronic acid (B), a sugar acid, glucosamine (C), an aminosugar, and deoxyribose (D), a deoxy sugar.

Sugars have essential functions on the biological systems and are important not only structurally and as source of energy to produce ATP, but also participate in sophisticated processes such as cellular communication, as information carriers for signal transmission. Attached to membranes glycoproteins and lipids, carbohydrates display antigenic properties, very important in cell-cell recognition processes and play important roles in adhesion, cell migration, blood clotting, immune response and increase the solubility of the macromolecules, too[2,4].

D-Glucose is the most abundant organic molecule[2] and is the parent sugar from which most carbohydrates are derived from[4]. Glucose plays a fundamental role in biology being the main source of energy of an enormous number of organisms and, moreover, can act as a building block to the synthesis of important structural and storage polymers as cellulose and starch[2].

1.1.2. Glycoconjugates

Glycoconjugates are very important compounds in life, occurring diverse essential natural glycoconjugates in different biological processes. Structurally, they comprises all the compounds containing a carbohydrate moiety of variable size and complexity as well as a covalently linked non-carbohydrate portion, the aglycone, such as proteins and lipids[5]. In general, bioactive carbohydrates, which plays the important biological roles described above, exist as glycoconjugates, mainly glycoproteins and glycolipids[4].

Despite those two types of glycoconjugates, there are a lot of other natural small molecules glycoconjugates, which can exert a variety of selective biological actions. Plants synthetize over than 100 000 natural products with a considerable proportion of them being glycosylated, as some alkaloids, phenols and polyphenols, sterol and terpenoids, being almost all classes of natural products able to be converted in glycosylated derivatives[6]. Figure 3 show some structures of natural glycosides[7-9]. In the majority of cases, the mono-, di-, or oligossacharides attached, contain D-glucose, but L-rhamnose, D- and L-fucose and L-arabinose monomers also occur quite frequently[1]. Nevertheless, it is imperative to note that the role of the sugar moiety looks completely different from plant physiology point of view and from drug development perspective[6].

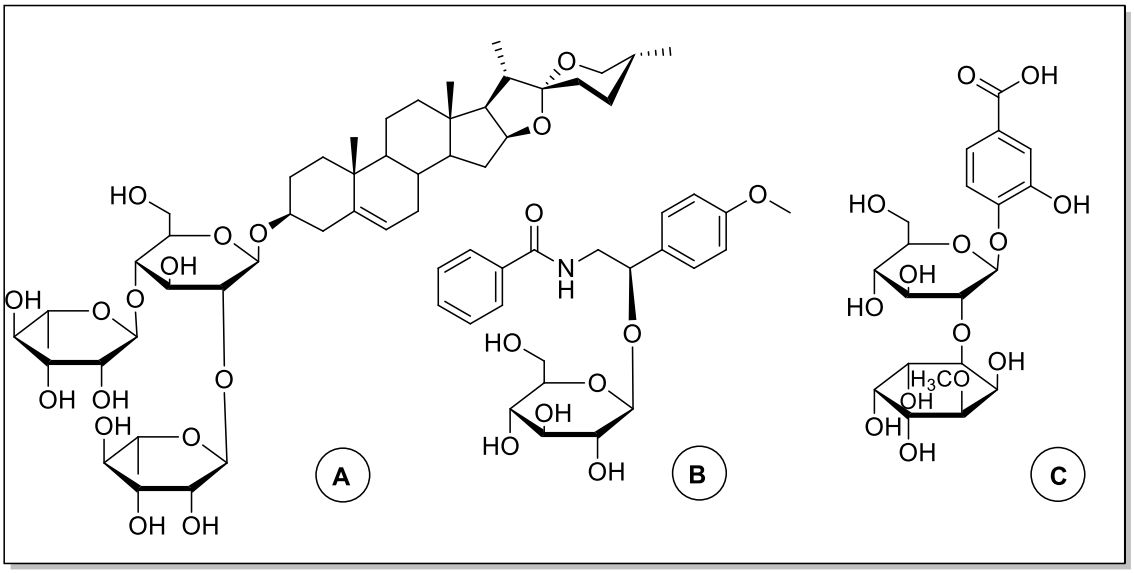

Figure 3 | Structures of diferent natural glycosides: A - dioscin[7]; B- an alkaloid glycoside[8]; C- a phenolic glycoside[9].

The understanding of the influence of natural glycoconjugates structural features is an extremely important issue in molecular and cellular biology, proteomics and medicine, since disorders on these systems can lead to severe diseases. Because of their different properties and biological functions, glycoconjugates have received attention as potential therapeutics, and the natural scaffolds can be used to design and synthesis of glycomimetics aims to improve features as bioactivity and biocompatibility[5]. It is known that structural modification on glycone or aglycone

moieties can be used to refine efficacy and selectivity of activity. Furthermore, the introduction of a glycone part offers ample opportunity for fine tune up of lipophilicity. This way, modifications of natural glycosides and glycosylation of other natural products through *O*-, *N*-, *S*- or *C*-glycosidic bonds can be key methods in preparation of new lead compounds on drug development process[6].

1.1.3. Carbohydrates and Drug Design and Development

Although carbohydrates are one of most important and diverse class of compounds in nature and act as excellent recognition molecules on cell surface, just a few carbohydrate-based drugs are on the market. In general carbohydrates possess high polarity due to hydroxyl groups (hydrogen bond donors and acceptors), which typically offers poor pharmacokinetic properties, as low tissue permeability because of their lack of lipophilicity required for passive absorption through biological membranes, and short serum half-lives, being quickly eliminated by renal excretion [10,11]. Also, in many cases, the binding affinities of carbohydrates are in the milli- or micromolar range, which means relatively weak interactions[11]. However, through several modifications, it is possible to turn them into more "drug-like" compounds. In this line, glycomimetics arise as a promising field on drug discovery improving features, maintaining the function and reaching higher affinities than the native carbohydrate[10,11].

In rational drug design, the first step is to fully understand the molecular base of the interaction between the functional carbohydrate epitope and its protein receptor. For this purpose, several techniques have been used to find the exact structure and binding conformation, as nuclear magnetic resonance (NMR) spectroscopy and X-ray crystallography. Using this information, molecules can be designed to eliminate or modify positions not involved in binding and optimize those areas that are crucial for interacting with the protein receptor surface, or even explore additional interactions. Concomitantly, enhancement of pharmacokinetic parameters has to be developed, a crucial process in the design of glycomimetics, wherein the modification of these properties is mandatory. All this process should be accomplished by a variety of strategies, including: incorporation of moieties to enhance binding to serum proteins and thus increase the half-life of the molecule, adjust of lipophilicity, decrease the number of hydrogen bond acceptors and donors and so on. It is possible to favour active transport by the appropriate addiction of side groups already recognized by active transport systems, for example, a bile acid transporter. In those cases, we have **glycoconjugates**[12].

Different glycomimetic drugs have been approved by the competent entities. Two well-known examples are the viral neuraminidase inhibitors zanamivir (Relenza™) and oseltamivir (Tamiflu™), which are used on the treatment of the Influenza A virus infection, and both drugs mimic the transition state of the hydrolysis of the terminal *N*-acetylneuraminic acid by neuraminidase[12].

Leading the treatment of type II diabetes *mellitus* (DM), different glycomimetic drugs have been approved to inhibit α-glucosidases in the brush boarder of the small intestine, for example

miglustat (Zavesca™), miglitol (Glyset™) and acarbose (Glucobay™), in which the transition state of the hydrolytic reaction is mimicked[11]. Moreover, some synthetic heparins (glycosaminoglycans) are used in clinic as anticoagulant drugs, by the inhibition of fibrin clots formation in blood[11,12]. The oligosaccharides streptomycin and neomycin are bactericidal aminoglycoside antibiotics able to interfere with the normal protein synthesis and are in the market for many years. Yet, sucralfate, a disaccharide basic aluminium sucrose sulfate complex, is a widely used drug with antipeptic and antiulcerative action, due to pepsin activity inhibition in gastric juice. Other important disaccharide drug available is lactulose, used to promote laxation[12].

In both academic and industrial research centres there are ongoing studies aiming the development of glycomimetic drugs and one of the most popular targets is the family of selectins. Selectins are adhesion proteins involved in the extravasation of cells from the bloodstream in different processes, including inflammatory diseases and infections. Inhibitors of these proteins can offer a wide range of applications on infectious diseases. Natural ligands of selectins are sialylated carbohydrates, and thus different glycomimetic compounds are being developed intending to the inhibit of these proteins, preventing the adhesion of pathogenic microorganisms or leucocytes in inflammatory diseases[11].

A considerable number of groups of small-molecules carbohydrate-based drugs are glycosides. Despite the fact of sometimes, sugars apparently do not show a pronounced therapeutic action, there is no doubt that their presence in natural structures and their mimetics have a dramatic effect on physical, chemical and biological properties. In fact, few research has been dedicated to the biological of pharmacological role of the sugar moieties, nevertheless it is clear that the aglycon itself is not active in most cases[13]. There are several examples of this drugs on the market:

- anthracycline antibiotics antitumor agents, as doxorubicin (Figure 4) and daunorubicine, characterized by the presence of an anthracycline and a glycosyl daunosamine moieties;
- antitumor and antiviral nucleotides and nucleoside agents and analogues, as fluradarabine phosphate, which inhibits DNA synthesis, exhibiting neoplastic activity, and stavudine, synthetic thymidine nucleoside analogues, which inhibits the replication of human immunodeficiency virus (HIV) in human cells;
- different antibiotics such as erythromycin (macrolide), which inhibit protein synthesis in susceptible organisms, microbial amphoteric glycopeptide antibiotic vancomycin, which inhibits bacterial cell-wall biosynthesis, antifungal antibiotics, as amphotericin B, which binds to the cell's sterols membrane of susceptible fungi and changes its permeability, causing cell death;
- chemotherapeutic agents as etoposide;
- cardiotonic glycosides, as digoxin (Figure 4). Digoxin, a steroidal glycoconjugate, inhibits sodium-potassium ATPase, leading to an increase of intracellular sodium and potassium, very useful in the presence of irregular heart beat or hear failure[12].

The structures of oseltamivir[14] (glycomimetic), digoxin[15] and doxorubicin[16] (glycosides) are shown on figure 4.

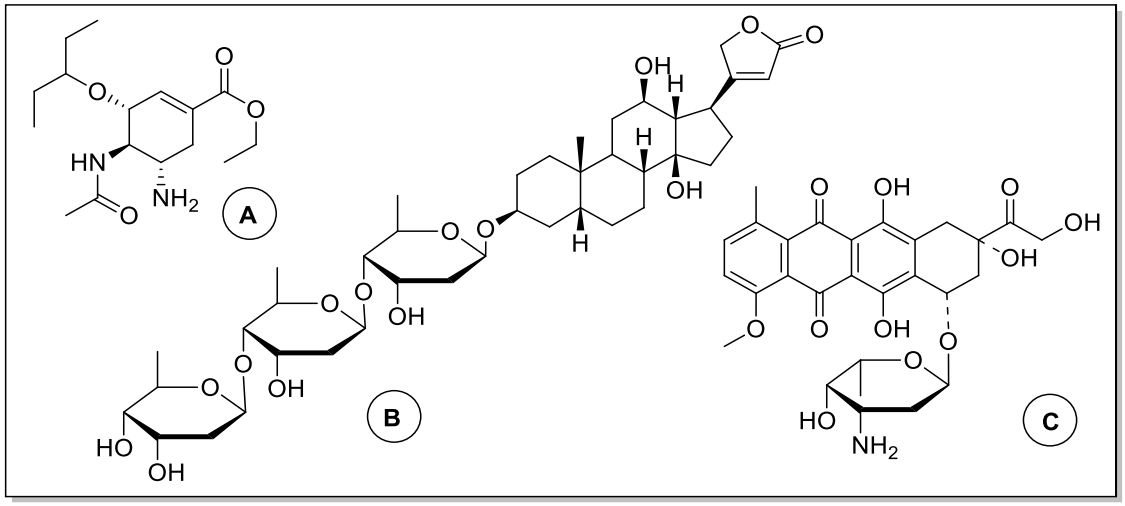

Figure 4 | Structures of glycomimetic/glycoside marketed drugs: A- Oseltamivir[14]; B- Digoxin[15]; C- Doxorubicin[16].

In the drug development field, there is another important area that is being investigated. By exploring differences between cell-surface glycosylation pattern of normal and diseased states, scientists have developed diverse vaccines to a variety of ailments including cancer. Carbohydrate-based vaccines are used to induce immunity since 1980's, and many developments have taken place. However, the use of carbohydrates in vaccines has been limited because of their poor immunogenic properties. Carbohydrate antigens activate independent T-cell humoral responses which create short-lived antibodies mobilizing immunoglobulin G. In contrast, proteins antigen which mobilize T cells and trigger the generation of highly specific and long-lived antibodies. To overcome this lack of immune response, different approaches have been successfully developed by using adjuvants, covalent attachment of carbohydrates to immune-stimulants (conjugate vaccines) or integration into complex multi-component vaccines.

Today there are many types of carbohydrate-based vaccines in study, namely antiviral, antibacterial, antifungal, anti-parasitic and anticancer vaccines, emerging new synthetic candidates every year. The main principle is to discover an antibody able to identify a conserved carbohydrate moiety of a characteristic glycoprotein (not human or aberrant surface carbohydrate structures) and produce the carbohydrate portion itself, a mimetic or a conjugate with peptide or lipid moieties, aiming the stimulation of biosynthesis of the critical antibody to elicit immune response[10].

1.1.3.1. Importance of glycosylation patterns

The treatment of diseases such as cancer or inflammation is extremely challenging since the pathology involves dysregulation of endogenous and often essential cellular processes.

Like cancer, diverse diseases present changes in glycosylation process, being a hallmark of the disease state. Generally, cancer cells exhibit carbohydrates at different levels or with expressively different structures than those observed on normal cells, as well as an inflammation process. Over the last years the huge development of genomics, proteomics and mass spectrometry promoted the knowledge about the recognition of specific carbohydrate structures in different states of the disease.

The availability of novel molecular targets that can distinguish unhealthy from healthy cells could deeply increase therapeutic opportunities, enhancing the selectivity and consequently the safety the new potential drugs. As aforementioned, the glycosylation pattern of a cell is therefore a code for cellular physiology, and the understanding of this code at both molecular and functional levels is now starting to emerge. In this context, it is necessary a continuous research to develop new methods towards detecting specific sugar moieties in a disease to prevent or destroy cells that exhibit them. The glycan moieties are formed on protein or lipid scaffolds by glycosyltransferases and glycosidases[17], with those enzymes also being key targets for a substantial number of possible therapeutic agents by the controlling of cell-surface carbohydrate structure and function[18].

Glycoproteins, glycolipids and proteoglycans have evolved from structural features of the cell to modulators of complex processes in higher organisms, which can include protein folding and trafficking, immune recognition and developmental regulation. Moreover, this kind of structures are involved in cell-cell communication and recognition, and cell adhesion, extremely important processes in tumour development and growth[18].

1.1.3.2. Iminosugars and glycosidase inhibition

Iminosugars (azasugar, or iminoalditol structures) are polyhydroxylated secondary and tertiary amines, in which the molecules resemble monosaccharide structures, where the endocyclic oxygen atom is replaced by a nitrogen atom. In case of bicyclic structures, they may be biologically considered disaccharides[19].

Those carbohydrate analogues are well known as investigation tools for better understanding of the structure, mechanism and function of carbohydrate processing enzymes such as glycoside hydrolases (glycosidase) and glycosyltransferases. Those enzymes are able to regulate vital processes, greatly affecting quality control, maturation, transport and secretion of glycoproteins as well as also being able to alter cell-cell recognition. The inhibition of dysfunctional types of these enzymes can prevent the formation of the aberrant N-linked oligosaccharides and may stop oncogenesis and tumour metastasis[18]. Glycosidase inhibition can also have positive effects in diverse carbohydrate-mediated diseases such as DM, viral infections, genetic disorders[20] and lysosomal storage diseases[21]. In specific, *a*-glucosidase exerts a very important action on carbohydrates digestion, and its selective inhibitors help retarding glucose's absorption and consequently supress hyperglycaemia events, important on type II DM treatment[22]. Furthermore, *a*-glucosidase is involved in aberrant glycosylation

of glycoproteins and glycolipids, which is fundamental at various pathophysiological steps of the tumour's progression[23].

In this context, and once iminosugars are able to inhibit carbohydrate's processing enzymes due to their analogy with their substrate, these compounds have been seen as potential therapeutic molecules, namely as anticancer agents. Unfortunately, in general, iminosugars display low availability due to their complex structure and require multistep synthesis. This way, the development of new synthetic approaches to reach already known active molecules is needed as well as the discovery of new related compounds in order to get further information about structure-activity relationship (SAR) with enzymes of interest[18].

Although many new natural iminosugars with a range of biological activities and good specificity have been identified, just few are available. However, modifications of some natural iminosugar templates have been successfully carried out in producing bioactive compounds, so the iminosugars field continues to be very interesting to explore, concerning the multiple opportunities for therapeutic agents discovery[19]. Castanospermine (Figure 5) was isolated in 1981 and it can be considered as a bicyclic derivative of 1-deoxynojirimycin plus an ethylene bridge between the hydroxymethyl group and the ring. The stereogenic centers of the six-membered ring correspond to the *gluco* configuration. Castanospermine has been shown to affect many properties of tumour cells both *in vitro* and *in vivo*, and is a natural and specific inhibitor of *α* and *β* glucosidases. Castanospermine prevents the morphological differentiation of endothelial cells leading to a deficient vascularization of the tumour and the posterior inhibition of tumour growth. Although it did not alter the proliferation of cultured endothelial cells or their ability to attach to various extracellular matrix molecules, the cells shown the reduce ability to migrate and to invade basement membrane gels, among other properties[18].

N-Methyl-1-deoxynojirimycin (Figure 5) is also a natural compound with the ability to inhibit glucosidases I and II, which are responsible to remove glucose residues from nascent glycoproteins in the rough endoplasmatic reticulum. Structurally related with castanospermine, N-methyl-1-deoxynojirimycin presents similar anti-metastic activity as well as the reduction of the tumour cells adhesion to the vascular endothelium. Furthermore, this compound is able to induce changes in oncogene glycosylation and the prevention of the endothelial cells' morphological differentiation, interfering on tumour growth.

Regarding the glucosidase inhibitor series structure-activity relationship, it is known that 1-deoxynojirimycin and castanospermine inhibit *α*-glucosidase I and II, but the first one inhibits *α*-glucosidase II strongly, whereas castanospermine has greater effect on *α*-glucosidase I. In contrast, *N*-methyl-1-deoxynojirimycin is a better inhibitor of *α*-glucosidase I, suggesting that the substitution of the ring nitrogen, as also occurr in castanospermine structure, favours the inhibition of this enzyme[18].

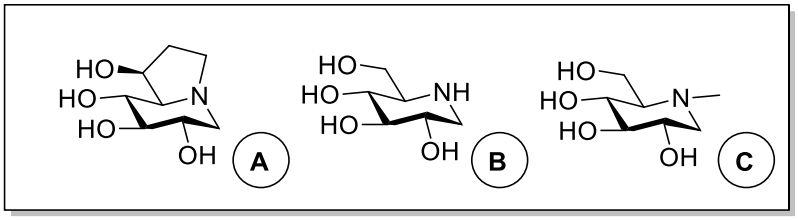

Figure 5 | Structures of natual iminodugars: A – castanospermine; B - 1-deoxynojirimicyn; C - *N*-methyl-1-deoxynojirimicyn[18]**.**

In spite of all the desirable properties of the natural iminosugars described above, in greater or lesser extent, they frequently are able to inhibit diverse types of glycosidase[23]. This poly-inhibition can lead to many side effects which can be avoided by the application of selective *α*-glucosidase inhibitors. In order to improve all of those properties and regarding all the achieved information, different related compounds have been prepared[24-30]. To improve anomeric selectivity to *α*-glucosidases was developed one family of glycomimetics with an endocyclic nitrogen having a higher sp^2-hybridation character (sp^2-iminosugars) instead of the usual sp^3-nitrogen atom, replaced by a carbamic type nitrogen[23,31]. The control of pseudoanomeric *α*-configuration in reducing sp^2-iminosugars (like (1*R*)-5*N*,6*O*-oxomethylidenenojirimycin derivative **1** (Figure 6)) can be obtained by the exploration of generalized anomeric effect (GAE), which results in very high anomeric selectivity for the inhibition of glycosidases. The resulting compounds revealed to have greater selectivity to α-glycosidase, with preference for the neutral isoform. Furthermore, it was proposed that the incorporation of axially-orientated substituents on pseudoanomeric position can be an important factor in aglycon-based modulation of inhibitory activity and in permeability through biologic membranes, considering the hydrophilicity of the initial compounds[23]. Also, the stability over the pseudoanomeric carbon has substantially increased, as well as configurational integrity in water[31]. This way, diverse castanospermine and nojirimycin iminosugar derivatives with sp^2-character have been synthesised, emerging a new class of potential α-glycosidase inhibitors with therapeutic applications[23,31,32].

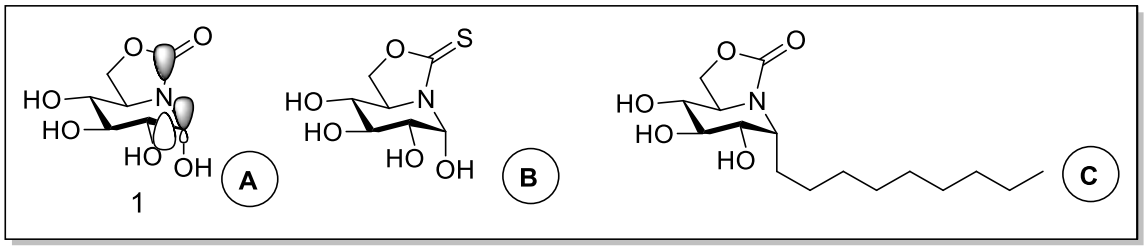

Figure 6 | Structures of (1*R*)-5*N*,6*O*-oxomethylidenenojirimycin **1** (A)[23], and two selective sp^2-iminosugars derivatives α-glycosidase inhibitors (B[31] and C[23]). The orbitals involved in negative hyperconjugation (generalized effect), thereby stabilizing the α-anomer, are depicted[23].

1.1.3.3. Potential Diabetes and Alzheimer treatment with carbohydrate based drugs

As described above, α-glycosidase is an important biological target in the treatment of type II DM[22]. In recent years, some studies shown that Alzheimer's disease (AD) and type II DM are most likely to appear together. Extensive efforts have been carried to unveil the relationship between DM and AD, and it was achieved that in both cases impairment of insulin is present. Insulin controls neuronal and synaptic functions in brain that are altered in individuals diagnosed with AD. In this context arises the need to develop potent dual inhibitors for the treatment of the two diseases. Acetylcholinesterase (AcCHE) inhibitors are used as therapeutic agents in AD, since they are able to prevent choline liberation in cholinergic synapses avoiding non-cholinergic events occurring in AD patients[33]. Also, these enzymes may potentiate both amyloid deposition and the toxicity of such deposits, as well as insulin resistance (related with hyperhomocystinemia, which leads to AcChE increased activity)[34]. Thus, developing of dual inhibitors for α-glycosidase and AcCHE can give rise to be valuable symptomatic therapeutic agents for both type II DM and AD.

1.2. Steroids

Beside carbohydrates, amino acids and nucleobases, steroids are a large class of natural compounds which plays important biologic functions in plant and animal cells. In mammals, the main sex hormones are steroids (testosterone and estrogens), as well as the plants sex hormones (brassiosteroids). Steroids also have an important role in metabolism regulation (glycocholic and taurocholic acid, vitamin D), and some of them, as glycosides, present interesting properties as cardioactive compounds (digoxin, gitoxin, scillaren A)[1,35]. Other steroids and their precursors or derivatives have also been reported as antitumor agents[36].

Structurally, steroidal compounds are originally modified triterpenoids with the tetracyclic ring system of lanosterol, the biogenetic precursor of steroids in animals, where three methyl groups on C-4 and C-14 are removed (Figure 7)[1,35]. These compounds are based on a backbone of four fused rings (A, B, C and D) arranged in a cyclopental[*a*]phenantrene, fully or partially reduced, with possibility of limited unsaturations (Figure 7)[1]. Although cychohexane may undergo a flip in conformation, steroids are rigid structures, once they possesses at least one trans fused ring system and this rings must to be diequatorial to each other. IUPAC numbering begins on A ring and proceeds around A and B, and then snakes around rings C and D until C-17[37]. The majority of the steroids have also one or two methyl groups. Unless specified, methyl groups, hydrogen atoms or substituents at the bridgehead positions C-8, 9, 10, 13 and 14 are assumed to have the 8*β*, 9*α*, 10*β*, 13*β* and 14 *α* configurations. In this way, these configurations can be omitted in compounds with natural

configurations. Configuration of C-5 can be *α* or *β*, once exist many steroids with one or the other configuration, then is necessary to identify the exactly configuration when the steroid is saturated in this position[1].

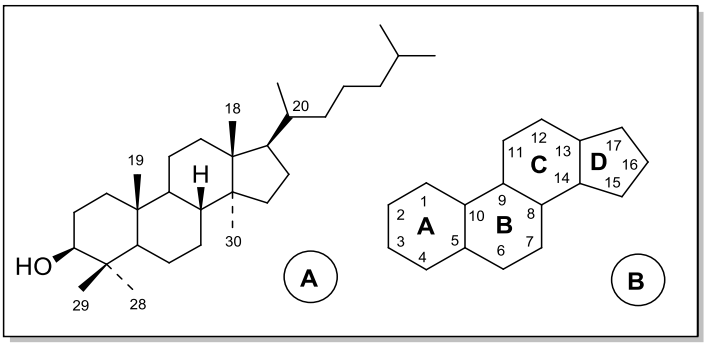

Figure 7 | Structure of lanosterol (A) and the steroid template with numbering system (B)[1].

Sterols are an extremely interesting group of steroids, abundantly widespread in animal and especially in plant kingdom. To sterols class belongs all the crystalline compounds that have a secondary hydroxyl group at C-3, generally in *β*-configuration, such as cholesterol and stigmasterol, and different side chains[1,35]. Modifications of functional groups in sterols molecules can provide compounds with high pharmacological activity[35].

In the point of view of biology, in mammals cholesterol is one of the most important steroids and by far the most abundant sterol, once is the base of all steroids biosynthesized and it is an essential component of all animal cell membranes[38].

1.2.1. Cholestane steroids (C_{27})

The cholestane group received this name from the best known compound of this class, cholesterol, structurally the precursor of almost all of the other sterols (Figure 8).

From this class, several others appear by the addition of one or more carbon atoms at side-chain positions, most commonly at C-24 (ergostanes, stigmastanes). Other are highly oxygenated cholestanes as ecdysteroids (Figure 8). Groups as spirostanes, furastanes and some steroidal alkaloids derived from cholestane too, by linking between two side-chain sites, or between a side-chain and a skeletal carbon, via an oxygen or nitrogen bridge. Alkylated cholestanes occur widely in plants, fungi and marine organisms[1].

Cholesterol

Cholesterol (cholest-5-en-3*β*-ol) is a very abundant lipidic molecule with fundamental biologic roles, being a structural constituent of cell membranes maintaining their integrity and a precursor of in the biosynthesis of bile acids, steroid hormones, neurosteroids and vitamin D. In mammalian cells cholesterol is mainly synthesized in the liver through mevalonate pathway or

acquired from dietary sources and it is very rare in plants and microorganisms[36,38]. Following the mevalonate pathway, cholesterol can be synthesised by to different routes, Bloch and Kandutsh-Russel pathways (Figure 9)[39].

Cholesterol is largely distributed in human body, mainly in brain and nervous tissues, muscles and connective tissues, which means that cholesterol content of cell membranes varies depending on cell type. Cell membranes with a high cholesterol ratio allow a high stability and low permeability, as the protective barrier of epidermis layer of skin[36]. On the other hand, low percentage of cholesterol mitochondria membranes are very fluidic and present high permeability. Cholesterol have also an important role in the maintenance of many neurotransmitter receptors and fluidity of nerve cells[36]. Various lipoproteins act as primary carriers of cholesterol through blood circulation, from liver to the tissues (low density lipoproteins– LDL) and back from liver (high density lipoproteins-HDL).

As precursor of all steroid hormones, cholesterol origin glucocorticoids (responsible for blood sugar regulation), mineralcorticoids (regulate mineral balance and blood pressure) and sex hormones. Pregnenolone is the first hormone in this biosynthesis cascade and after follows cortisol, progesterone and testosterone. Other important derivatives of cholesterol are bile acides, the amphipatic compounds that are responsible for emulfying the dietary fats, essential process for a proper digestion of food[36].

Biochemistry of cholesterol and its metabolites have been studied for many years and today is known that some of the oxidation derivatives of cholesterol are implicated in the initiation and progression of several chronic diseases, including atherosclerosis, neurodegenerative processes, DM, kidney failure, and ethanol intoxication. It have been also demonstrated that some oxidation products present also cytotoxic activity, as well as apoptotic and pro-inflammatory effects[38].

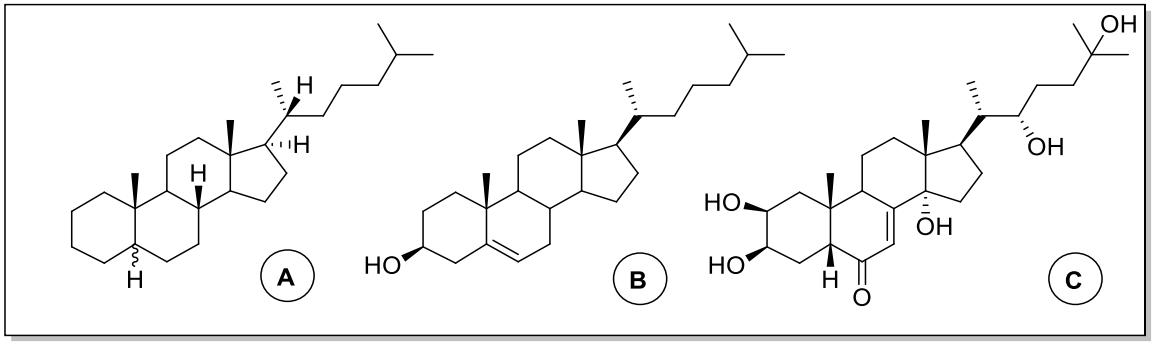

Figure 8 | Structures of cholestane (A), cholesterol (B) and ecdysone, an ecdysteroid (C)[1].

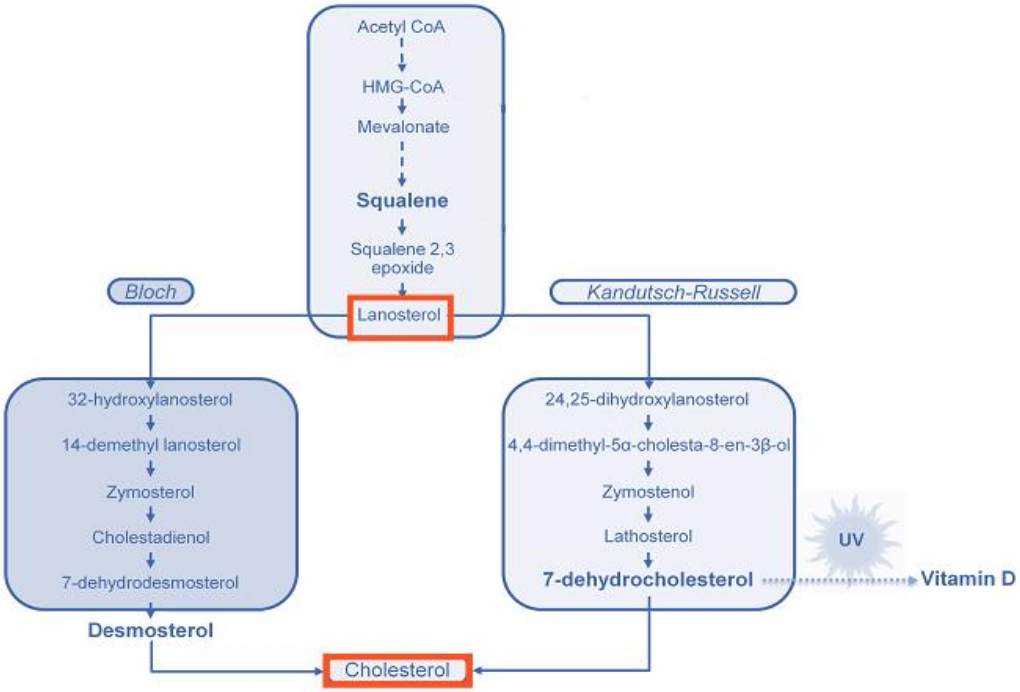

Figure 9 | Cholesterol biosynthesis by Bloch and Kanddutsch-Russel pathways, showing the different intermediary precursors[39].

Cholestanol

Cholestanol (5*α*-cholestan-3*β*-ol) (Figure 10) is a minor physiological sterol in animals, occurring in far lower concentrations than cholesterol. Structurally, the only difference between this two similar compounds it is the presence in cholesterol of a double bond in C5. Cholestanol is biosynthesised in the body from cholesterol with 4-cholesten-3-one as an intermediate, and the natural concentration of this sterol in the body, is around 1/500 of cholesterol concentration make difficult to understand its exact role[40]. The hereditary disease *cerebrotendious xanthomasis* is characterized by the sterol 27-hydroxylase deficiency in humans, wherein occur an increase of cholestanol concentration and its subsequent deposition[41]. The accumulation of this sterol causes several symptoms, namely tendon xanthomas, cerebellar ataxia, pyramidal signs, cataracts and dementia. Also, when partially replaces cholesterol, cholestanol reduces the fluidity of membranes, causing failure in calcium channel opening and induces apoptosis[40].

However, synthetic and natural cholestanol derivatives have shown interesting biological properties, for example the cholestanol conjugated with a ß-lactam ring (Figure 10)[35] and cholestanol glucoside[42] with anticancer and antioxidant effects.

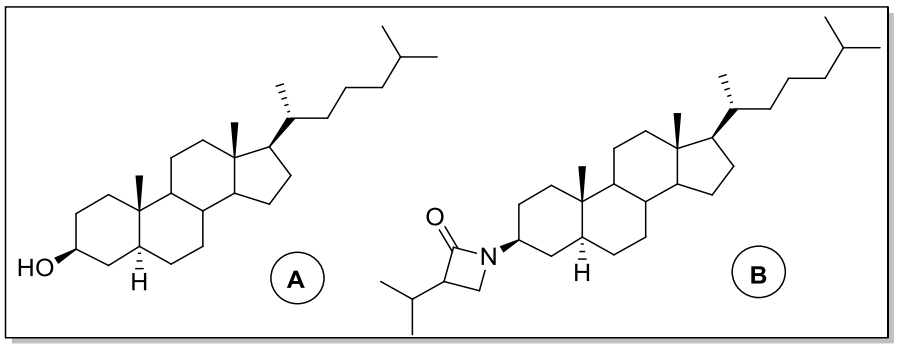

Figure 10 | Structure of cholestanol and a bioactive cholestanol conjugate (with ß-lactam ring[35]

1.2.2. Pregnane steroids (C_{21})

Pregnane (Figure 11) is the parent hydrocarbon of progesterone and of the great majority of the corticosteroids, as many other natural products. This sub-group is the largest of all steroids. In structural terms, the backbone of pregnane compounds present 21 carbons, with an ethyl group at C17[1].

Pregnenolone

Pregnenolone (3ß-hydroxypregn-5-en-20-one) (Figure 11) is one of the most important intermediaries in the steroid biosynthesis, precursor of several hormones such as cortisone, progesterone, estrogen and testosterone[43]. The conversion of cholesterol into pregnenolone is the first step in the synthesis of steroidal hormones that is consistent from amphibians to mammalians, in the diverse steroidogenic tissues, gonads, adrenal glands, placenta and also in brain. At first, occurs mobilization of cholesterol into the inner mitochondrial membrane, and then is allowed the cleavage of the lateral chain by cytochrome P45011A1(CYP11A1) to pregnenolone, being this step the limiting one for the synthesis of all steroid hormones. The steroids biosynthesised in brain, are recognized as neurosteroids, which are able to modulate brain functions. They are synthesised on the central and peripheral nervous system, in glial cells and also in neurons from cholesterol or steroidal precursors imported from peripheral sources. The main pregnenolone metabolites, are sulphated pregnenolone, 17ß-hydroxypregnenolone which results in dehydroepiandrosterone (DHEA) or 17ß-hydroxyprosgesterone, and progesterone. Through these metabolites it is also possible to biosynthesise glucocorticoids, androgens and estrogens (Figure 12)[44].

Neurosteroids act on membrane receptors that trigger signalling cascades, involving mainly inhibitory and excitatory aminoacid receptors, $GABA_A$ and NMDA, respectively. Pregnenolone derivatives as sulphated pregnenolone and allopregnenolone can interact with those systems. The first one possesses an inhibitory effect and the second is excitatory. Pregnenolone itself is known to interact with sigma1 receptors (agonist, learning and memory, functions) and stress-anxiety and

depression related functions), cytoplasmatic microtubules (agonist, modulates assembly and stabilization) and recently discovered, with type-1 cannabinoid receptor (inhibitor of the action of THC-mediated effects).

Pregnenolone has real potential as therapeutic agent and the development of synthetic steroids that can display better bioavailability and efficacy might constitute promising novel strategies for the treatment of certain disorders like depression, Alzheimer disease and schizophrenia. Several pregnenolone derivatives have been synthesised and show interesting biological properties with potential therapeutic applications including in psychosis, mental retardation, metabolic disorders, skin diseases[44], neuroinflammation[45] and cancer[46].

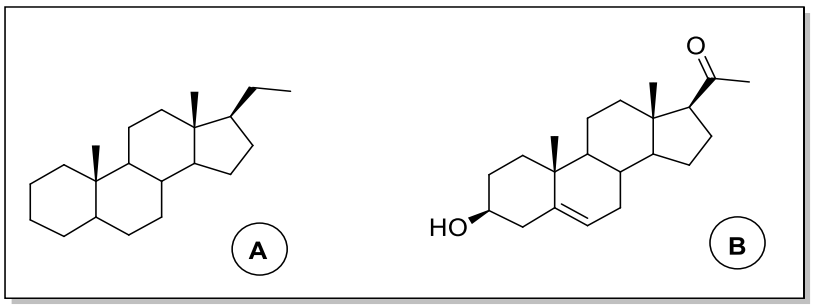

Figure 11 | Structures of pregnane (A) and pregnenolone (B)[1].

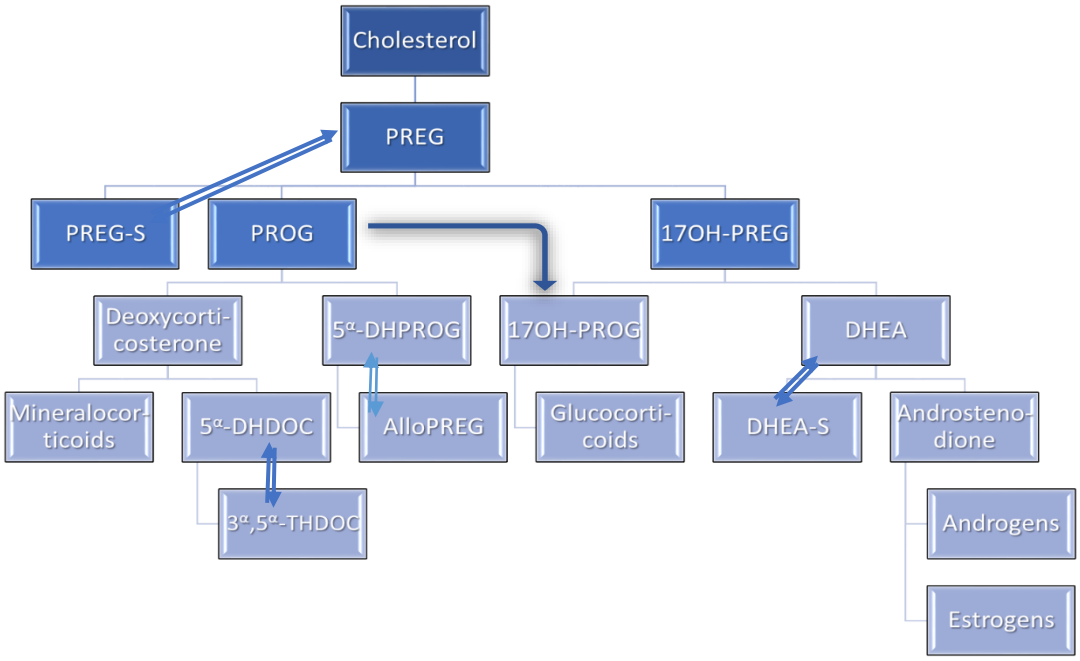

Figure 12 | Main metabolic pathways for the biosynthesis of the major classes of steroidal hormones in humans and rodents. PREG - pregnenolone; PREG-S - pregnenolone sulphate; 17OH-PREG - 17α-hydropregnnolone; PROG - progesterone; 17OH-PROG - 17α-hydroprogesterone; 5α-DHDOC - dihydrodeoxycorticosterone; 3α,5α-THDOC - tetrahydrodeoxyxorticosterone; DHEA-S - DHEA sulphate. Adaptated[44].

1.2.3. Androstane steroids (C_{19})

As the parent hydrocarbon of testosterone and its derivatives and metabolites, androstane (Figure 13) give the name to its group. Structurally, these compounds present two bridgehead methyl groups at C-10 and C-13 as many other steroid groups. On the other hand, in this family there are no sidechains at C-17[1].

DHEA

DHEA (3ß-hydroxyandrost-5-en-17-one) (Figure 13) is the most abundant steroid hormone in human blood, and it is present in serum mainly as a sulfate ester (DHEA-S), which concentration decreases dramatically with age[47]. In this context, in recent years was hypothesized that DHEA play an important role in cognitive performance. Conversely, the available data lead to reject the hypothesis of the usefulness of DHEA supplementation in improving or maintaining memory and other cognitive domains in older individuals[48].

After conversion of cholesterol into pregnenolone, CYP17A1 regulate pregnenolone conversion to 17-hydroxypregnenolone and further to DHEA (half-life~30min), which is inter-convertible into DHEA-S (half-life~10h), more stable, process controlled by SULT2A1 T and steroid sulfatase (STS). DHEA synthesis occur in adrenal cortex (*zona reticularis*), gonads and in central nervous system, and can be substrate for testosterone and estrogen formation[49]. DHEA along with DHEA-S accounts for 50% of androgens in men and 75% of estrogens in premenopausal women.

Besides the fact of DHEA/S is able to exert many biological actions, the exact mechanism is broadly unknown. The effects of those compounds are thought to be mainly mediated by a specific G protein coupled plasma membrane receptor as well as a nuclear DHEA specific binding complex. They seem to bind to estrogen receptors exerting some estrogen-like activities, independent of its conversion to estradiol. Also, the presence of some skeletal muscle binding sites can explain specific influence of DHEA/S on muscle function. Moreover, DHEA can act in immune system, increasing interleukin 2 production, through the interaction with specific receptor-binding complex in T cells[48]. As neurosteroids, DHEA and a variety of its free and sulphated derivatives are efficient neuromodulators in both central nervous system and peripheral tissues (Figure 14)[50]. Some clinical and experimental studies also show that DHEA/S is a multifunctional steroid related in fisiopathologic/pharmacologic processes, including in obesity, DM, arteriosclerosis and antiviral, antidepressant, anti-inflammatory and antitumor actions[51,52]. Leading to found different biological active compounds, mainly to improved anticancer activity several derivatives have been prepared[52-54].

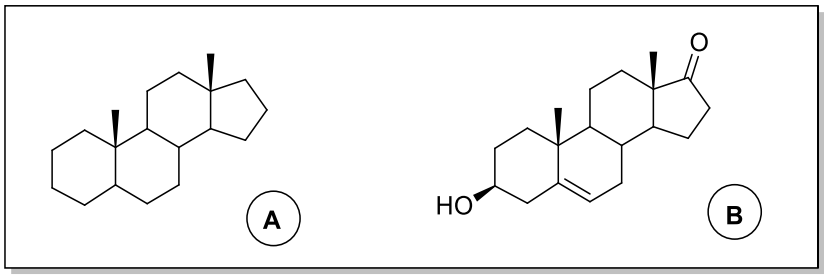

Figure 13 | Structures of androstane (A) and DHEA (B)[1].

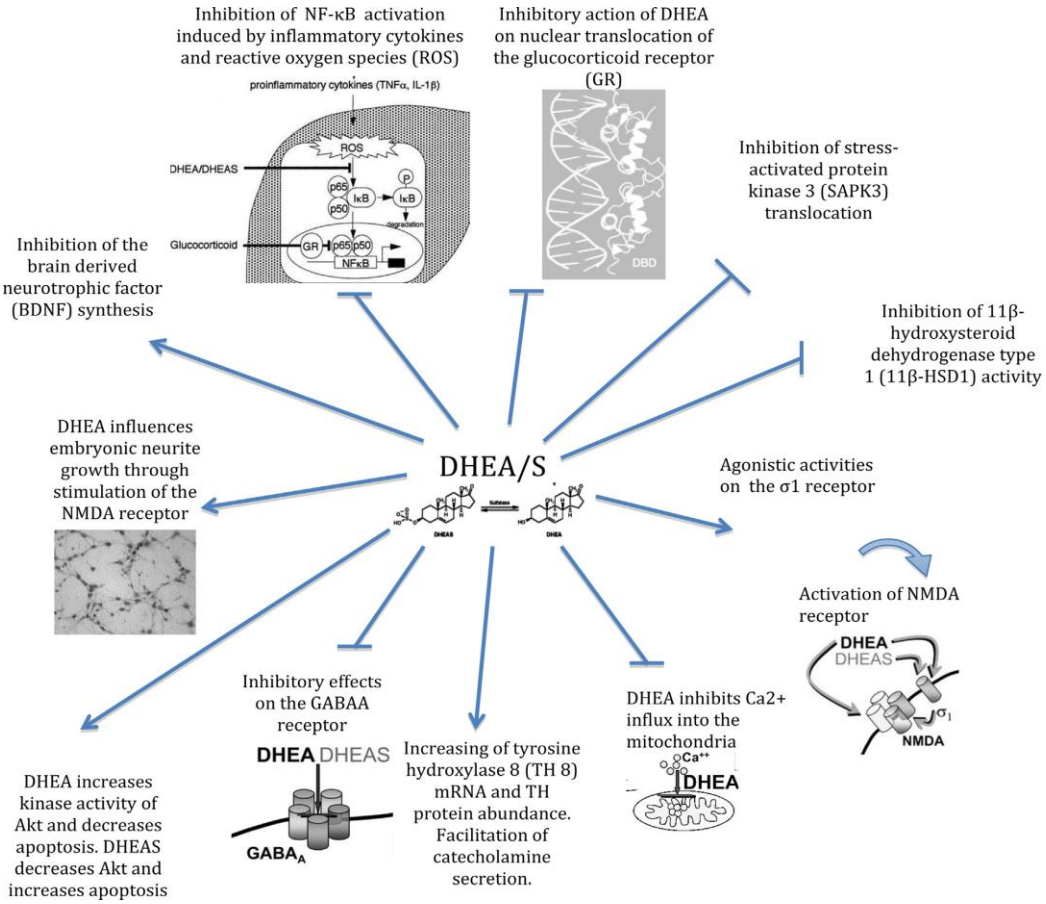

Figure 14 | Potential molecular mechanisms of DHEA/DHEA-S in cognitive function[48].

1.2.4. Stigmastane steroids (C_{29})

Stigmastane-based nomenclature derived from the very common plant sterol stigmasterol, nevertheless they are originally 24-ethylcholestanes[1].

Stigmasterol

Stigmasterol (Figure 15) is an unsaturated phytosterol present in several plants[55]. Stigmasterol has essential roles along with other phytosterols like sitosterol and campesterol in structure and function of cell membranes, like cholesterol in mammalian cells. They regulate the fluidity of membranes, restricting the motion of fatty acyl chains. As cholesterol, stigmasterol also modulate ATPase activity, by stimulation of export of H^+ at low concentrations, unlike all the other sterols[56]. Stigmasterol act as precursor in the synthesis of progesterone and as intermediate in the biosynthesis of androgens, oestrogens, corticoids and in the synthesis of vitamin D_3. Actually, stigmasterol is used as raw material, on the design of synthetic and semisynthetic compounds for the pharmaceutical industry. Recently, stigmasterol biosynthesis was attributed to mevalonate and deoxy-xylulose pathways with relatively equal contributions.

This phytosterol has been isolated from many medicinal plants, being assigned it different biological activities such as anti-inflammatory, antimutagenic, antioxidant, hypoglicemic, anti-tumour, cytotoxic, anti-osteoarthritic and anti-hypercolestrolemic activities. Furthermore, its derivatives have also shown similar properties as fucosterol (antioxidant and antidiabetic) and spinasterol (anti-tumour), or quite different but not least as dehydrooogoniol, an female activating hormone, cyasterone, with anti-feeding properties or stigmasterol glucoside, a neurotoxic compound[55]. Other natural and synthetic stigmasterol derivatives have been evaluate as antiviral and antimicrobial agents (Figure 15)[57,58].

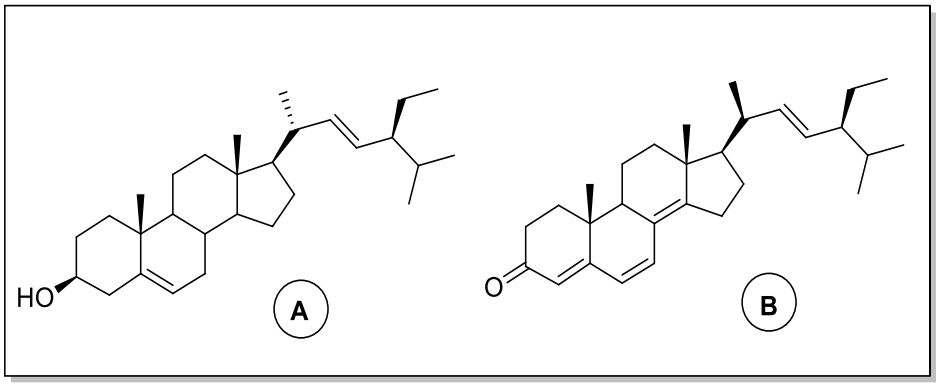

Figure 15 | Structures of stigmasterol (A) and a derivative with antiviral properties (B)[57].

1.2.5. Spirostan steroids (C_{27})

Compounds of spirostan class are found in many plants, being diosgenin the most know, one of the main sources of steroidal intermediates for synthesis of steroidal hormones and pharmaceutical analogues. In fact, spirostans are 16*β*,22:22,26-diepoxycholestanes, what means it is not a class of hydrocarbons[1].

Diosgenin

Diosgenin ((25R)-spirost-5-en-3ß-ol) (Figure 16) is a very abundant sapogenin of diverse saponins as a glucoside and dioscin, and it is found in several plant species, of *Trigonella*, *DIoscorea* and *Costus* famillies. Besides its important role for the semisynthesis of industrial and pharmaceutic steroids, diosgenin have revealed different biological activities, including in the improvement of blood circulation, anti-inflammatory, antioxidant and cytotoxic effects[59,60]. Diosgenin is also able to control blood cholesterol levels and the production of DHEA. Furthermore, this steroid affects the lipidic biosynthesis, acting as antagonist on nuclear liver X receptors in liver, which is also related with type II DM and hypercholesterolemia. In this context, diosgenin itself is used for the treatment of leukaemia, climacteric syndrome and colon cancer[59]. Despite the fact of its biotransformation by microorganisms[61], plants[62] and ruminants[63], it is not known any metabolism of the molecule by the human enzymatic machinery.

Leading to improve diosgenin properties and selectivity different derivatives have been prepared, namely as anti-inflammatory and anti-proliferative agents[60,64–66].

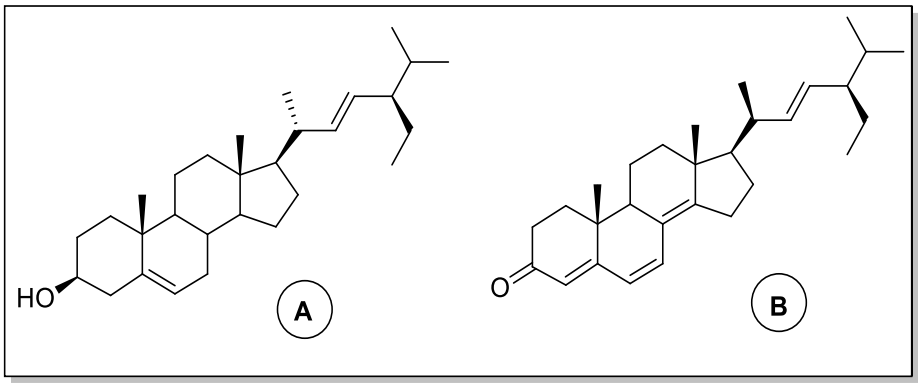

Figure 16 | Structures of stigmasterol (A) and a derivative with antiviral properties (B)[57].

1.2.6. Steroidal conjugates

The steroid connection with natural products such as pyrimidine, purine, alkaloids, sugars or polyamines allow to obtain new compounds with different biological activities, complexing or gelling

agents, being all this type of compounds classified as steroid conjugates[35]. Steroid conjugates are actually used in a variety of biological, medicinal or supramolecular chemistry, being a target of interest on design and synthesis of new compounds. There are different applications for these compounds on medicinal chemistry such as new drug complexing agents, drug delivery systems or even the drug itself[35].

Currently, there are several examples of biological active steroidal conjugates in study or already used in clinic. For the last decades, cholesterol, the most abundant steroid in mammals, and its derivatives and conjugates have received much attention. Conjugation of cholesterol with active compounds is an attractive approach for diagnostic and treatment, since cholesterol can be considered a drug delivery system. For example, cholesterol (lipophilic compound) conjugated with a more polar and active molecule can go through the blood brain barrier and achieve the brain. Also, cholesterol can drive an anticancer molecule until ovaries, where there are, in general, high levels of cholesterol (precursor of sex hormones), or just redirect those anticancer agents to any tumour, wherein the cells need an extra uptake of cholesterol, once there are overexpression of LDL receptors[36].

Through the action of several enzymes, including CYP3A4 on cholesterol, metabolites like bile acids are synthesised. The application of those compounds in drug improvement is of great interest, mainly in the synthesis of prodrugs such as chlorambucil (cytostatic agent) conjugates (Figure 17), much less toxic than the free drug, or a oxaprolylopeptide conjugated with cholic acid (liver cirrhosis treatment), much well absorbed. Also, the agglutination of bile acids with active pyrimidine or purine moieties, like the antiviral acyclovir can improve drastically the absorption, permeability and stability of the compounds.

Alkaloids are a class of secondary metabolites containing basic nitrogen atoms which usually plays very important biological activities. In the natural molecule pachystermine A a *β*-lactam ring is attached to the steroidal moiety[35]. This compound showed ability to block the active site of some enzymes like antiestrogen binding site receptor in breast cancer cell line[35,67]. Still in the field of nitrogenous compounds, conjugated steroids with triazole moieties apparently constitutes an important strategy in the preparation of bioactive compounds, namely with antimicrobial and antiviral properties[35]. In addition, other approach to reach biological active compounds, such as antiproliferative agents, has been successfully applied the conjugation of natural cytotoxic nitrogenated motif with steroids[68].

Ionophores are very important molecules able to transport ions like K^+, or Rb^+ cross the biologic membranes, and usually show antibiotic properties. Conjugation of this known compounds with steroids results in very selective complexation agents of cations (Figure 17).

Steroids also can be conjugated to form diverse macrocycles with steroidal skeleton or steroidal dimmers with different linkers. Those macrocycles can be very useful to coordinate ions or neutral molecules. Other macromolecules can be synthesised based on steroidal skeleton. In recent

years much attention was given to molecular pockets (Figure 17), umbrellas and *quasi podands* and the presence of natural compounds as steroids can be useful. These compounds present important properties as delivery vehicles for biological molecules, molecular containers as well as hydrogelators[35].

Other large and important class of conjugates are the steroidal glycosides, which includes structurally and biologically diverse synthetic and natural molecules, isolated from a wide variety of both plant and animal species[13].

The possibilities of major biomedical applications based on glycobiology have dramatically in demand of glycoconjugates such as steroidal glycosides. Curiously, among the huge number of glycoconjugates used in traditional Chinese medicine, steroidal glycosides are found as the main components[13]. An example is a spirostan saponin isolated from the rhizome of Anemarrhena asphodeloides Bunge (*Liliaceae*), used in the treatment of DM and inhibition of platelet aggregation for many years[69].

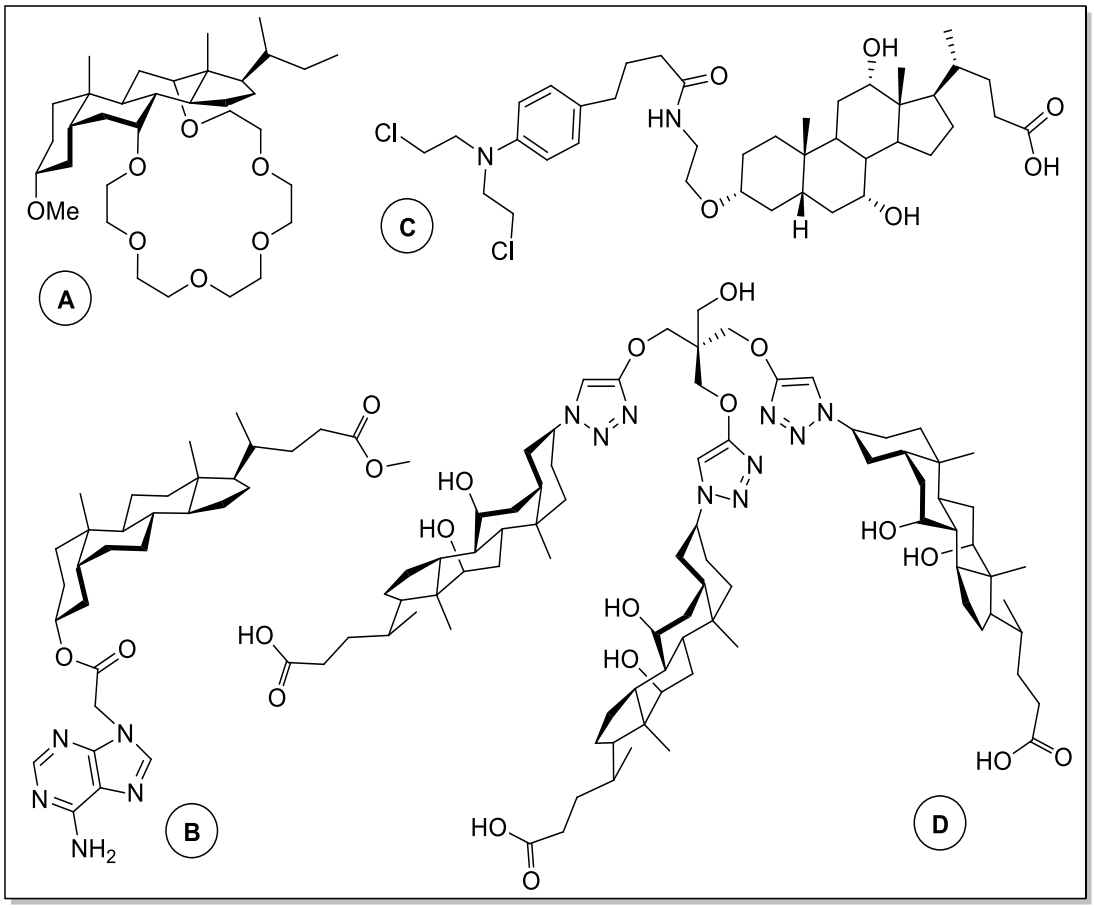

Figure 17 | Structures of a synthetic ionophore containing a steroidal moiety (A), a bile acid conjugated with a purine (B) and the drug chlorambucil (C), and a molecular pocket composed by three steroidal moieties[35].

1.3. Steroidal glycoconjugates

As described above, steroid conjugates are actually used in a variety of biological, medicinal or supramolecular chemistry, being a target of interest on design and synthesis of new compounds[35], and steroidal glycosides is one of the most promising classes in terms of drug development. On the first half of the XX century, some researchers already believed that plants sterols and their natural glycosides can serve as rich and efficient source of raw materials for chemical synthesis of mammalian hormones, and today it is confirmed by the massive utilization of compounds as diosgenin and progesterone of plant origin by large scale industries[6].

Natural products are the main source of all the drugs in the market, playing a dominant role in the discovery of leads for the drug development, being themselves the active agent or inspiring the synthesis of mimetics[70]. Saponins are a widely distributed group of naturally occurring plant glycosides, found in roots, tubers, leaves, blooms and seeds. Initially, this class was characterized by foam-forming properties in aqueous solution. Structurally they are described as triterpene or steroidal glycosides[71], consisting in a hydrophobic sapogenin (genin, aglicone) and a hydrophilic sugar moiety (glycone). Their amphiphilic structure is intrinsically related with their biological functions, including haemolytic activity[72]. The glycone portion are in general oligosaccharides in a linear or branched fashion[71], and the most common monosaccharides units present in natural (and synthetic) steroidal saponins are *β*–D-glucopyranose, *α*-L-rhamnopyranose and *β*–D-galactopyranose. However, due to nature of amino group which confers specific properties, also glucosamine seem to open a broad spectrum of possibilities in biological activities, if present in steroidal saponins. Glucosamine is an aminosugar of great biological importance that is frequently present as a constituent of many naturally occurring poly and oligosaccharides, glycoproteins and glycolipids[73].

In last decades saponins have received significant attention due to their physiological and pharmacological activities[13], including expectorant, anti-inflammatory, vasoprotective, hypocholesterolemic, immunomodulatory, hypoglycaemic, antifungal, antiparasitic, chemopreventive and antiproliferative effects[71,72], and also can be use as adjuvant in vaccines formulation. In economy these compounds are very important too, since they are important raw materials for the pharmaceutical industry in the production of steroidal hormones[72]. The identification and development of saponins have greatly contributed to medical treatment of cancer and some of them are in fact used in clinical practise[71]. The combined application of saponins with other antitumor compounds may increase cytotoxic activity of the latter, being also an interesting new possibility in cancer treatment[71,72]. In general, saponins induce apoptosis instead of necrosis, a really desired property concerning the avoidance of side effects [71].

Concerning structure-activity relationship, some structural features of were already identified as promoters or reducers of the activity. For example, in relation to the aglycone, in similar

compounds, the presence of a hydroxyl group at C16 appears to enhance the activity, unlike the same group at C17, which seems to reduce the cytotoxic activity. Also, the stereochemical configuration of a methyl group and the presence of an F ring instead of an open chain can change the selectivity of the compound[71]. The presence or lack of an unsaturation at C5 seems to not affect the activity, although there is a spatial difference in conformation of A and B rings. In spirostanol derivatives, the introduction of a nitrogen atom on F ring indicate an enhancement of activity. About the glycone part, it is in general attached to a sterol by the hydroxyl group of C3[72], but can be added or naturally appear in different positions such as C16. Different factors can affect the potency/activity of the compound such as the linkage between the sugar monomers, the extension of the chain, their lipophilicity and the sequence. More lipophilic sugar molecules with acyl groups seem to be more active, as well as glycosyl moieties[71]. Other features in both aglycone and glycone moieties seem to be relevant but more studies are needed to clarify this point, especially for steroidal saponins[72].

Among all natural steroidal saponins, the most promising classes as antiproliferative agents are spirostanes and furostanes[71]. Polyphyllin D (Figure 18), formosanin C and dioscin are examples of diosgenyl (spirostane) saponins with strong-anticancer and immunostimulative activity[74-76]. Furostanes as protoneodiscin, protodioscin, protoneogracillin and protogracillin have also showed promising cytotoxic activity[77]. **Diosgenyl glycosides** and spirostane glycosides in general, natural and synthetic, are probably by far the most studied saponins. Different approaches have been applied to reach more selective and efficient agents in order to obtain potent antiviral[78-80], antimicrobial[81-83], anti-inflammatory[84,85] and mainly antiproliferative[64,73,86-94] compounds.

Cardenolides are another important class of natural saponins, in which the cardiotonic glycoside like digoxin are present, and show also diverse cytotoxic agents[95-98] (Figure 18). Inspired in ketones as pregnenolone, different glycosides have been found and synthesised. **Pregnenolone glycosides** and derivatives found in *Cynanchum saccatum* have revealed to possess some antiproliferative potential[99], others, extracted from *H. gordonii* and *A. incarnata* roots have showed influence on corticosteroid releasing[100].

OSW, probably the most known cholestane glycoside, has attracted great attention due to its potent cytotoxic properties. OSW was isolated dorm bulbs of Ornothogalum saundersiae[101] and since than different derivatives have been synthesised[96,101-105]. **Cholesterol glycosides** and analogues have also been synthesised, namely as vascular leakage blockers[106] and for the development of liposomal gene delivery systems[107].

Cholestanol glycosides are promising steroidal sugars, concerning antioxidant and anticancer potentialities[42]. In some types of cancer such as gastric, ovarium, colorectal and pancreatic cancers, the major form of recurrence is by peritoneal dissemination, through the adhesion to the surface of the peritoneum. To prevent this adhesion some synthetic sugars have been developed, including cholestanol conjugates, with mono- di- or tri-saccharides attached at 3- position. This compounds have shown a strong inhibiting activity of colorectal and gastric cancer cells by inducing apoptotic

cell death. In contrast, cholestanol itself present total ineffectiveness. Furthermore, this type of compounds have demonstrated potential multi-target anticancer activity against human esophageal cell lines, since they induce apoptotic cell death trough modulating the Bcl-2 family, caspase cascade, PARP and VEGF-A[36].

Stigmasterol glycosides have also been investigated and the results have shown that some of them present anti-inflammatory[108], antimutagenic[109] and neurotoxic[110] activities. Polyhydroxylated steroidal glycosides of *Vernonia nigritiana Oliv. & Hiern*. (*Asteraceae*) present to be 80% more active as topical anti-inflammatories than indomethacin (reference compound)[108]. In the other hand, stigmasterol glucoside (Figure 18), isolated from diferent species, is related with neurotoxicity via liberation of large amounts of glutamate that can lead to NMDA receptors activation[110]. Antimutagenic studies were carried out using an extract of *Momordica charantia* containing steroidal glycosides and the well-known mutagen mitomycin C. The study revealed that the extract reduce 80% of the modifications induced by mitomycin C, probably through the penetration of the sterol glycosides on the plasma membranes affecting the permeability towards mitomycin C[109].

Besides all of this large spectrum of activities and potentialities, most of available data suggests that these steroidal glycosides are typically poorly absorbed following oral administration to animals and humans. However, new strategies to increase absorption of such amphiphilic compounds as saponins have been developed. Studies have been carried out in this order and was found that worse permeability from gastrointestinal tract can be due to the surface activity that imposes self-assemble as micelles in solution. The formation of those micellar aggregates of increased molecular size and hydrophilic character results in an expected poor permeability. To enhance bioavailability of this type of compounds different formulations were developed, such as a lipid-based formulation that aims the prevention of aggregation, which provided an improvement of almost thirty-fold in bioavailability of a gisenoside (triterpene saponin). Other example is a micronized formulation of another gisenoside (Rh_2) that enhanced two-fold the bioavailability. These micro-particles seemed to be better dissolved in the intestinal juice and transported across the intestinal epithelial cells[72].

In summary, a lot of steroidal conjugates with great biological actions, as selective anticancer activity, have been found or synthetized having as base natural scaffolds, however more research in this field is needed, including design of new steroidal glycosides and wider range of biological evaluations[73].

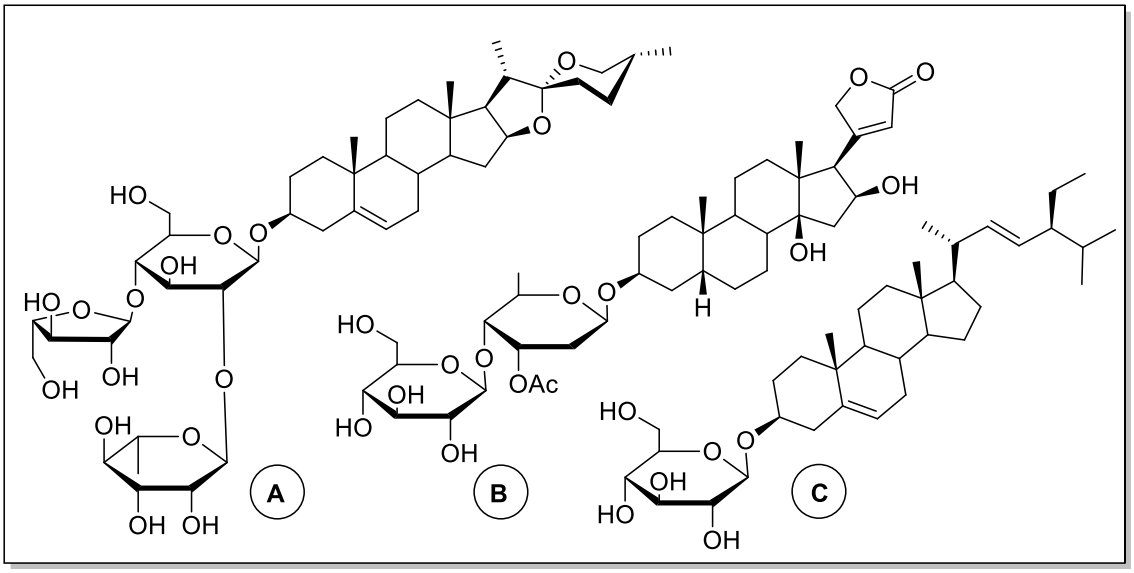

Figure 18 | Structures of steroidal glycosides: polyphyllin D (A)[74], a cardenolide glycoside (B)[95] and stigmasterol glucoside (C)[109].

2. Aims

Regarding all the information above, the project here described aimed the synthesis of a series of six new steroidal glycosides, through the hybridization of well-known, natural and available sterols (cholesterol, 5α-cholestanol, pregnenolone, DHEA, stigmasterol and diosgenin) and a promising synthetic sp^2-iminosugar ((1*R*)-5*N*,6*O*-oxomethylidenenojirimycin **1**), selective inhibitor of *α*-glucosidases[23]. After the synthesis and proper purification and characterization of the compounds, it was proposed their biological evaluation as potential glycosidase inhibitors. As structurally these compounds can be considered saponins, a class of compounds known by the significant antiproliferative properties (among others)[71], it is of major interest the evaluation of the cytotoxicity of these compounds, by the colorimetric 3-(4,5-dimethylthiazol-2-yl)-2,5-diphenyltetrazolium bromide (MTT) assay. In order to clarify the results of this assay, flow cytometry studies were also performed.

In the course of this dissertation project was noticed that dual *α*-glucosidase and AcCHE inhibitors can be very useful agents on the treatment of type II DM and AD[34]. Thus, as some steroidal derivatives have also shown potential in the treatment of same diseases[69,111], it was also performed molecular docking studies in order to predict biding energies and the possible interactions with AcCHE.

3. Results and Discussion

3.1. Synthesis

The synthesis of six new steroidal conjugates consisting in a steroidal moiety attached to a sp^2-iminosugar portion was developed in this project. To synthesise the desired compounds, it was followed a strategy which start with the preparation of the sp^2-iminosugar (1*R*)-5*N*,6*O*-oxomethylidenenojirimycin **1** until is ready to be glycosidated. After the glycosidation procedure, it is only necessary to deprotect the acetylated hydroxyl groups (Figure 19). After several steps, twelve new compounds were successfully synthesised and fully characterized (acetylated and hydroxyl free final products).

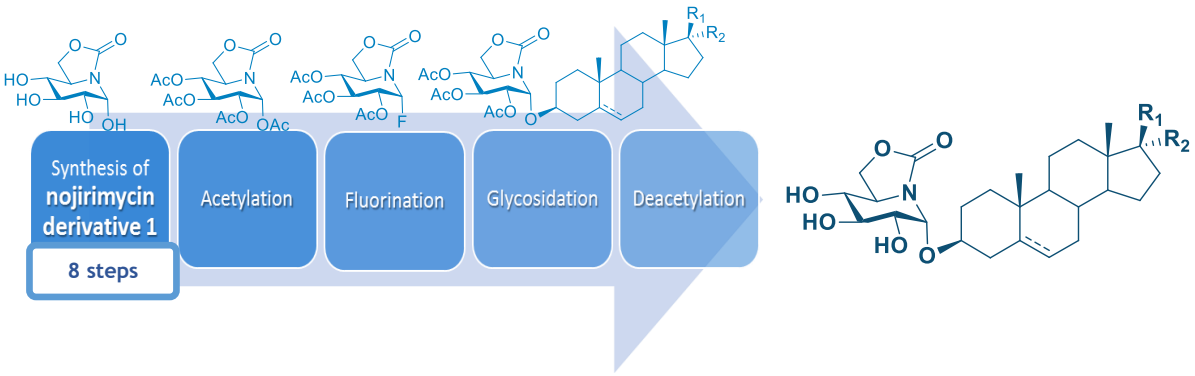

Figure 19 | Schematic synthesis process to obtain steroidal conjugates bearing a sp^2-iminosugar moiety.

For the synthesis of the sp^2-iminosugar 1 a 8 steps strategy was followed (Scheme 1), a quite complex process involving different types of experimental conditions[31].

The process started with the nucleophilic substitution (S_N2) with stereochemistry inversion of the free -OH group of by a chlorine atom in the presence of SO_2Cl_2 and pyridine, on the substrate 1,2-*O*-isopropylidene-ß-L-idofuranurono-6,3-lactone **2**, wherein the two -OH groups at C1 and C2 protected by an isopropylidene group. Here, pyridine displaces chlorine from the sulphur and there is no internal return as usually happen in reactions with SO_2Cl_2 and an alcohol.

After, the lactone was reduced to a diol derivative, with ring opening in presence of the strong reducing agent $LiBH_4$. The next step was the protection of the reactive –OH at C6 with a tetrahydropiran (THP) moiety. This molecule also displays another –OH group at C3, but this one is much less reactive. THP was the protecting group chosen due to it is stable at strong basic conditions[112], such as the basic medium needed to proceed to the introduction of the azide functional group by displacement of the chlorine leaving group. After C6 –OH deprotection with *p*-TsOH, the azide group was reduced by hydrogenation to afford a primary amine. Then, the addition of the

reactive triphosgene triggered a quick cyclic carbamate formation. Finally, the bicyclic compound **1** was obtained, resulting from acid catalysis by trifluoroacetic acid (TFA).

Product **1** possess a very particular stereochemistry. Aside the fact that this compound is derived from a natural product, it was designed thoroughly to present specific characteristics. The carbamic group, where the endocyclic nitrogen presents high sp^2-character, affects remarkably the stereoelectronic properties, since it is produced a very efficient overlap between the symmetrical orbital located on the lone-pair of endocyclic nitrogen and the σ* antibonding orbital of the anomeric C-X bond, which imparts chemical, conformational and configurational stability to the axially oriented pseudo-aglycone substituent. This effect seems to be the responsible for the remarkable α-anomeric selectivity[113].

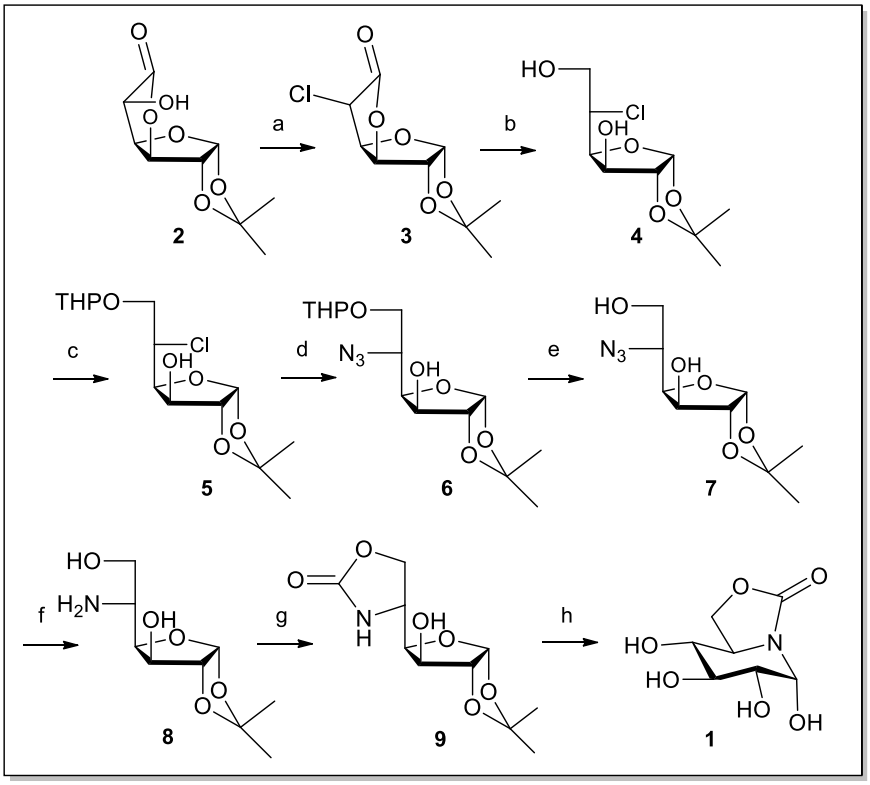

Scheme 1 | Synthetic strategy and results of (1*R*)-5*N*,6*O*-oxomethylidenenojirimycin preparation. Conditions and yields: a) SO_2Cl_2, Py, anydrous DCM, 0ºC, 90 min, 91%; b) $LiBH_4$ 1M in THF (anhydrous THF, 0→ 20 ºC), 4h, 84%; c) DHP, PPTS, DCM, r.t., 1h, 68%; d) NaN_3, anhydrous DMF, 130 ºC, 72h, 50%; e) *p*-TsOH (1:1) DCM:MeOH, 2h, r.t., 87%; f) H_2, Pd/C, MeOH, 1 atm, 2h15min, 69%; g) Triphosgene, DIPEA, DCM, 0ºC, 30 min, 72%; h) 90% TFA-H_2O, 30 min, r.t., 89%.

To proceed to the glycosydation with sterols, it is necessary to enhance the nucleofilicity of the alcohol group. In order to do this, it was proposed to synthesise a fluorine derivative of **1** to generate a better leaving group. At first, all the four –OH groups were protected with acetyl groups. After, a substitution of the acetyl group on the pseudoanomeric C1 by a fluorine atom occurred

(Scheme2). This compound presents very characteristic NMR spectra, wherein it is observed a splitting on the ^{13}C NMR spectrum. This happens because fluorine atom can couple with carbon nuclei in a similar manner to which is seen in C-H couplings and it was not applied any kind of C-F decoupling to prevent signal splitting.

Finally, it is possible to proceed to the hybridization between the iminosugar moiety and the sterol. Until this step, all the products described have already been fully characterized[23,31,114], and the yields were, in general, in accordance to the expected.

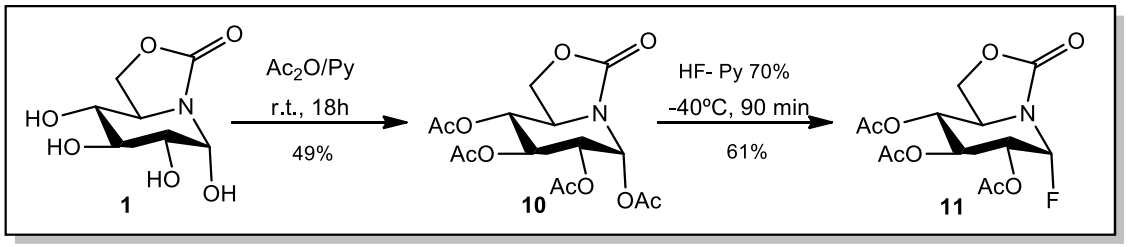

Scheme 2 | Preparation of fluorine per-*O*-acetylated derivative of 1. Yields: 10-49%; 11- 61%.

The use of glycosyl fluoride as glycosyl donor possess notable advantages, including the fact that it is more stable thermal and chemically when compared to the low stability of other glycosyl halides. This is due to the higher strength of the carbon-halogen bond, which can even allow to purify the glycosyl product by column chromatography. Through the use of boron trifluoride etherate ($BF_3{\cdot}OEt_2$) as catalyst it is possible to achieve highly stereoselective glycosylations, since this non-hydrolytically sensitive and non-volatile catalyst allows the avoidance of a heterogeneous reaction[13]. In this case, the departure of the fluorine leaving group is catalysed by $BF_3{\cdot}OEt_2$ and assisted by the formation of an azacarbenium cation species. This species allow the subsequent addition of the sterol alcohol nucleophile under a strict control of the anomeric effect[113]. NMR spectra seem to confirm this hypothesis, once only the α-anomer was observed in all the new synthesised compounds. This was figured out by the observation of coupling constants (*J*) between H-1' and H-2'. According to the dihedral angles, two axial protons possess higher J (ex:9.5 Hz), and vicinal equatorial-axial protons possess lower J (ex:4.0 Hz)[115]. All of results indicate that the *J* value between H-1' and H-2' is low (3.6 to 4.2). Also, *J* between H-2' and H-3' are all quite high (9.0 to 9.8 Hz). This means that at C-1 the substituent is axial (α-anomer) and at C-2 and C-3 is equatorial (NMR spectra on Attachment 1).

The described glycosydation reaction (Scheme 3) generates two main products, tri- and di-acetylated conjugates in variable global yields (44-89%) (Table 1). In fact, after glycosidation of a certain amount of **11** starts to deacetylate which leads to an incomplete reaction. By the NMR technique, it is simple to identify tri- and di-acetylated compounds, since the first one display three consecutive singlet signs at ~2.00 ppm on ^{1}H NMR spectrums and the di-acetylated just two. By comparison of the NMR spectra between **11** and the synthesised compounds it is possible to see that, in fact, the reaction occurred: at first, duplet signals in ^{13}C NMR spectrum of C1 disappeared and only

one signal appeared, as well as in ^{1}H spectrum, wherein the double duplet of H-1 became just a duplet and changed the displacement to a lower field. The other signals are very similar with the spectrum junction of the two precursors.

The final step of the conjugates synthesis requires deprotection of hydroxyl functions, in this case, carried out under standard sodium methoxide catalysis. This was a quite straightforward reaction, wherein high yields (85-97%) (Table 2) were achieved. ^{1}H and ^{13}C NMR spectra showed the disappearance of the signals of acetate groups, confirming the synthesis of the final compound.

All the new compounds (all the triacetylated and deacetylated final products (Figure 20), as well as the di-acetylated compound 12b, to serve as example) were fully characterized through NMR, mass spectroscopy, elemental analysis, and optical rotatory power, confirming the preparation of the pure desired compounds. Compound 20 was even analysed via X-ray diffraction.

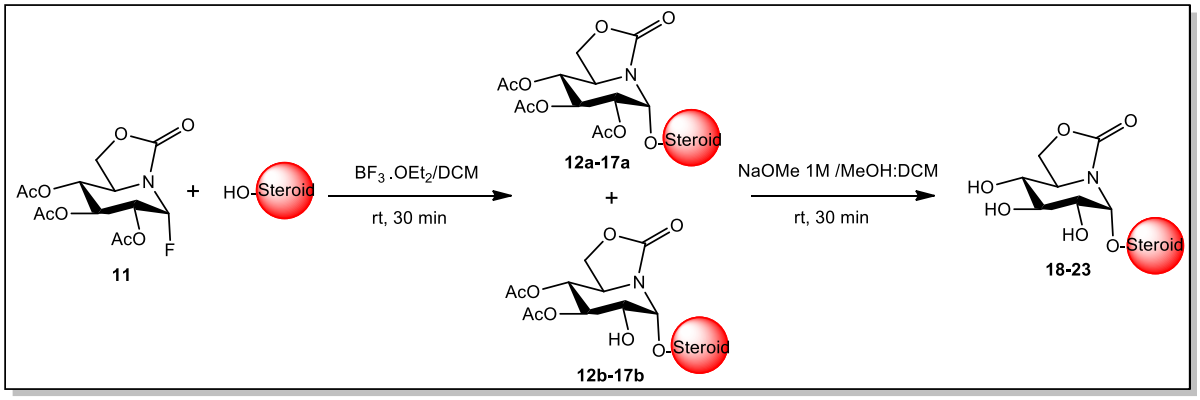

Scheme 3 | Preparation of the steroidal conjugates via glycosydation of fluoride derivative of 10.

Table 1 | Synthesis of acetylated sp^2-iminosugar-sterol conjugates: steroidal precursor, products and yields. Reactional conditions: BF_3 Et_2O/DCM, r.t., 30 min.

Steroid	Product	Yield %
Cholesterol	12a	57
	12b	11
Cholestanol	13a	22
	13b	22
Pregnenolone	14a	34
	14b	37
DHEA	15a	80
	15b	9
Stigmasterol	16a	56
	16b	16
Diosgenin	17a	19
	17b	42

Table 2 | Synthesis of sp^2-iminosugar-sterol conjugates (deacetylated final products): precursor, products, and yields. Reaction conditions: NaOMe 1M /1:1 MeOH-DCM, r.t. 30 min.

Substrate	Product	Yield %
12a+12b	18	97
13a+13b	19	93
14a+14b	20	96
15a+15b	21	96
16a+16b	22	92
17a+17b	23	85

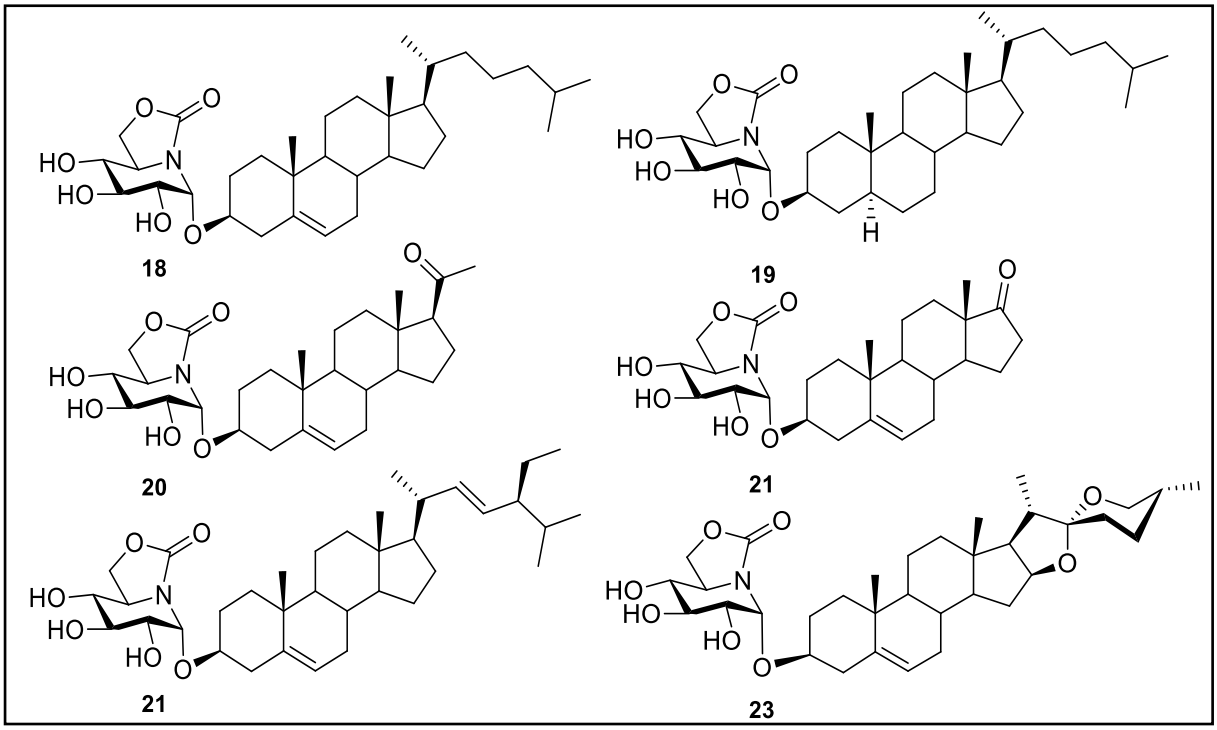

Figure 20 | Final products – steroidal conjugates (18-23).

3.2. X-ray Structural Analysis of compound 20

To best characterize the synthesised compounds, it was proceeded a X-ray structural analysis. Giving the similarity between all the compounds, just one compound was analysed through this method. To this end, it was necessary to obtain crystals of the compound with proper size. After selection of the crystals, X-rays diffraction was carried out, by impinging electromagnetic radiation (X-rays) on them, and collecting the information about the diffraction patterns observed. After, the data (table 3) is analysed and it is possible to determine, with precision, the structure of the compound.

The established complete structure and relative stereochemistry of 20 obtained by this method shows a huge similarity with the optimized drawn structure. In agreement with the expected and NMR experiments, this data confirm the *α*-configuration of the substituent at pseudoanomeric carbon of the iminosugar, and the ß-configuration of the substituent at C-3 of sterol moiety (Figure 21).

Through the analysis of the data it is possible to assume that are the hydrogen bonds between the iminosugar moieties of the compounds and water molecules that are responsible by the formation of the unit cell, as shown in figure 21. Therefore, this can be the major type of interactions able to maintain the crystal cohesion (For more data see attachment 2)

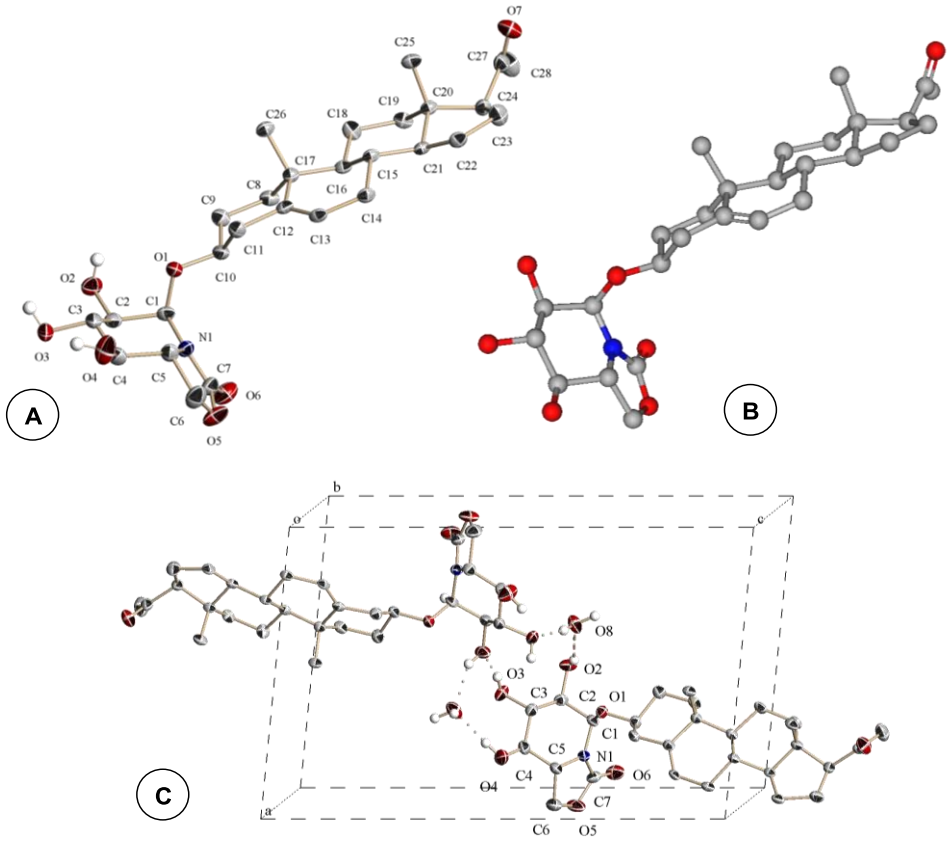

Figure 21 | A – Structure of 311 (different numbering system); B – Drawn structure of 311 (MarvinSpace 15.11.9.0); C – Interactions between molecules in a unit on crystalline structure. C-H···O interactions are represented by dotted lines.

Table 3 | Cristal data and structure refinement for **20**

Parameters	Data
Empirical formula	$C_{28}H_{43}NO_8$
Formula Weight	521.63
Temperature	193 (2) K
Wavelenght	0.71073 Å
Crystal System	Monoclinic
Space group	P 2_1
Unit Cells dimension	*a* = 11.9796(12) *Å* *a* = 90° *b* = 11.9796(12) *Å* *B* = 98.969(3)° *c* = 19.0244(16) *Å* γ = 90°
Volume	1334.0(2) $Å^3$
Z	2
Density (calculated)	1.299 Mg m^{-3}
Absorption coeficiente	0.094 mm^{-1}
F(000)	564
Crystal size	0.55 x 0.15.0.10 mm
Theta range for data collection	1.89 to 25.25°.
Index ranges	-14 ≤ h ≤ 14, -7 ≤ k ≤ 7, -22 ≤ l ≤ 22
Reflections collected	18791
Independent reflections	2573 [R(int) = 0.0356]
Completeness to theta = 25.25	96.8 %
Absorption correction	Semi-empirical from equivalents
Max. and min. transmission	0.9906 and 0.9633
Refinement method	Full-matrix least-squares on F2
Data / restraints / parameters	2573 / 4 / 347
Goodness-of-fit on F^2	1.150
Final R indices [I>2sigma(I)]	R1 = 0.0443, wR2 = 0.0980
R indices (all data)	R1 = 0.0474, wR2 = 0.0992
Largest diff. peak and hole	0.283 and -0.194 e.$Å^{-3}$

3.3. Glycosidase inhibition

After preparation of pure steroidal conjugates, the inhibitory activity was evaluated against a panel of commercial glycosidases (Table 4). In this is assay a solution of the compound is added to an enzyme solution in the optimal conditions. The activity was evaluated via spectrophotometric measurements. With this assay it is possible to achieve the inhibitory potential of the new steroidal conjugates as well as to analyse the effect of both sterol lateral chain and the presence/absence of the unsaturation at C5.

The new compounds exhibit specific selectivity to glucosidases, since no inhibition was observed for α- and ß- manosidases or α- and ß-galactosidases. The α- *versus* ß-glucosidase activity was significantly high, however the synthesised compounds show all potential to inhibit both enzymes, even in different extents, in these experimental conditions.

Compounds **20** and **21** are remarkably strong mixed inhibitors of neutral α-glucosidase, standing out the presence of a small lateral chain, presenting a hydrogen bond acceptor. All the other compounds showed competitive inhibition, with preference for α-glucosidase instead of ß-glucosidase, isomaltase, and amyloglucosidase, excluding compound 19, which displays more affinity for bovine liver ß-glucosidase. The difference between 18, a strong α-glucosidase inhibitor, and 19 relies only in the absence of the unsaturation in C5. It may be concluded that this structural difference on B ring of the steroid system is crucial for selectivity.

Lineweaver-Burk equation was the linearization method applied to treat enzymatic kinetic data and access K_i and K_i' for the compounds **20** e **21** against baker´s yeast α-glucosidase. Therefore, graphics 1 and 2 represent the steady state of α-glucosidase by compounds 20 and 21, ploting the initial velocity and substrate concentration in the presence of inhibitors (five concentrations) and their absence. Both graphics show mixed inhibition, being found two Ki values, of E-I binding (K_{ic}) and E-S-I binding (K_{iu}). It is possible to observe that both V_{max} and K_m change with 20/21 binding to *a*-glucosidase, consisting with mixed inhibition. Apparent V_{max} decreases with the inhibitor concentration increasing, showing that there is not only a binding site for the inhibitor exert its action, however, in the same time, apparent K_m increases with the concentration of the inhibitor, revealing that there is also a non-competitive component (Graphic 1 and 2).

The other compounds show strictly competitive inhibition mode. Nevertheless, mixed inhibition can slightly improve the inhibitory potency, since the compound can both compete with the substrate for the binding site, but can also bind allosterically and inhibit the enzyme, too.

Table 4 | Inhibitory activity: K_i values (μM) against a panel of glycosidases[a]

Enzymes	23	22	18	19	21	20
α-glucosidase (baker´s yeast)	91 ± 11	46 ± 6	19 ± 2	161 ± 20	1.3 ± 0.2[c] 4.9 ± 0.5[c]	0.7 ± 0.08[c] 6.0 ± 0.7[c]
isomaltase (baker´s yeast)	619 ± 55	487 ± 50	420 ± 45	285 ± 30	27 ± 3	79 ± 8
Amyloglucosidase (*Aspergillus niger*)	463 ± 49	647 ± 65	274 ± 30	353 ± 38	390 ± 42	730 ± 75
ß-glucosidase (almonds pH 7.3)	n.i.[b]	n.i.	n.i.	n.i.	n.i.	n.i.
ß-glucosidase (bovine liver)	196 ± 20	116 ± 12	170 ± 20	144 ± 15	90 ± 8	126 ± 15

[a]No inhibition was observed for any compound at 2 mM concentration on *Escherichia coli* ß-galactosidase, green coffee bean α-galactosidase, Jack bean α-mannosidase and *Helix pomatia* ß-mannosidase.

[b]n.i., no inhibition observed at 2 mM concentration of the inhibitor (K_i >1000 mM).

[c]Mixed type inhibition mode was observed, with inhibition constant for the E-I binding and E-S-I binding.

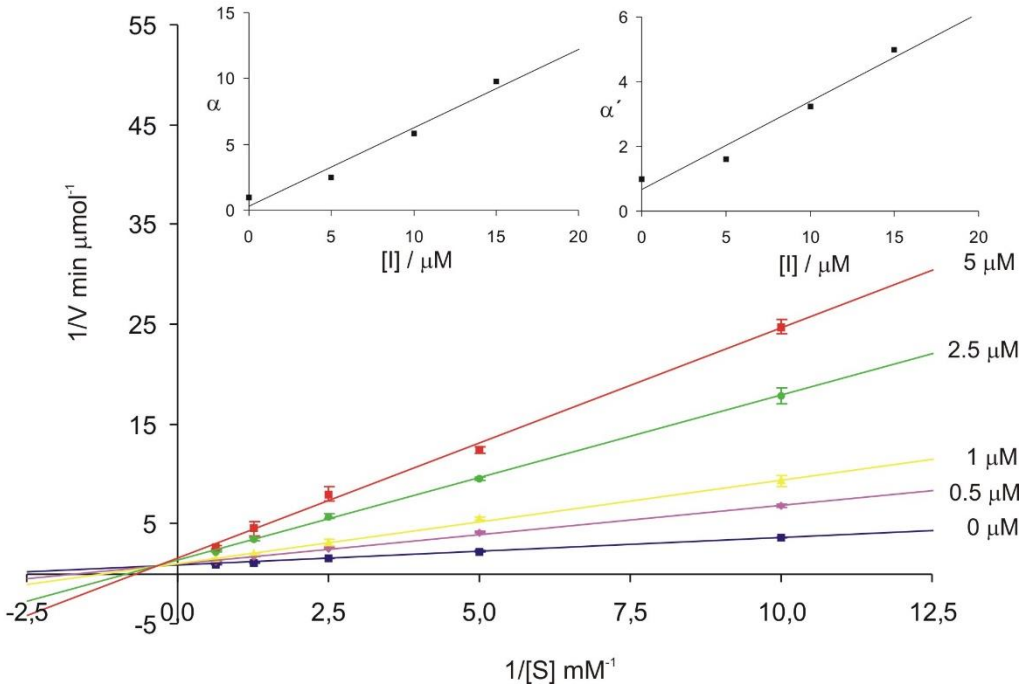

Graphic 1 | Lineweaver-Burk Plot for K_{ic} and K_{iu} determination (1.3 and 4.9 μM) of 20 against baker´s yeast α-glucosidase.

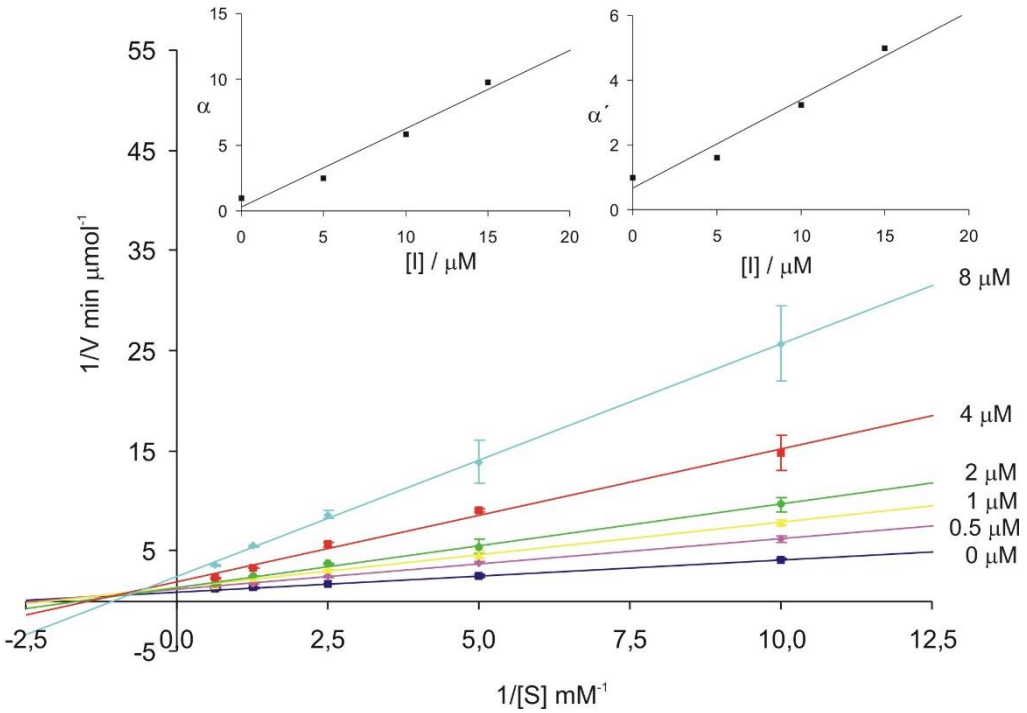

Graphic 2 | Lineweaver-Burk Plot for K_{ic} and K_{iu} determination (0.7 and 6.0 µM) of 21 against baker´s yeast α-glucosidase.

3.4. Anti-proliferative evaluation

The anti-proliferative evaluation was carried out through the MTT method, involving cell culture process, the subsequent cell treatment with the compounds and the MTT assay itself and posterior analysis. The biological evaluation through this method is a reliable procedure, being widely used[116].

The cell culture is affected by multifactorial issues, which means that cells maintenance, proliferation and death it is not so straightforward. The effect of the synthesised compounds was compared with the parent sterols and the sp^2-iminosugar **1**, as well as a positive control (5-fluorouracil – 5-FU), in cell lines of prostate (LNCaP) and breast (T-47D) cancer, and normal dermal skin cells (NHDF). These cell lines are widely used, and they are specially interesting in this study, once both cancer cell lines are steroidal hormone-dependent. It is also important to test compounds on healthy cells towards understanding the toxic effects, whereby it is also important use NHDF cells.

In this assay, the MTT molecule is reduced by succinate dehydrogenase in viable cells resulting in its water insoluble, purple formazane derivative. For this reason, the biosynthesis of formazan is considered proportional to the cell number, so the more intense purple colour, the greater the number of living cells. This intensity is then quantified spectrophotometrically[117].

At first, all the compounds were tested at two different concentrations (10 and 50 µM) as a preliminary assay in the three cell lines. Results are shown on the graphic 3. Throughout the analysis

it is possible to say that generally there is no added value in conjugate the employed sterols with **1** concerning their antiproliferative effect. In general, all the compounds show less antiproliferative effect than they precursors in the three cell lines, excluding the effect of iminosugar precursor **1,** which present almost no antiproliferative effect on the three cell lines, in these experimental conditions. Furthermore, at 10 μM only few synthesised compounds showed any significant antiproliferative effect, although some precursors such as cholesterol, cholestanol and stigmasterol show a strong effect at that concentration. Also, just diosgenin and its derivative **23** have showed prominent cytotoxic effects. For this reason, compound 23, along with diosgenin and the positive control 5-FU, was the only synthesised molecule which proceeds to concentration-response curve studies and subsequently to IC_{50} determination on the three cell lines.

This dissertation also presents the synthesis of the acetylated precursors (**12-17**) of the final products (**18-23**). In general, ester groups can be easily cleaved *in vivo*[118], and as these molecules display three different acetyl moieties, at this level, it is not possible to know how many groups rest in the molecule until it produces its effect. From this point of view, there is not a great interest to evaluate these molecules. Nonetheless we evaluated the acetylated compound **17a** to find out what is its influence in comparison with the sterol precursor (diosgenin) and its deacetylated derivative **23**. The results have shown that this compound show significantly less antiproliferative effect than the related compounds on the three cell lines.

By comparison of the effects on the three cell lines, it is possible to realize that all the compounds affect cell proliferation much less in non-cancer cell line NHDF than in prostate and breast cancer cells. This fact indicates that there is some selectivity, once it seems that the synthesised compounds show less toxicity to normal cells than to cancer cells. Also, there is similarity on the results of the two cancer cell lines.

Looking broadly to graphic 3, it is also noted that some compounds, mainly DHEA and pregnenolone, seem to stimulate the cell proliferation at low concentrations (10 μm). This is not so surprisingly, since this compounds are precursors of important essential hormones, even more on the hormone-dependent cancer cells[119]. At higher concentrations, it is already possible to see a reduction on cell proliferation.

Concentration-response curves of the positive control (5-Fu), diosgenin and diosgenin derivative **23** towards accessing IC_{50} values were performed on the three cell lines. Table 5 show IC_{50} values found in the study. As observed, compound 23 is less potent than 5-FU on the three cell lines. On T-47D cells, the IC_{50} of diosgenin was considerable lower than IC_{50} of compound 23, which present similar values, 12.84 and 13.03, for both cancer cell lines LNCaP and T-47D (respectively). Unfortunately, IC_{50} of compound 23 was lowest for healthy NHDF cells.

Regarding those results, it was proceeded to flow cytometry studies on LNCaP cells to verify the effect of compound **23** on cell viability, along with its precursor diosgenin and 5-FU.

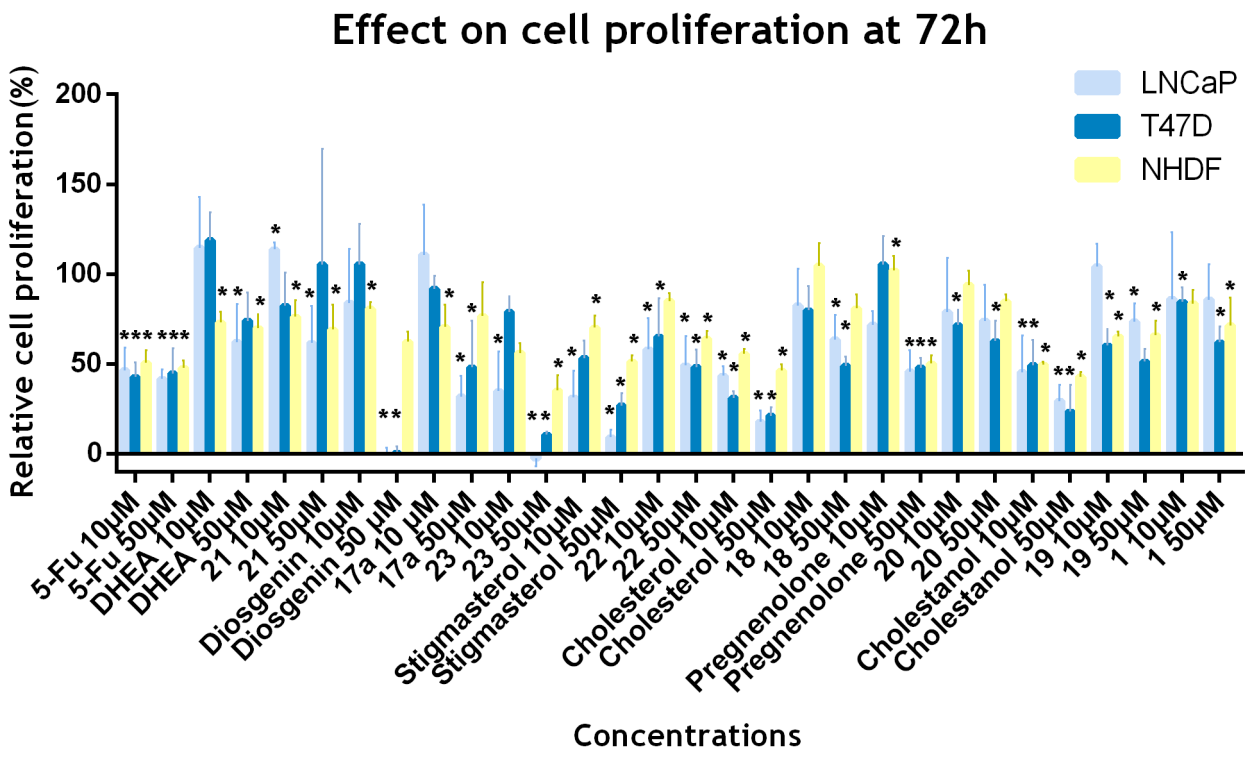

Graphic 3 | Results of preliminary studies of cell viability at two concentrations, 10 and 50 µM. The effect of all the synthesised final products 18-23 was evaluated a long with sterol and iminosugar precursors. * p< 0.5 in relation to a negative control (*t*-student test).

Table 5 – Half maximal proliferation inhibitory concentration activity (IC_{50}) values (µM) – 95% Confidence intervals.

Compound	LNCaP		T-47D		NHDF	
	IC_{50}	r^2	IC_{50}	r^2	IC_{50}	r^2
5-FU	1.50	0.99	0.70	0.99	0.11	0.85
Diosgenin	ND[a]	-	3.19	0.90	ND[a]	-
23	12.84	0.99	13.03	0.99	**4.39**	0.99

[a] – ND- Not defined

3.5. Flow Cytometry

Compound 23 was the only synthesised compound that revealed pronounced effects on cell proliferation. To analyse cell viability after treatment of compound 23 along with the precursor diosgenin and the positive control 5-FU, flow cytometry assays were performed on LNCaP cell line. On this method, propidium iodide (PI) was applied to identify death cells, since it is able to be permeate compromised cell membranes. This compound intercalates DNA and emit fluorescence proportional to DNA content of the cell[120].

Aiming the study of cells morphology, 24h and 72h after treatment with the compounds, photographs were taken to cells (Figure 22). On the negative control, cells without treatment, the area of cells are considerable higher at 24h than at 72h. In comparison with negative control, the number of cells which suffered treatment with 5-FU or compound 23 are evidently lower. Furthermore, cells morphology is clearly different, since treated cells present a rounded form unlike non treated cells. The difference between treated cells at 24h and 72h is also significant, since just few and rounded cells are present.

After all procedures, results of preliminary flow cytometry studies were analysed. Representative contour plots of FSC intensity versus PI intensity, displaying a view of the size of events against the fluorescence at 24h and 72h, are shown on figures 23 and 24, respectively. The events are subdivided in three different regions, R1, R2 and R3. In R1 population the events have, in general, great size and negative fluorescence, being considered viable cells. Generally, the R2 population present lower size and positive fluorescence. R3 possess intermediate size and fluorescence, being considered early apoptotic or oncotic cells, cell debris or autofluorescent cells[121]. Attending to the its considerable number of events, this area cannot be discarded. Events out of those three main areas were not considered in the analysis.

By the analysis of graphics 4 and 5, it is verified that after 24h hours there were not a great difference on mortality between treated and untreated cells. Besides the fact that at 72h there were less events at R1, the scenario changes and it is notorious the greater number of events at R3, the undefined zone.

Comparing positive control 5-FU with compound 23 results, they seem to have a comparable effect on morphology changes and mortality. At 72h, the cells treated with 5-FU present less alive cells (on R1), however the number of deaths (R2) and events in R3 is quite similar in cells treated with compound 23. However, these results coming from preliminary studies that should be refined. For example, 72h of treatment maybe is a too long period of exposition resulting on only debris and undefined events. Therefore, further studies are needed to better understand the behaviour of cells treated with the mentioned compounds.

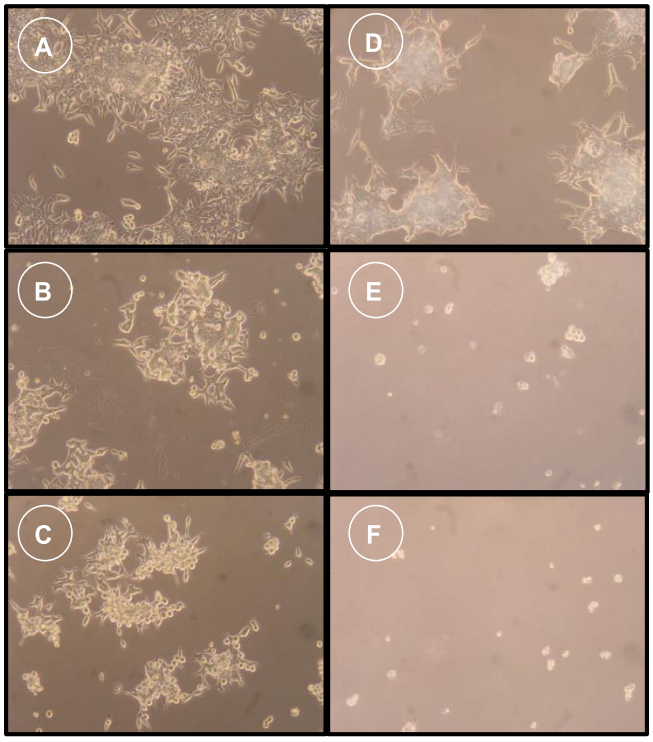

Figure 22 | Cells morphology after 24h (left –A,B,C) and 72h (right- D,E,F) of treatment. A and D – non treated cells (negative control); B and E – cells treated with 5-FU (positive control); C and F – cells treated with compound 23. Zoom: 100 X.

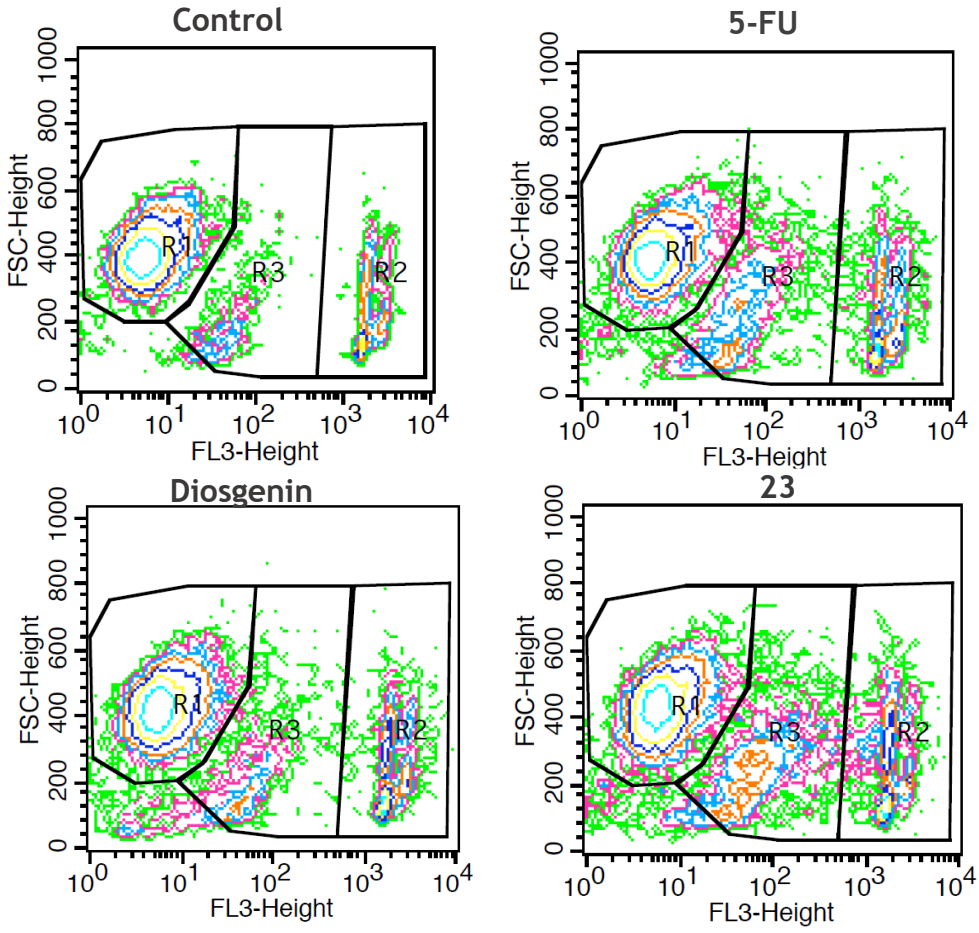

Figure 23 | Contour plots resulting from the analysis of the non-staining/ staining cells with PI (size of events versus intensity of fluorescence) 24h after cell treatment. R1- living cells; R2-death cells; R3- intermediate population.

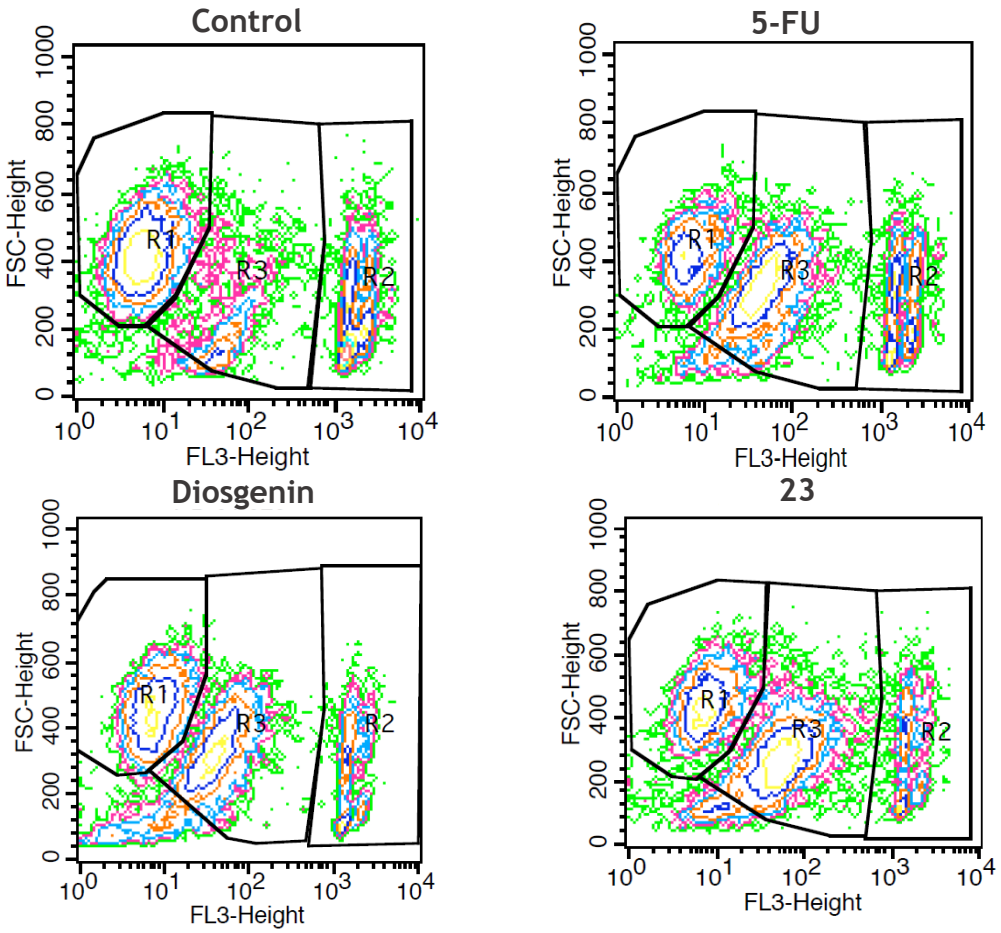

Figure 24 | Contour plots resulting from the analysis of the non-labelled/ labelled cells with PI (size of events versus intensity of fluorescence) 72h after cell treatment. R1- living cells; R2-death cells; R3- intermediate population.

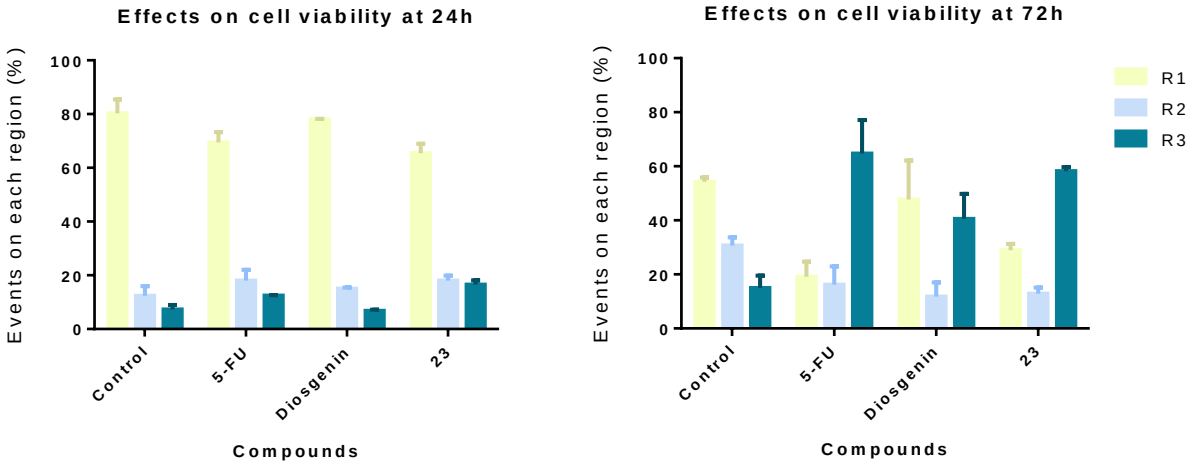

Graphic 4 and 5 | Graphics of the effects on cell viability at 24h (left) and 72h (right) - results for the three regions (R1, R2 and R3).

3.6. Molecular Docking

A molecular docking study was carried out to obtain information about a possible interaction between AcCHE and the synthesised steroidal conjugates. It was also considered to check the interactions between the mentioned compounds and the experimentally tested panel of glycosydases. However, of all the tested enzymes just few are in fact available on Protein Data Bank[122]. Moreover, the structure of human α-glucosidase is also not available, whereby an extrapolation of the results for the human real target would not be possible too.

At the beginning of the experience, it was proceeded to a method validation, which was performed using territrem B (**TB**), the ligand crystalized in complex with the protein, and by comparison with results obtained in the literature for tacrine[123], a well-known inhibitor of AcCHE, as well as other potential inhibitors (A-H)[123,124]. This ligand TB was docked and the resulting conformation was similar (mean RMSD = 1.94) with the crystalized ligand, and the interactions obtained are related with those ones found in the crystalized ligand-protein complex (Figure 25). Comparing results of eight inhibitors from the literature with the ones obtained here (not shown), it is possible to verify the similarity between the values. Those facts suggest that the method used is able to generate docking models that include the protein's local in analysis, being useful to give information about possible bindings with potential ligands.

Thereafter, the docking study was performed with the synthesized compounds. The results are presented on table 7. Giving the resemblance between all the compounds in study, it is not surprising that the results are very similar. Comparing the obtained values with the potent inhibitor TB[125], it is possible to say that there is potential in the synthesized compounds to inhibit AcCHE. Interactions between the compounds are also very similar to the ones involved on TB binding (Table 8). We should also note that there is high resemblance between the structures.

Although all the compounds present low binding energies, pharmacokinetic issues of each compound can change the results and produce very different effects *in vitro* and *in vivo*.

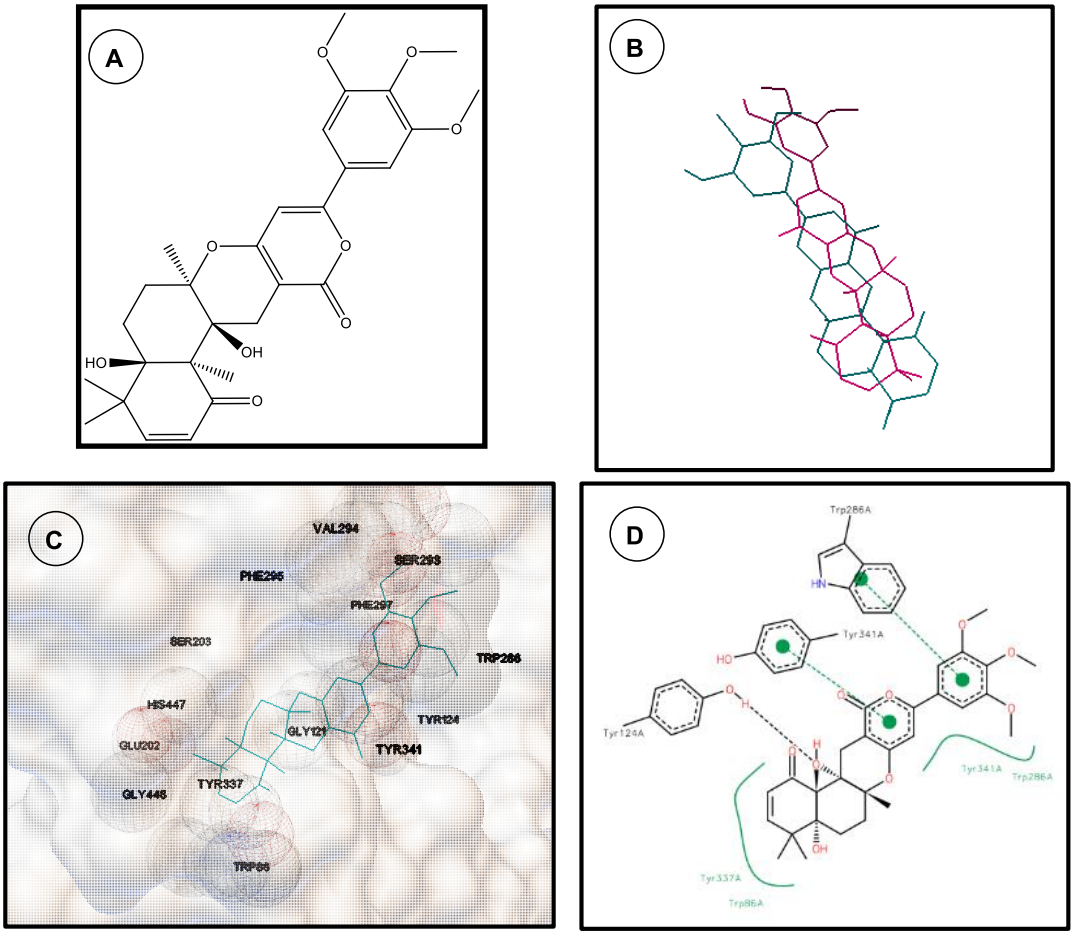

Figure 25 | Important structures for method validation: A- 2D structure of TB (drawn on Chem Draw pro 12.0 software); B- Overlap pf TB crystalized structure (pink) and resulting docking structure (blue); C- Docked TB structure interaction with AcCHE; D- Real main interactions between TB and AcCHE[125]; B and C obtained by docking analysis through AutoDock Tools 1.5.6 software.

Table 6 | Main molecular docking results of compounds 18-23.

Compound	Clusters	Binding Energy (BE)			Number of conf. in cluster
		Lowest	Run	Mean	
TB	1	**-14.04**	4	-13.55	49
	2	-12.82	6	-12.82	1
18	1	**-14.83**	48	-12.87	8
	2	-14.63	25	-13.17	13
	3	-13.09	23	-11.20	12
	4	-12.57	4	-11.80	6
	5	-12.50	19	-12.50	1
	6	-12.14	41	-11.55	4
	7	-10.98	39	-10.98	1
	8	-10.41	24	-10.28	2

	9	-10.34	37	-10.34	1
	10	-10.16	18	-10.16	1
	11	-9.20	34	-9.20	1
19	1	**-14.74**	24	-13.08	27
	2	-12.18	26	-11.21	8
	3	-11.80	42	-11.06	5
	4	-11.34	13	-9.86	7
	5	-10.52	20	-10.52	1
	6	-10.45	7	-10.45	1
	7	-8.44	6	-8.44	1
20	1	**-13.73**	6	-13.29	47
	2	-13.45	35	-13.45	1
	3	-12.98	25	-12.98	1
	4	-12.54	15	-12.54	1
21	1	**-12.64**	13	-12.41	38
	2	-12.38	30	-12.32	3
	3	-12.24	46	-12.15	6
	4	-12.90	16	-11.85	3
22	1	**-15.08**	22	-15.08	1
	2	-14.75	43	-12.62	8
	3	-14.23	4	-11.56	17
	4	-12.20	33	-12.00	4
	5	-11.73	2	-11.06	11
	6	-10.69	14	-9.83	7
	7	-10.64	36	-10.46	2
23	1	**-11.54**	37	-10.85	50

Table 7 | Resume of interactions between TB and synthesised compounds (18-23), and AcCHE.

Compound	Residues present in main interactions
TB	Arg296 – HB, GLU202, GLY120, GLY121, GLY448, HIS447, PHE297, PHE338, SER283, **TRP86, TRP286, TYR124**, **TYR337**, **TYR341**, VAL294;
18	ARG296-HB, GLU202, GLY120, GLY121, GLY126, GLY448, HIS447, PHE297, PHE338, SER293, **TRP86, TRP286, TYR124**, TYR133, **TYR337**;
19	ASP74, GLU202, GLY120, GLY126, HIS447, LEU130, PHE297, PHE338, SER203, **TRP86, TRP286,** TYR72-HB**, TYR124**, TYR133**, TYR337, TYR341;**
20	ARG296-HB, GLU202, GLY121, GLY448, HIS447, ILE451, PHE295-HB, PHE297, PHE338, SER293, **TRP86, TRP286**, **TYR124**, TYR133, **TYR337**, **TYR341**, VAL294;
21	ASP74, GLU202, HYS447, PHE297, PHE338, SER203, **TRP86, TRP286**, TYR72-HB, **TYR337**, **TYR341**;
22	ARG296, GLU202, GLY120, GLY121, GLY126, PHE295, PHE297, PHE338, SER125, SER293, **TRP86, TRP286**, **TYR124**, TYR133, **TYR341**, VAL294;
23	GLU202, GLY120, GLY126, GLY448, HIS447, LEU76, PHE297, PHE338, SER125, **TRP86, TRP286**, **TYR124**, TYR133-HB, **TYR341.**

4. Conclusion and future perspectives

In summary, in this work it was performed to the synthesis of six new sp^2-iminosugar-steroid conjugates, their evaluation as glycosidase inhibitors and as antiproliferative agents. The effect on cell viability was also quantified by flow cytometry. Moreover, *in silico* molecular docking was performed fitting the described compounds on active centre of AcCHE.

Specifically, several new steroidal- sp^2-nojirimycin derivative conjugates were successfully prepared, although in variable yields. Beside the differences in the natural reactivity of the different steroids, it could be interesting to optimize the synthesis procedure to obtain improved yields. By means of an analysis via X-ray diffraction it was possible to confirm the exact structure of the molecules as well as how their spatial disposition and the interactions in the crystal.

The compounds were evaluated as potential glycosidase inhibitors, revealing greater selectivity and potency to inhibit α-glucosidase enzymes, especially compounds **20** and **21**, acting by mixed inhibition. In this assay it was concluded that a carbonyl group on steroidal lateral chain can be important for the activity, as well as the double bond at C-5. In the future, it can be important to use human glycosidases, to further improve the biological interest of these compounds in this context.

The evaluation of the antiproliferative effect of the synthesised compounds through the MTT assay, it was found out that compound 23 show prominent antiproliferative effect as well as its precursor diosgenin. In addition, there is no added value in the conjugation of the sterols with the sp^2-iminosugar **1**, in cell proliferation effects. Also, these assays revealed that it seems to exist some selectivity towards cancer cells in comparison with healthy cells. Flow cytometry studies on LNCaP cells, with untreated and treated cells (with 5-FU, diosgenin and compound 23), revealed that at 24h the presence of the different compounds did not affect significantly the cell viability. However, at 72h, the effects on viability are more pronounced and compound 23 seems to act similarly with 5-FU. In this context, it will be important carry out cell cycle studies and investigate if there are similarity on their mode of action.

Molecular docking studies were performed to predict the binding energies between the synthesised compounds and active site of AcCHE, which revealed that there is potential in these compounds as AcCHE inhibitors, comparing with a well-known inhibitor. Therefore, in the future, these compounds will be experimentally evaluated as AcCHE inhibitors, looking for dual inhibitors of both α-glucosidase and AcCHE inhibitors with high potential therapeutic interest.

As it was observed, the synthesised steroidal conjugates have demonstrated high potential as bioactive compounds, being of interest further synthesis of similar conjugates of this or other series and after their biological evaluation, as well as investigate other potential biological targets, by *in silico* and experimental methods. In fact, the conjugation of bioactive compounds with steroids can

promote changes at properties such as molecular weight and hydrophilicity/hydrophobicity which can affect dramatically their pharmacokinetic and efficacy profile.

5. Experimental Section

5.1. Synthesis

5.1.1. General Data

All the reagents and solvents purchased from commercial sources were used without further purification.

Thin-layer chromatography (TLC) was carried out on aluminium coated with Silica Gel 60 F254 Merck (0.25 mm), with visualization by UV light (λ = 254 nm) and by carrying with 10% H_2SO_4 in ethanol; 0.1% ninhydrin in ethanol; 0.2% w/v cerium(IV) sulphate-5% ammonium molybdate in 2 M H_2SO_4 and heating at 100 ºC. Column chromatography was performed on Chromagel (SDS silice 60 A.C.C 35-70 µm). Optical rotations were measured at 20 ± 2 ºC in 1 cm or 1 dm tubes on a Jasco P-2000 polarimeter using Na D line (λ 589 nm), 0.2-1% (w/v) solutions and 1 cm cells. Elemental analyses were performed on elemental analyser Leco CHNS-932 or Leco TruSpec CHN. ^{1}H and ^{13}C NMR spectra were recorded at 300 (75.5) MHz, 400 (100.6) MHz and 500 (125.7) MHz with, respectively, Bruker AVANCE 300, Bruker AVANCE 400 and Bruker AVANCE DRX 500 spectometers. 2D COSY (Correlated Spectroscopy), ^{1}H-^{13}C HSQC (Heteronuclear Single Quantum Coherence experiment) experiments were used to assist on NMR assignments. $CDCl_3$, CD_3OD and DMSO-d_6 have been used as solvents. ESI mass spectra were recorded in the positive mode on an Esquire 300 ion-trap mass spectrometer (Bruker Daltonik GmbH). Typically, samples were dissolved in appropriate volumes of MeOH and MeCN to give sample concentrations of 50 mg/L. Aliquots were mixed with 25:25:1 deionised water-methanol-trifluoroacetic acid, generally in a ratio of 1:10, to give a total volume of 200 µl. Samples were introduced by direct infusion, using a Cole-Parmer syringe at a flow rate of 2 µl/min. Ions were scanned between 300 and 3000 Da with a scan speed of 13000 Da/s at unit resolution using resonance ejection at the multipole resonance of one-third of the radio frequency (Ω = 781.25 kHz). Calibration of the mass spectrometer was performed using Electrospray ionization (ESI) tuning mix (Hewlett Packard). Recorded data were processed using Bruker Daltonics Esquire 5.0 software (Bruker).

5.1.2. Synthesis of starting materials

The starting materials 1,2,3,4–Tetra-*O*-acetyl-5*N*,6*O*-oxometylidenenojirimycin **10**[31] and (1*R*)-2,3,4-Tri-*O*-acetyl-1-fluoro-5*N*,6*O*-oxometylidenenojirimycin **11**[23] were prepared as described previously.

5-Cloro-5-deoxy-1,2-*O*-isopropylidene-ß-L-idofuranurono-6,3-lactone (3):

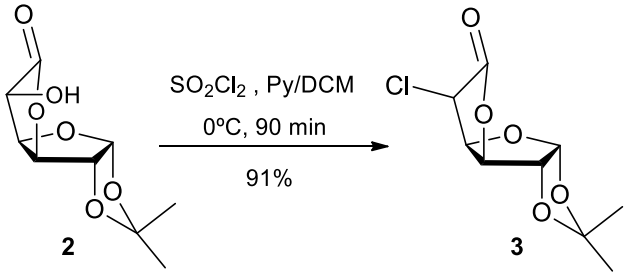

Scheme 4 | Preparation of 3 from 2. Yield:91%

To a solution of 1,2-*O*-isopropylidene-α-D-glucofuranurono-6,3-lactone **2** (3.00 g, 14.06 mmol) in DCM (46 mL) and pyridine (4.55 mL) at 0 ºC, sulphuryl chloride (1.7 mL, 0.6 eq) was added dropwise. The reaction mixture was stirred at 0 ºC for 90 min (TLC monitoring). Then, the mixture was diluted with DCM (20 mL), washed with aqueous HCl 5% (2 x 20 mL) and saturated aqueous solution of $NaHCO_3$ (20 mL). The organic layer was dried ($MgSO_4$), filtered and concentrated. The residue was purified by column chromatography (1:1 EtOAc/Cyclohexane) to afford the corresponding chloro-derivative **3**. Yield: 3.74 g (91%). Rf 0.82 (1:1 EtOAc/Cyclohexane).

5-Cloro-5-deoxy-1,2-*O*-isopropylidene-ß-L-idofuranose (4):

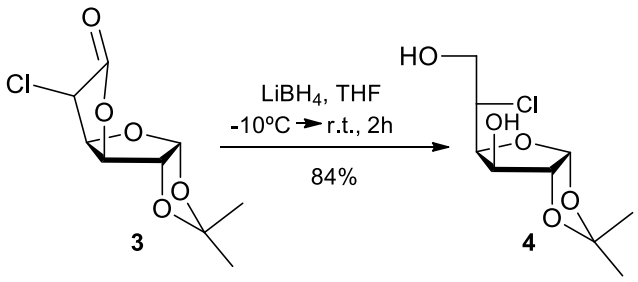

Scheme 5 | Preparation of 4 from 3. Yield:84%.

To a solution of 5-cloro-5-deoxy-1,2-*O*-isopropylidene-ß-L-idofuranurono-6,3-lactone **3** (2.99 g, 12.76 mmol) in anhydrous THF (24 mL) at -10 ºC, $LiBH_4$ in THF 2 M (3,8 mL, 0.6 eq) was added dropwise. The reaction mixture was stirred at -10 ºC for 2 h and allowed to reach r.t. for 2 h more (TLC monitoring). The excess of $LiBH_4$ was deactivated by adding water slowly until no reaction was observed. Then, the reaction was neutralized with Amberlite IRA 120 H+ ion exchange resin, stirred for 10-15 min (pH 6), filtered, concentrated and coevaporated several times with MeOH (3 x 20 mL). The residue was purified by column chromatography (1:2→2:1 EtOAc/Cyclohexane) to give **4**. Yield: 2.55 g (84%). Rf 0.44 (2:1 EtOAc-Cyclohexane).

5-Cloro-5-deoxy-1,2-*O*-isopropylidene-6-O-tetrahydropyranyl-ß-L-idofuranose (5):

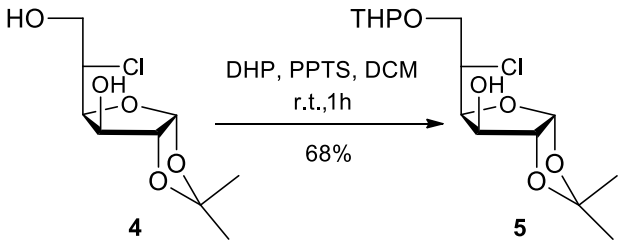

Scheme 6 | Preparation of 5 from 4. Yield:68%.

3,4-Dihydro-2*H*-pyran (1.3 mL, 13.91 mmol, 1.3 eq) and pyridinium *p*-toluenesulfonate (2.55 g, 10.70 mmol, 1.0 eq) were added to a solution of 5-cloro-5-deoxy-1,2-*O*-isopropylidene-ß-L-idofuranose **4** (2.55 g, 10.70 mmol) in DCM (40 mL). The reaction mixture was stirred at r.t. for 17 h, diluted in DCM (30 mL), washed with saturated aqueous solution of $NaHCO_3$ (30 mL), dried ($MgSO_4$), and concentrated. The resulting residue was purified by column chromatography (1:3→1:1 EtOAc:Cyclohexane) to afford the tetrahydropyranyl derivative **5**. Yield: 2.35 g (68%). Rf 0.26 (1:1 EtOAc-Cyclohexane).

5-Azido-5-deoxy-1,2-*O*-isopropylidene-6-*O*-tetrahydropyranyl-α-D-glucofuranose (6):

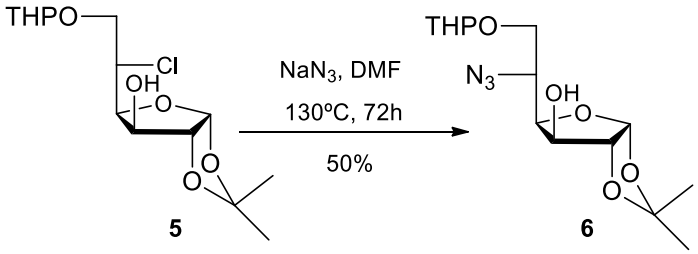

Scheme 7 | Preparation of 6 from 5. Yield:50%

NaN_3 (2.01 g, 30.87 mmol, 4.5) dried over P_2O_5 was added to a stirred solution of the corresponding chloride-derivative **5** (2.21 g, 6.86 mmol, 1.0 equiv.) in dry DMF (33 mL) at 90 ºC. The reaction mixture was stirred at 130 ºC for 3 days (TLC monitoring) and concentrated. The residue was dissolved in DCM (50 mL) and washed with water (2 x 20 mL). The aqueous layer was extracted with DCM (2 x 15 mL). The organic layer was dried ($MgSO_4$), filtered and concentrated. The residue was purified by column chromatography (1:4→1:3 EtOAc:Cyclohexane) to give the azido-derivative **6**. Yield: 1.13 g (50%). Rf 0.68 (1:1 EtOAc-Cyclohexane).

5-Azido-5-deoxy-1,2-*O*-isopropylidene-α-D-glucofuranose (7):

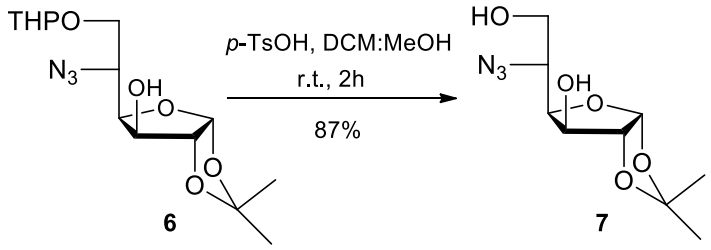

Scheme 8 | Preparation of 7 from 6. Yield:87%

To a solution of 5-azido-5-deoxy-1,2-*O*-isopropylidene-6-*O*-tetrahydropyranyl-α-D-glucofuranose **6** (1.13 g, 3.43 mmol, 1.0 equiv.) in DCM:MeOH (50 mL, 1:1), p-toluenesulfonic acid (131.25 mg, 0.69 mmol, 0.2 equiv.) was added. The reaction mixture was stirred at r.t. for 2 h (TLC monitoring), diluted with DCM (75 mL) and washed with saturated aqueous solution of $NaHCO_3$ (2 x 10 mL). The aqueous layer was extracted with EtOAc (2 x 50 mL) and the organic layer dried ($MgSO_4$) and concentrated. Yield: 731 mg (87%). Rf 0.40 (1:1 EtOAc/Cyclohexane).

5-Amino-5-deoxy-1,2-*O*-isopropylidene-α-D-glucofuranose (8):

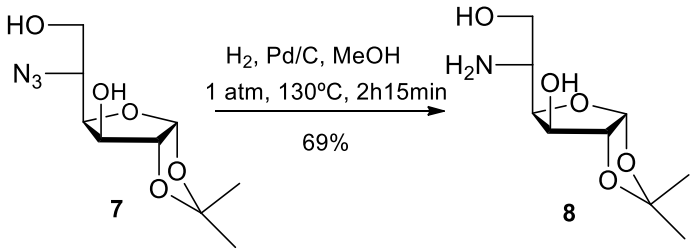

Scheme 9 | Preparation of 8 from 7. Yield:69%

A solution of 5-azido-5-deoxy-1,2-*O*-isopropylidene-α-D-glucofuranose **7** (731 mg, 2.98 mmol) and Pd/C (300 mg) in MeOH (10 mL) was hydrogenated under an atmospheric pressure of hydrogen. The suspension was stirred for 2h at r.t., filtered through a pad of celite and concentrated to give the corresponding amine **8**, which was used in the next step without further purification. Yield: 451 mg (69%).

5-Amino-5-deoxy-1,2-*O*-isopropylidene-α-D-glucofuranose-5,6-(Cyclic carbamate) (9):

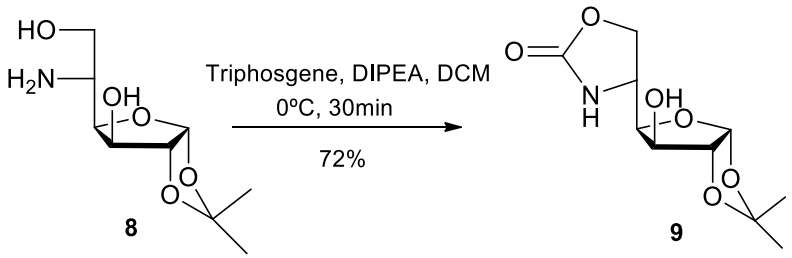

Scheme 10 | Preparation of 9 from 8. Yield:72%

To a stirred solution of the amine **8** (451 mg, 2.06 mmol, 1.0 equiv.) in DCM (50 mL) at 0 ºC, diisopropylethylamine (DIPEA, 3.4 mL, 20.60 mmol, 10.0 equiv.) and triphosgene (0,917 g, 3.09 mmol, 1.5 equiv.) were added. After 30 min, the solvent was removed under reduced pressure, and the residue was purified by column chromatography (EtOAc →1:10 EtOH:EtOAc). Yield: 363 mg (72%).

(1*R*)-5*N*,6*O*-oxomethylidenenojirimycin (1):

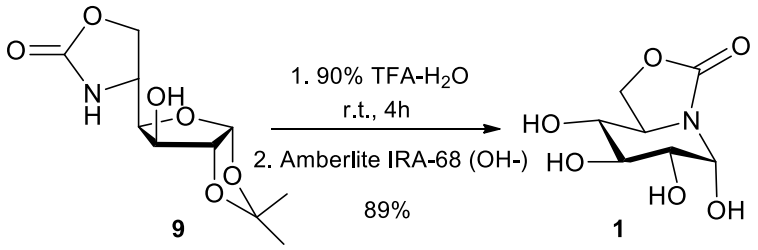

Scheme 11 | Preparation of 1 from 9. Yield:89%

The cyclic carbamate **9** (363 mg, 1.48 mmol) was treated with 90% TFA/water (3,6 mL) at r.t. for 4h (TLC monitoring). The reaction mixture was concentrated and the residue coevaporated several times with water to remove traces of acid. The resulting residue was purified by column chromatography using 40:10:1 DCM/MeOH/H_2O as eluent to give 1. Yield: 270 mg (89%).

^{1}H NMR (400 MHz, D_2O) δ 5.41 (d, $J_{1,2}$ = 4.0 Hz, 1H; H-1), 4.66 (t, $J_{6a,6b}$ = $J_{5,6a}$ = 8.8 Hz, 1H; H-6a), 4.35 (dd, $J_{5,6b}$ = 6.8 Hz, 1H; H-6b), 4.00 (ddd, $J_{4,5}$ = 9.5 Hz, 1H; H-5), 3.74 (t, $J_{3,4}$ = $J_{2,3}$ = 9.4 Hz, 1H; H-3), 3.62 (dd, 1H; H-2), 3.57 (t, 1H; H-4).

^{13}C NMR (100.6 MHz, D_2O) δ 157.7 (CO), 74.5 (C-1), 73.5 (C-4), 72.3 (C-3), 71.1 (C-2), 67.6 (C-6), 53.1 (C-5).

(1*R*)-1,2,3,4-Tetra-O-acetyl-5*N*,6*O*-oxomethylidenenojirimycin (10):

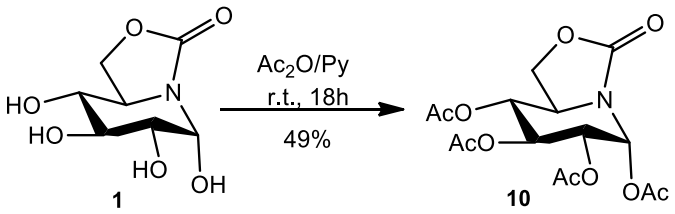

Scheme 12 | Preparation of 10 from 1. Yield:49%.

Acetylation was carried out by dissolving the sp^2-iminosugar **9** (270 mg, 1.32 mmol) in Ac_2O-Py (1:1, 2,7 mL) at 0 ºC. The reaction mixture was stirred at rt for 18 h (TLC monitoring), then poured into water/ice and extracted with DCM. The organic layer was washed with 1N HCl and saturated aqueous solution of $NaHCO_3$, dried ($MgSO_4$) and concentrated. The resulting residue was purified by column chromatography (1:2 EtOAc-Cyclohexane) to give the peracetylated compound **10**. Yield: 242 mg (49%).

^{1}H NMR (300 MHz, CDC_{l3}) δ 6.70 (d, $J_{1,2}$ = 4.0 Hz, 1H; H-1), 5.48 (t, $J_{3,4}$ = $J_{2,3}$ = 10.0 Hz, 1H; H-3), 5.08 (dd, 1 H, H-2), 4.96 (t, $J_{4,5}$ = 10.0 Hz, 1H; H-4), 4.43 (dd, $J_{6a,6b}$ = 9.3 Hz, $J_{5,6b}$ = 8.0 Hz, 1H; H-6a), 4.26 (dd, $J_{5,6b}$ = 8.0 Hz, 1H; H-6b), 4.03 (dt, 1H; H-5), 2.12-1.98 (4 s, 12 H, MeCO).

^{13}C NMR (75.5 MHz, $CDCl_3$) δ 169.9-168.5 (MeCO), 154.1 (CO), 72.3 (C-1), 72.3 (C-4), 69.0 (C-2), 68.9 (C-3), 66.9 (C-6), 52.7 (C-5), 20.6-20.3 (*Me*CO).

(1*R*)-1-Fluoro-2,3,4-Tri-O-acetyl-5*N*,6*O*-oxomethylidenenojirimycin (11):

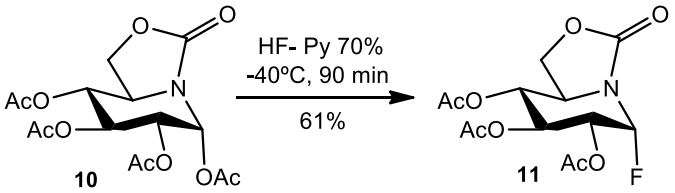

Scheme 13 | Preparation of 11 from 10. Yield:61%

Compound 10 (242 mg, 0.65 mmol) was placed in a polyethylene vessel, cooled at -40ºC and treated with poly(hydrogen fluoride)pyridinium complex (70% HF,1.2 mL, 2.8M). The reaction mixture was stirred at that temperature for 90min (TLC monitoring), diluted with Et_2O (30 mL), washed with saturated aqueous KF (15 mL) and extracted with Et_2O (3 X 30 mL). The organic layer was washed with saturated solution of $NaHCO_3$, (10 mL) dried ($MgSO_4$) and concentrated. The resulting residue was purified by column chromatography (1:2 EtOAc-Cyclohexane) to afford compound 11. Yield: 132 mg (61%).

^{1}H NMR (500 MHz, $CDCl_3$) δ= 6.17 (dd, $J_{1,F}$ = 52.5 Hz, $J_{5,6}$ = 3.5 Hz, 1H; H-1), 5.60 (t, $J_{2,3}$ = $J_{3,4}$ = 10.0 Hz, 1H; H-3), 5.00 (ddd, $J_{2,F}$ = 14.0 Hz, 1H; H-2), 4.99 (t, $J_{4,5a}$ = 10.0 Hz, 1H; H-4), 4.51 (dd, $J_{6a,6b}$ = 9.0 Hz, $J_{6a,5}$ = 8.0 Hz, 1H; H-6a), 4.32 (t, $J_{6b,5}$ = 9.0 Hz, 1H; H-6b), 4.17-4.09 (m, 1H; H-5), 2.15-2.09 (3 s, 9H; MeCO).

^{13}C NMR (125.7 MHz, $CDCl_3$) δ= 170.0-169.5 (MeCO), 154.2 (CO), 87.5 (d, $J_{C5,F}$ = 211.6 Hz, 1C; C-1), 72.0 (C-4), 69.8 (d, $J_{C6,F}$ = 24.8 Hz, 1C; C-2,), 68.6 (C-3), 67.2 (C-6), 52.0 (C-5), 20.4 (MeCO).

5.1.3. General procedure for preparation of conjugates of triacetylated nojirimicyn derivatives and sterols

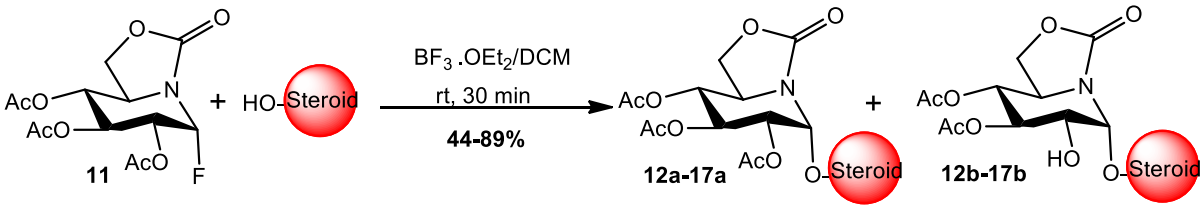

Scheme 14 | Preparation of 12a-17b from 11 and a commercial sterol. Yields: 44-89%

BF_3. Et_2O (0.5 eq., 15.2 µL, 0.12 mmol) was added to a stirred solution of 11 (1eq, 8 0.24 mmol) and the sterol (1 eq., 0.24 mmol) in anhydrous DCM (2.6 mL) at room temperature under Ar atmosphere. After consumption of substrate (30 min) (TLC monitoring), the mixture was concentrated under reduce pressure. The resulting residue was purified by column chromatography to give two products: the triacetylated and its corresponding 3,4-diacetylated compound in variable quantities. Triacetylated compounds were fully characterized, diacetylated compounds were not characterized with the exception of compound 12b.

3β-O-(2',3',4'-Tri-*O*-acetyl-5'*N*,6'*O*-oxometylidenenojirimycin-1'-yl)-cholest-5-ene (12a)

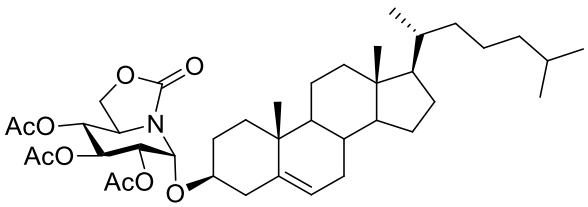

Figure 26 | Structure of 12a.

Sterol: Cholesterol. Column chromatography EtOAc/Cyclohexane, (1:4) → (1:3); Yield: 95.4 mg (57%). amorphous solid; R_f= 0.49 (2:1 AcOEt/Cyclohexane); $[\alpha]_D$= +46.6 (c=0.7 in DCM).

^{1}H NMR (300 MHz, $CDCl_3$): δ= 5.54 (t, $J_{2',3'}$= $J_{3',4'}$= 9.6 Hz, 1H; H-3'), 5.5 (d, $J_{1',2'}$= 3.6 Hz, 1H; H-1'), 5.31 (d, $J_{6,7}$= 5.1 Hz, 1H; H-6), 4.92 (t, $J_{4',5'}$= 9.6 Hz, 1H; H-4'), 4.79 (dd, 1H; H-2'), 4.43 (t, $J_{5',6a'}$= $J_{6b',6a'}$= 8.7 Hz 1H; H-6a'), 4.23 (dd, $J_{5,6b'}$= 7.2 Hz 1H; H-6b'), 4.00 (ddd,1H; H-5'), 3.37-3.32 (m, 1H; H-3), 2.07–2.02 (3s, 9H; MeCO), 0.98 (s, 3H; H-18), 0,89 (d, $J_{21,20}$= 6.3 Hz 3H; H-21), 0.84 (dd, $J_{26/27,25}$=6.6, $J_{26,27}$= 1.2 6H; H-26,27), 0.66 ppm (s, 3H; H-19).

^{13}C NMR (75.5 MHz, $CDCl_3$): δ= 170.0-169.8 (MeCO), 155.4 (CO), 140.0 (C-5), 122.3 (C-6), 77.9 (C-3), 76.4 (C-1'), 72.9 (C-4'), 70.7 (C-2'), 69.3 (C-3'), 66.6 (C-6'), 56.7, 56.1, 51.7 (C-5'), 50.0, 42.3, 39.8, 39.7, 39.5, 36.8, 36.6, 36.2, 35.8, 31.2, 28.2, 28.0, 27.4, 24.3, 23.8, 22.8-22.5 (2C; C-26,C-27), 21.0, 20.6-20.5 (*Me*CO),19.4 (C-19), 18.7 (C-21), 11.8 ppm (C-18).

ESIMS: m/z 722.5 $[M + Na]^+$.

HRMS: Calculated for $C_{40}H_{61}NO_9Na$: 722.4239, found 722.4217.

3β -O-(3',4'-Di-*O*-acetyl-5'*N*,6'*O*-oxometylidenenojirimycin-1'-yl)-cholest-5-ene (12b)

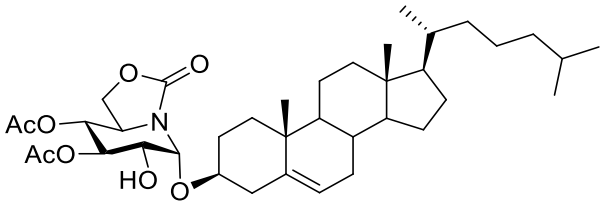

Figure 27 | Structure of 12b.

Sterol: Cholesterol. Column chromatography EtOAc/Cyclohexane, (1:4) → (1:3); Yield: 17.3 mg (11%) amorphous solid; R_f= 0.36 (2:1 AcOEt/Cyclohexane); $[\alpha]_D$= +57.8 (c=0.7 in DCM).

^{1}H NMR (300 MHz, $CDCl_3$): δ= 5.34 (d, $J_{1',2'}$= 4.2 Hz, $J_{6',7'}$= 4.2 Hz, 2H; H-1',H-6), 5.26 (t, $J_{2',3'}$= $J_{3',4'}$= 9.6 Hz, 1H; H-3'), 4.89 (t, $J_{4',5'}$= 9.6 Hz, 1H; H-4'), 4.43 (t, $J_{5',6a'}$= $J_{6b',6a'}$= 8.7 Hz 1H; H-6a'), 4.24 (dd, $J_{5,6b'}$= 6.6 Hz 1H; H-6b'), 3.95 (ddd,1H; H-5'), 3.67-3.59 (m, 1H; H-2'), 3.50-3.41 (m, 1H; H-3), 2.09–2.05 (2s, 6H; MeCO), 0.99 (s, 3H; H-19), 0,90 (d, $J_{21,20}$= 6.3 3H; H-21), 0.85 (dd, $J_{25,26}$ =6.6, $J_{26,27}$= 1.2 Hz 6H; H-26,27), 0.66 ppm (s, 3H; H-18).

^{13}C NMR (75.5 MHz, $CDCl_3$): δ= 170.8-170.1 (MeCO), 155.7 (CO), 139.8 (C-5), 122.5 (C-6), 78.5 (C-1'), 77.9 (C-3), 72.3 (2C; C-3', C-4'), 70.5 (C-2'), 66.5 (C-6'), 56.7, 56.1, 51.9 (C-5'), 50.0, 42.3, 39.9, 39.7, 39.5, 36.8, 36.6, 36.2, 35.8, 31.9, 31.8, 28.2, 28.0, 27.6, 24.3, 23.8, 22.8-22.6 (2C; C-26,C-27), 21.0, 20.8-20.6 (*Me*CO),19.4 (C-19), 18.7 (C-21), 11.9 ppm (C-18).

ESIMS: m/z 680.6 $[M + Na]^+$. Anal.Calc for $C_{38}H_{59}NO_8$: C, 69.38; H, 9.04; N, 2.13. Found: C, 69.53; H, 9.21; N, 1.90.

3β -O-(2',3',4'-Tri-*O*-acetyl-5'*N*,6'*O*-oxometylidenenojirimycin-1'-yl)-5α-cholestane (13a)

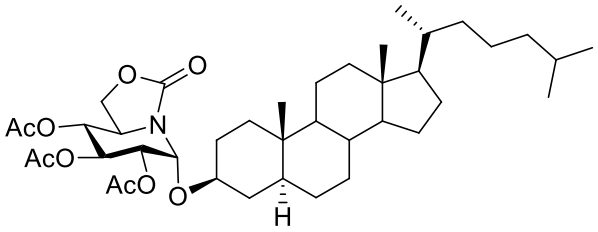

Figure 28 | Structure of 13a.

Sterol: Cholestanol. Column chromatography EtOAc/Cyclohexane, (1:3); Yield: 24.3 (22%) amorphous solid; R_f=0.45 (1:2 AcOEt/Cyclohexane); $[\alpha]_D$= 63.2 (c=0.7 in DCM).

^{1}H NMR (300 MHz, $CDCl_3$): δ= 5.536 (t, $J_{2',3'}$= $J_{3',4'}$= 9.9 Hz, 1H; H-3'), 5.50 (d, $J_{1',2'}$= 4.2 Hz, 1H; H-1'), 4.91 (t, $J_{4',5'}$= 9.9 Hz, 1H; H-4'), 4.78 (dd, 1H; H-2'), 4.42 (t, $J_{5',6a'}$= $J_{6b',6a'}$= 8.1 Hz 1H; H-6a'), 4.23 (t, $J_{5,6b'}$= 8.1 Hz 1H; H-6b'), 4.00 (q,1H; H-5'), 3.40-3.1 (m, 1H; H-3), 2.07–2.02 (3s, 9H; MeCO), 0,89 (d, $J_{21,20}$= 6.6 Hz, 3H; H-21), 0.85 (dd, $J_{26/27,25}$=6.6, $J_{26,27}$= 1.2 6H; H-26,27), 0.79 (s, 3H; H-18), 0.63 ppm (s, 3H; H-19).

^{13}C NMR (75.5 MHz, $CDCl_3$): δ= 170.1-169.7 (MeCO), 155.5 (CO), 78.0 (C-3), 76.8 (C-1'), 72.9 (C-4'), 70.7 (C-2'), 69.3 (C-3'), 66.7 (C-6'), 56.4, 56.2, 54.2 (C-5'), 51.7, 44.8, 42.6, 40.0, 39.5, 36.6, 36.1, 35.8, 35.8, 35.5, 35.5, 32.0, 28.7, 28.2, 28.0, 27.4, 24.2, 23.8, 22.8-22.6 (2C; C-26, C-27), 21.2, 20.6- 20.5 (*Me*CO), 18.7 (C-21), 12.3-12.1 ppm (C-18,19).

ESIMS: m/z 724.6 $[M + Na]^+$. Anal.Calc for $C_{40}H_{63}NO_9$: C, 68.44; H, 9.05; N, 2.00. Found: C, 68.51; H, 9.20; N, 1.78.

3β -O-(3',4'-Di-*O*-acetyl-5'*N*,6'*O*-oxometylidenenojirimycin-1'-yl)-5α-cholestane (13b)

Sterol: Cholestanol. Column chromatography EtOAc/Cyclohexane, (1:3); Yield: 23.3 (22%); amorphous solid; R_f=0.30 (1:2 AcOEt/Cyclohexane).

3β-O-(2',3',4'-Tri-*O*-acetyl-5'*N*,6'*O*-oxometylidenenojirimycin-1'-yl)-pregn-5-en-20-one (14a)

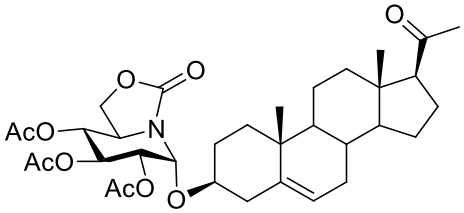

Figure 29 | Structure of 14a.

Sterol: Pregnenolone. Column chromatography EtOAc/Cyclohexane, (1:3) → (1:1); Yield: 35.2 mg (34%) amorphous solid; R_f=0.29 (2:3 AcOEt/Cyclohexane); $[\alpha]_D$= + 81.07 (c=0.7 in DCM).

^{1}H NMR (300 MHz, $CDCl_3$): δ= 5.55 (t, $J_{2',3'}$= $J_{3',4'}$= 9.6 Hz, 1H; H-3'), 5.52 (d, $J_{1',2'}$= 3.6 Hz, 1H; H-1'), 5.32 (d, $J_{6,7}$= 5.1 Hz, 1H; H-6), 4.92 (t, $J_{4',5'}$= 9.6 Hz, 1H; H-4'), 4.79 (dd, 1H; H-2'), 4.44 (t, $J_{5',6a'}$= $J_{6b',6a'}$= 9.0 Hz 1H; H-6a'), 4.24 (dd, $J_{5,6b'}$= 7.2 Hz 1H; H-6b'), 4.02 (q,1H; H-5'), 3.41-3.32 (m, 1H; H-3), 2.11 – 2.03 (3s, 9H; MeCO), 0.99 (s, 3H; H-19), 0.61 ppm (s, 3H; H-18).

^{13}C NMR (75.5 MHz, $CDCl_3$): δ= 209.6 (C-20), 170.1-169.8 (MeCO), 155.5 (CO), 140.0 (C-5), 122.0 (C-6), 77.8 (C-3), 76.5 (C-1'), 72.9 (C-4'), 70.7 (C-2'), 69.3 (C-3'), 66.7 (C-6'), 63.7 (C-17), 56.8 (C-5'), 51.7, 49.8, 44.0, 39.8, 38.8, 36.8, 36.7, 31.8, 31.7, 31.5, 29.7, 24.5, 22.8, 21.0 (C-21), 20.7-20.5 (*Me*CO), 19.3 (C-19), 13.2 ppm (C-18).

ESIMS: m/z 652.6 $[M + Na]^+$. Anal.Calc for $C_{34}H_{47}NO_{10}$: C, 64.85; H, 7.52; N, 2.22 Found: C, 65.03; H, 7.66; N, 1.97.

3β-O-(,3',4'-Di-*O*-acetyl-5'*N*,6'*O*-oxometylidenenojirimycin-1'-yl)-pregn-5-en-20-one (14b)

Sterol: Pregnenolone. Column chromatography EtOAc/Cyclohexane, (1:3) → (1:1); Yield: 35.0 (37%): amorphous solid; R_f= 0.15 (2:3 AcOEt/Cyclohexane);

3β-O-(2',3',4'-Tri-*O*-acetyl-5'*N*,6'*O*-oxometylidenenojirimycin-1'-yl)- androst-5-en-17-one (15a)

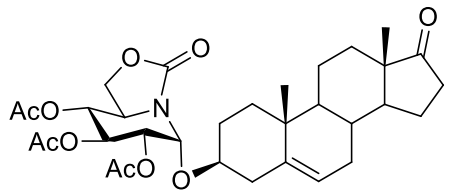

Figure 30 | Structure of 15a.

Sterol: DHEA. Column chromatography EtOAc/Cyclohexane, (1:3) → (2:1); Yield: 116 mg (80%); amorphous solid; R_f=0.35 (2:3 AcOEt/Cyclohexane); $[\alpha]_D$= 89.18 (c=0.7 in DCM).

^{1}H NMR (300 MHz, $CDCl_3$): δ= 5.51 (t, $J_{2',3'}$= $J_{3',4'}$= 9.5 Hz, 1H; H-3'), 5.47 (d, $J_{1',2'}$= 3.6 Hz, 1H; H-1'), 5.32 (d, $J_{6,7}$= 5.1 Hz, 1H; H-6), 4.91 (t, $J_{4',5'}$= 9.5 Hz, 1H; H-4'), 4.78 (dd, 1H; H-2'), 4.41 (t, $J_{5',6a'}$= $J_{6b',6a'}$= 8.7 Hz, 1H; H-6a'), 4.22 (dd, $J_{5,6b'}$= 7.5 Hz 1H; H-6b'), 3.99 (q,1H; H-5'), 3.35-3.32 (m, 1H; H-3), 2.04 – 2.00 (3s, 9H; MeCO), 0.98 (s, 3H; H-19), 0.84 ppm (s, 3H; H-18).

^{13}C NMR (75.5 MHz, $CDCl_3$): δ= 220.8 (C-17), 169.9-169.6 (MeCO), 155.3 (CO), 140.1 (C-5), 121.4 (C-6), 77.7 (C-3), 76.4 (C-1'), 72.7 (C-4'), 70.5 (C-2'), 69.1 (C-3'), 66.5 (C-6'), 51.5 (C-5'), 51.5, 49.9, 47.4, 39.6, 36.6, 36.6, 35.7, 31.3, 31.2, 30.6, 27.3, 21.7, 20.5-20.4 (*Me*CO), 20.2,19.2 (C-19), 13.5 ppm (C-18).

ESIMS: m/z 624.5 $[M + Na]^+$. Anal.Calc for $C_{32}H_{43}NO_{10}$: C, 63.88; H, 7.20; N, 2.33. Found: C, 64.04; H, 7.35; N, 2.26.

3β-O-(3',4'-Di-*O*-acetyl-5'*N*,6'*O*-oxometylidenenojirimycin-1'-yl)- androst-5-en-17-one (15b)

Sterol: DHEA. Column chromatography EtOAc/Cyclohexane, (1:3) → (2:1); Yield: 13 mg (9%); amorphous solid; R_f= 0.20 (2:3 AcOEt/Cyclohexane);

3β-O-(2',3',4'-Tri-*O*-acetyl-5'*N*,6'*O*-oxometylidenenojirimycin-1'-yl)-24*S*-stigmast-5,22-diene (16a)

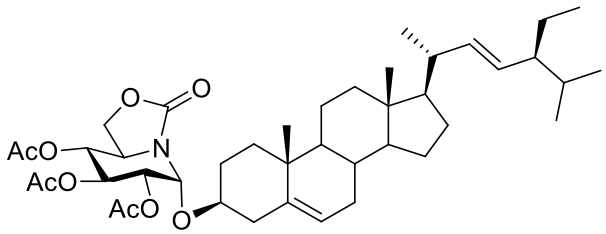

Figure 31 | Structure of 16a.

Sterol: Stigmasterol. Column chromatography EtOAc/Cyclohexane, (1:4); Yield: 97.6 mg (56%); amorphous solid; R_f=0.40 (1:2 AcOEt/Cyclohexane); $[\alpha]_D$= +37.9 (c=0.7 in DCM).

^{1}H NMR (300 MHz, $CDCl_3$): δ= 5.56 (t, $J_{2',3'}$= $J_{3',4'}$= 9.8 Hz, 1H; H-3'), 5.52 (d, $J_{1',2'}$= 3.6 Hz, 1H; H-1'), 5.33 (d, $J_{6,7}$= 5.1 Hz, 1H; H-6), 5.20-5.02 (2 dd, $J_{20,22}$= $J_{23,24}$= 8.6 Hz, 2H; H-22, H-23), 4.93 (t, $J_{4',5'}$= 9.8 Hz, 1H; H-4'), 4.80 (dd, 1H; H-2'), 4.42 (t, $J_{5',6a'}$= $J_{6b',6a'}$= 8.4 Hz 1H; H-6a'), 4.24 (dd, $J_{5',6b'}$= 7.2 Hz 1H; H-6b'), 4.06-3.97 (m,1H; H-5'), 3.41-3.32 (m, 1H; H-3), 2.08 – 2.03 (3s, 9H; MeCO), 1.02 (d, $J_{20,21}$= 6.6 Hz, 3H; H-21), 1.00 (s, 3H; H-19), 0.86-0.78 (m, 9H; H-24b, H-26, H27), 0.69 ppm (s, 3H; H-18).

^{13}C NMR (75.5 MHz, $CDCl_3$): δ= 170.0-169.7 (MeCO), 155.4 (CO), 140.0 (C-5), 138.3-129.2 (2C; C-22, C-23), 122.3 (C-6), 77.9 (C-3), 76.4 (C-1'), 72.9 (C-4'), 70.7 (C-2'), 69.3 (C-3'), 66.6 (C-6'), 56.7, 55.9, 51.6 (C-5'), 51.2, 50.0, 42.2, 40.4, 39.8, 39.6, 36.7, 36.6, 31.8, 28.8, 27.4, 26.9, 25.3, 24.3, 21.2, 21.1, 21.0, 20.6-20.5, (*Me*CO), 19.4 (C-19), 19.0 (2C; C-26, C-27), 12.2 (C-24b), 12.0 ppm (C-18).

ESIMS: m/z 748.6 $[M + Na]^+$. Anal.Calc for $C_{42}H_{63}NO_9$: C, 69.49; H, 8.75; N, 1.93. Found: C, 69.63; H, 8.86; N, 1.77.

3β -O-(3',4' - Di-*O*-acetyl-5'*N*,6'*O*-oxometylidenenojirimycin-1'-yl)-24*S*-stigmast-5,22-diene (16b)

Sterol: Stigmasterol. Column chromatography EtOAc/Cyclohexane, (1:4); Yield: 26.2 mg (16%); amorphous solid; R_f=0.24 (1:2 AcOEt/Cyclohexane).

3β -O-(2',3',4' - Tri-*O*-acetyl-5'*N*,6'*O*-oxometylidenenojirimycin-1'yl)- 25*R*-spirost-5-ene (17a)

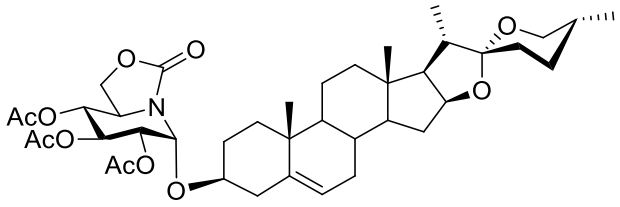

Figure 32 | Structure of 17a.

Sterol: Diosgenin. Column chromatography EtOAc/Cyclohexane, (1:3) → (1:2); Yield: 33.2 mg (19%) amorphous solid; R_f=0.38 (2:1 AcOEt/Cyclohexane); $[\alpha]_D$= -1.99 (c=0.7 in DCM).

^{1}H NMR (300 MHz, $CDCl_3$): δ= 5.55 (t, $J_{2',3'}$= $J_{3',4'}$= 9.8 Hz, 1H; H-3'), 5.51 (d, $J_{1',2'}$= 3.9 Hz, 1H; H-1'), 5.32 (d, $J_{6,7}$= 5.1 Hz, 1H; H-6), 4.92 (t, $J_{4',5'}$= 9.8 Hz, 1H; H-4'), 4.79 (dd, 1H; H-2'), 4.47-4.36 (m, 2H; H-6a', H-16), 4.24 (dd, $J_{5,6b'}$= 7.2 Hz 1H; H-6b'), 4.00 (q,1H; H-5'), 3.49-3.324 (m, 3H; H-3, H-27a, H-27b), 2.07–2.03 (3s, 9H; MeCO), 1.00 (s, 3H; H-19), 0,96 (d, $J_{25,27}$= 6.9 Hz, 3H; H-26), 0.78 (d, $J_{20,21}$=5.1 Hz, 3H; H-21), 0.77 ppm (s, 3H; H-18).

^{13}C NMR (75.5 MHz, $CDCl_3$): δ= 170.1-169.8 (MeCO), 155.4 (CO), 140.0 (C-5), 122.0 (C-6), 109.3 (C-22), 80.8 (C-16), 77.8 (C-3), 76.4 (C-1'), 72.9 (C-4'), 70.7 (C-2'), 69.3 (C-3'), 66.8-66.7 (2C; C-6', C-27), 62.1, 56.4, 51.7 (C-5'), 49.9, 41.6, 40.2, 39.8, 39.7, 36.8, 36.7, 32.0, 31.8, 31.4, 30.3, 29.7, 28.8, 27.4, 20.8, 20.7-20.6 (*Me*CO), 19.4 (C-19), 17.1-16.3 (2C; C-18, C-21), 14.5 (C-26).

ESIMS: m/z 750.6 $[M + Na]^+$. Anal.Calc for $C_{40}H_{57}NO_{11}$: C, 66.00; H, 7.89; N, 1,92. Found: C, 66.09; H, 7.75; N, 1.81.

3β -O-(3,4 - Di-*O*-acetyl-5*N*,6*O*-oxometylidenenojirimycin-1'yl)-25*R*-spirost-5-ene (17b)

Sterol: Diosgenin. Column chromatography EtOAc/Cyclohexane, (1:3) → (1:2); Yield: 69.3 mg (42%); amorphous solid; R_f=0.23 (2:1 AcOEt/Cyclohexane).

5.1.4. General procedure for preparation of conjugates of nojirimicyn derivatives and sterols.

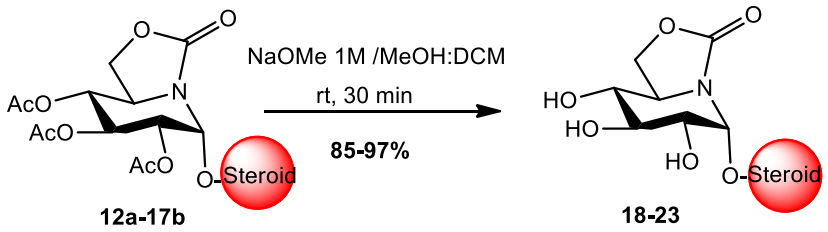

Scheme 15 | Preparation of compounds 18-23 from acetylated precursors 12a-17b.

The conjugates were obtained by conventional de-*O*-acetilation of their corresponding triacetylated and diacetylated compounds. To a stirred solution of triacetylated and/or diacetylated compound in MeOH:DCM (1:1) was added NaOMe (0.1 eq for each acetyl group) at room temperature for 30 min (TLC monitoring). The reaction was stopped with Amberlite IRA-68 (OH-), filtrated and concentrated under reduced pressure to give the corresponding deacetylated compound.

3β -O-(5'*N*,6'*O*-oxometylidenenojirimycin-1'-yl)-cholest-5-ene (18)

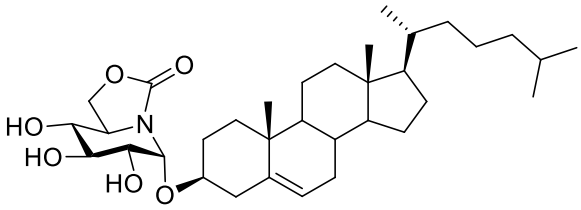

Figure 33 | Structure of **18**.

Starting material: 95.4 mg (0.136 mmol) of **12a**; Yield: 75.8 mg (97%); amorphous solid; R_f=0.67 (5:1 AcOEt/MeOH); $[\alpha]_D$= + 30.7 (c=0.6 in py);

^{1}H NMR (500 MHz, DMSO-d_6): δ= 5.31 (d, $J_{6,7}$= 4.0 Hz, 1H; H-6), 5.02 (d, $J_{1',2'}$= 4 Hz, 1H; H-1'), 4.48 (t, $J_{5',6a'}$= $J_{6b',6a'}$= 8.5 Hz 1H; H-6a'), 4.11 (dd, $J_{5,6b'}$= 6.5 Hz 1H; H-6b'), 3.65-3.61 (dd, $J_{4',5'}$= 9.0 Hz 1H; H-5'), 3.47 (t, $J_{2',3'}$= $J_{3',4'}$= 9.0 Hz, 1H; H-3'), 3.34-3.30 (m, 1H; H-3), 3.26 (dd, 1H; H-2'), 3.19 (t, 1H; H-4'), 0.99 (s, 3H; H-18), 0,93 (d, $J_{20,21}$= 7.0 Hz 3H; H-21), 0.88 (dd, $J_{26/27,25}$=6.5, $J_{26,27}$= 1.5 Hz, 6H; H-26,27), 0.69 ppm (s, 3H; H-19).

^{13}C NMR (125.7 MHz, DMSO-d_6): δ= 156.1 (CO), 141.1 (C-5), 121.6 (C-6), 80.2 (C-1'), 77.3 (C-3), 74.9 (C-4'), 73.3 (C-3'), 72.2 (C-2'), 67.2 (C-6'), 56.8, 56.4, 53.9 (C-5'), 50.3, 42.5, 39.9, 39.5, 37.2, 36.8, 36.3, 35.6, 32.1, 31.9, 28.1, 27.8, 24.3, 23.8, 22.9, 22.8, 21.2 (2C; C-26, C-27), 19.5-19.1 (2C; C-19, C-21), 12.2 ppm (C-18).

ESIMS: m/z 596.5 $[M + Na]^+$. Anal.Calc for $C_{34}H_{55}NO_6$: C 71.17, H 9.66, N 2.44. Found: C 70.97, H 9.52, N 2.23.

3β -O-(5'*N*,6'*O*-oxometylidenenojirimycin-1'-yl)-5α-cholestane (19)

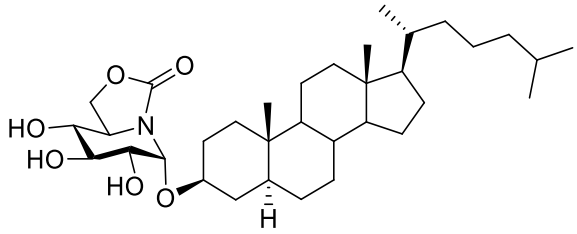

Figure 34 | Structure of **19**.

Starting material: 23.3 mg (0.035 mmol) of 13b; Yield: 18.9 mg (93%); amorphous solid; R_f=0.68 (5:1 AcOEt/MeOH); $[\alpha]_D$= +63.5 (c=0.5 in py);

^{1}H NMR (500 MHz, 333K, DMSO-d_6): δ= 5.10 (d, J= 5.1 Hz 1H; OH), 4.99 (d, $J_{1',2'}$= 4.0 Hz, 1H; H-1'), 4.58 (d, J= 4.7 Hz 1H; OH), 4.46 (t, $J_{5',6a'}$= $J_{6b',6a'}$= 8.6 Hz 1H; H-6a'), 4.10 (dd, $J_{5,6b'}$= 6.0 Hz 1H; H-6b'), 3.62-357 (m,1H; H-5'), 3.46-3.37 (m, 2H; H-3, H-3'), 3.24-3.16 (m, 2H; H-2', H-4'), 0,90 (d, $J_{21,20}$= 6.6 Hz, 3H; H-21), 0.87 (dd, $J_{26/27,25}$=6.7, $J_{26,27}$= 1.8 Hz 6H; H-26,27), 0.78 (s, 3H; H-19), 0.65 ppm (s, 3H; H-18).

^{13}C NMR (125.7 MHz 333K, DMSO-d_6): 155.2 (CO), 79.3 (C-1'), 75.7 (C-3), 74.0 (C-4'), 72.3 (C-3'), 71.3 (C-2'), 66.2 (C-6'), 55.6, 55.5, 53.4 (C-5'), 53.0, 44.1, 41.2, 38.6, 36.0, 35.3, 35.0, 34.8, 34.7, 34.7, 31.2, 28.0, 27.3, 26.9, 26.6, 23.4, 22.8, 22.1-21.9 (2C; C-26, C-27), 20.4, 18.2 (C-21), 11.6 (C-19), 11.5 ppm (C-18).

ESIMS: m/z 574.6 $[M - H]^-$. Anal.Calc for $C_{34}H_{57}NO_6$: C, 70.92; H, 9.98; N, 2.43. Found: C, 70.74; H, 9.81; N, 2.19.

3β -O-(5'*N*,6'*O*-oxometylidenenojirimycin-1'-yl)-pregn-5-en-20-one (20)

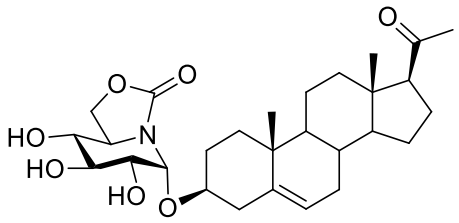

Figure 35 | Structure of **20**.

Starting material: 12.8 mg (0.025 mmol) of 14a and 22.3 mg (0.035 mmol) of 14b; Yield: 29.0 mg (96%); amorphous solid; R_f=0.65 (5:1 AcOEt/MeOH); $[\alpha]_D$= + 61.1 (c=0.9 in py);

^{1}H NMR (500 MHz, $CDCl_3/CD_3OD$ (1:1): δ= 5.35 (t, $J_{6,7a}$= $J_{6,7b}$= 2.8 Hz 1H; H-6), 5.22 (d, $J_{1',2'}$= 4.5 Hz 1H; H-1'), 4.52 (t, $J_{5',6a'}$= $J_{6b',6a'}$= 8.5 Hz 1H; H-6a'), 4.24 (t, $J_{5,6b'}$= 6.0 Hz 1H; H-6b'), 3.79-3.74 (ddd, $J_{5,4'}$= 9.5 Hz 1H; H-5'), 3.64 (t, $J_{2',3'}$= $J_{3',4'}$= 9.5 Hz, 1H; H-3'), 3.36-3.29 (m, 2H; H-3, H-2'), 3.24 (t, 1H; H-4'), 2.12 (1s, 3H; H-21 1.02 (s, 3H; H-19), 0.64 ppm (s, 3H; H-18).

^{13}C NMR (125.7 MHz, $CDCl_3/CD_3OD$ (1:1): δ= 211.0 (C-20), 156.7 (CO), 140.4 (C-5), 121.6 (C-6), 79.4 (C-1'), 77.6 (C-3), 74.4 (C-4'), 73.3 (C-3'), 71.7 (C-2'), 67.0 (C-6'), 63.6 (C-17) , 56.8, 53.4 (C-5'), 50.0, 44.0, 39.6, 38.7, 36.9, 36.7, 31.9, 31.6, 30.8, 29.4, 24.3, 22.8, 21.0 (C-21), 18.9 (C-19), 12.7 ppm (C-18).

ESIMS: m/z 526.5 $[M + Na]^+$. Anal.Calc for $C_{28}H_{41}NO_7$: C, 66.78; H, 8.21; N, 2.78. Found: C, 66.51 ; H, 7.99; N, 2.53.

3β -(5'*N*,6'*O*-oxometylidenenojirimycin-1'-yl)- androst-5-en-17-one (21)

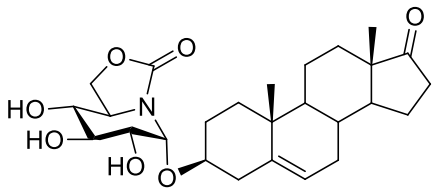

Figure 36 | Structure of **21**.

Starting material: 101.0 mg (0.169 mmol) of 15a; Yield: 77.2 mg (96%); amorphous solid; R_f=0.66 (6:1 AcOEt/MeOH); $[\alpha]_D$= +29.4 (c=1.0 in DMSO);

^{1}H NMR (300 MHz, DMSO-d_6): δ= 5.38 (d, J= 5.1 Hz, 1H; OH) 5.34 (d, $J_{6,7}$= 5.1 Hz, 1H; H-6), 4.95 (d, $J_{1',2'}$= 3.9 Hz, 1H; H-1'), 4.93-4.86 (2H, OH), 4.48 (t, $J_{5',6a'}$= $J_{6a',6b'}$= 8.4 Hz, 1H; H-6a'), 4.08 (dd, $J_{5',6b'}$= 6.3 Hz, 1H; H-6b'), 3.59 (ddd, $J_{5',4'}$= 9.0 Hz, 1H; H-5'), 3.44-3.14 (m, 4H; H-3, H-2',H-3',H-4'), 0.98 (s, 3H; H-19), 0.80 ppm (s, 3H; H-18).

^{13}C NMR (75.5 MHz, DMSO-d_6): δ= 219.6 (C-17), 155.7 (CO), 140.5 (C-5), 120.9 (C-6), 79.4 (C-1'), 76.2-71.4 (C-3,2',3',4'), 66.8 (C-6'), 53.2 (C-5'), 50.8, 49.6, 46.8, 40.3, 38.7, 36.4, 36.3, 35.3, 31.1, 30.9, 30.2, 27.0, 21.4, 19.9, 19.0 (C-19), 13.1 ppm (C-18).

ESIMS: m/z 498.4 $[M + Na]^+$. Anal.Calc for $C_{26}H_{37}NO_6$: C, 65.66; H, 7.84; N, 2.95. Found: C, 65.77; H, 8.02; N, 2.78.

3β -(5'*N*,6'*O*-oxometylidenenojirimycin-1-yl)- 24*S*-stigmast-5,22-diene (22)

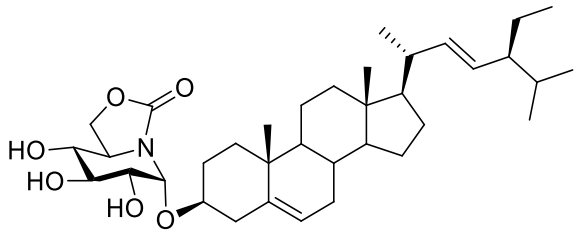

Figure 37 | Structure of **22**.

Starting material: 88.0 mg (0.121 mmol) of 16a; Yield: 66.7 (92%); amorphous solid; R_f=0.62 (5:1 AcOEt/MeOH); $[\alpha]_D$= +19.51 (c=0.9 in py);

^{1}H NMR (500 MHz, DMSO-d_6): δ= 5.32 (d, $J_{6,7}$= 4.0 Hz, 1H; H-6), 5.27-5.08 (2 dd, 2H; H-22, H-23), 5.03 (d, $J_{1',2'}$= 4.0 Hz, 1H; H-1'), 4.47 (t, $J_{5',6a'}$= $J_{6b',6a'}$= 8.5 Hz 1H; H-6a'), 4.12 (t, $J_{5',6b'}$= 6.0 Hz 1H; H-6b'), 3.66-3.61 (ddd, $J_{5',4'}$= 9.0 Hz 1H; H-5'), 3.48 (t, $J_{2',3'}$= $J_{3',4'}$= 9.0 Hz, 1H; H-3'), 3.35-3.32 (m, 1H; H-3), 3.26 (dd, 1H; H-2'), 3.20 (t, $J_{4',5'}$= 9 Hz, 1H; H-4'), 1.03 (d, $J_{20,21}$= 7.0 Hz, 3H; H-21), 1.00 (s, 3H; H-19), 0.87-0.81 (m, 9H; H-24b, H-26, H27), 0.71 ppm (1s, 3H; H-18).

^{13}C NMR (125.7 MHz, DMSO-d_6): δ= 155.0 (CO), 140.1 (C-5), 137.1-128.7 (2C; C-22, C-23), 120.5 (C-6), 79.2 (C-1'), 76.4 (C-3), 73.9 (C-4'), 72.3 (C-3'), 71.3 (C-2'), 66.1 (C-6'), 55.9, 55.2, 53.0 (C-5'), 50.0, 49.4, 41.7, 38.9, 38.8, 38.7, 36.2, 35.8, 31.1, 30.9, 30.7, 30.6, 30.0, 29.5, 28.3, 27.5, 26.8, 24.1, 23.3, 20.4, 20.1, 20.0, 18.4, 18.3, 11.3-11.2 ppm (2C; C-18, C-24b).

ESIMS: m/z 598.5 $[M - H]^-$. Anal.Calc for $C_{36}H_{57}NO_6$: C, 72.08; H, 9.58; N, 2.34. Found: C, 71.81; H, 9.48; N, 2.20.

3β -O-(5'*N*,6'*O*-oxometylidenenojirimycin-1'-yl)- 25*R*-spirost-5-ene (23)

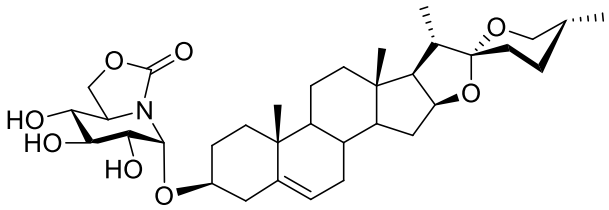

Figure 38 | Structure of **23**.

Starting material: 69.3 mg (0.101 mmol) of 17b; Yield: 21.9 mg (85%); amorphous solid; R_f= 0.68 (5:1 EtOAc/MeOH); $[\alpha]_D$= -6.59 (c=0.6 in py).

^{1}H NMR (500 MHz, $CDCl_3/CD_3OD$ (2:1)): δ= 5.14 (t, $J_{6,7a}$= $J_{6,7b}$= 2.5 Hz, 1H; H-6), 5.02 (d, $J_{1',2'}$= 4.0 Hz, 1H; H-1'), 4.32 (t, $J_{5',6a'}$= $J_{6a',6b'}$= 8.5 Hz, 1H; H-6a'), 4.21 (q, $J_{15,16}$= $J_{16,17}$= 7.5 Hz, 1H; H-16), 4.05 (dd, $J_{5',6b'}$= 6 Hz 1H; H-6b'), 3.58-3.53 (ddd, $J_{5',4'}$= 9.0 Hz 1H; H-5'), 3.44 (t, $J_{2',3'}$= $J_{3',4'}$= 9.0 Hz, 1H; H-3'), 3.27-3.10 (m, 5H; H-3, H-26a, H-26b, H-2', H-4'), 0.83 (s, 3H; H-18), 0,76 (d, $J_{25,27}$= 6.7 Hz, 3H; H-27), 0.59 (s, 3H; H-19), 0.59 ppm (d, $J_{20,21}$= 6.0 Hz, 3H; H-21).

^{13}C NMR (100.6 MHz, $CDCl_3/CD_3OD$ (2:1)): δ= 156.7 (CO), 140.1 (C-5), 121.5 (C-6), 109.3 (C-22), 80.7 (C-16), 79.1 (C-1'), 77.0 (C-3), 74.2 (C-4'), 73.2 (C-3'), 71.4 (C-2'), 66.8-66.6 (2C; C-6', C-27), 61.9, 56.2, 53.2 (C-5'), 49.8, 41.4, 40.0, 39.4, 36.6, 36.6, 31.7, 31.4, 31.2, 31.0, 29.9, 29.3, 28.4, 26.9, 20.5, 18.8 (C-19), 16.5-15.8 (2C; C-21,C-18), 13.9 ppm (C-26).

ESIMS: m/z 624.5 $[M + Na]^+$. Anal.Calc for $C_{34}H_{51}NO_8$: C, 67.86; H, 8.54; N, 2.33. Found: C, 67.69; H, 8.42; N, 2.05.

5.2. X-ray Structural Analysis of compound 20

One crystal of suitable size for X-ray diffraction analysis (white needle, 0.40 x 0.20 x 0.10 mm) was coated with dry perfluoropolyether and mounted on glass fiber and fixed in a cold nitrogen stream (T = 213 K) to the goniometer head. Data collection was performed using monochromatic radiation λ(Mo Kα) = 0.71073 Å, by means of ω and φ scans with a width of 0.50°. The data were reduced (SAINT)20 and corrected for absorption effects by the multiscan method (SADABS).21. The structures were solved by direct methods (SIR-2002)22 and refined against all F2 data by full-matrix least-squares techniques ($_{SHELXTL}$-6.12)23 minimizing w[Fo 2 − Fc 2].2 All the non-hydrogen atoms were refined with anisotropic displacement parameters. Hydrogen atoms were included in calculated positions and allowed to ride on the attached atoms with the isotropic temperature factors (U_{iso} values) fixed at 1.2 times (1.5 times for methyl groups) those U_{eq} values of the corresponding attached atoms.

Crystal data for 20. $C_{28}\,H_{41}NO_7$, M = 521.63, monoclinic, a = 11.980(12) Å, b = 5.926(5) Å, c = 19.024(16) Å, α = 90.00°, ß = 98.97(3)°, γ = 90.00°, V = 1334.0(2) $Å^3$, T = 193(2) K, space group $P2_1$, Z = 2, 18791 reflections measured, 2573 independent reflections (Rint = 0.0356). The final R1 values were 0.0443 (I > 2σ(I)). The final wR(F2) values were 0.0980 (I > 2σ(I)). The final R1 values were 0.0474 (all data). The final wR(F2) values were 0.0992 (all data). The goodness of fit on F2 was 1.150.

5.3. Biological Evaluation

5.3.1. General procedures for glycosidase inhibition assays

Inhibitory potencies were determined by spectrophotometrically measuring the residual hydrolytic activities of the glycosidase against the respective *o*- (for β-glucosidase from bovine liver and β-galactosidase from *E. coli*), *p*-nitrophenyl α- or ß-D-glycopyranoside and *p*-nitrophenyl-*N*-acetyl-b-D-glucoseaminide/galactosaminide in the presence of the corresponding compound. Each

assay was performed in phosphate buffer at the optimal pH for each enzyme. The Michaelis-Menten constant (K_m) values for the different glycosidase used in the tests and the corresponding working pHs are listed herein: α-glucosidase (from yeast), K_m = 0.35 mM (pH 6.8); isomaltase (yeast) K_m = 1.0 mM (pH 6.8), ß-glucosidase (from almonds), K_m = 3.5 mM (pH 7.3); ß-glucosidase (from bovine liver), K_m = 2.0 mM (pH 7.3); ß-galactosidase (*E. coli*), K_m = 0.12 mM (pH 7.3); α-galactosidase (from coffee beans), K_m = 2.0 mM (pH 6.8); amyloglucosidase (from *Aspergillus niger*), K_m = 3.0 mM (pH 5.5); ß-mannosidase (*Helix pomatia*), K_m = 0.6 mM (pH 5.5); α-mannosidase (from jack bean), K_m = 2.0 mM (pH 5.5). The reactions were initiated by addition of enzyme to a solution of the substrate in the absence or presence of various concentrations of inhibitor.

The mixture was incubated for 10-30 min at 37 ºC or 55 ºC (for amyloglucosidase), and thereafter the reaction was quenched by addition of 1 M Na_2CO_3. The absorbance of the resulting mixture was determined at 405 nm. The K_i value and enzyme inhibition mode were determined from the slope of Lineweaver-Burk plots and double reciprocal analysis.

5.3.2. Cell studies

After the synthesis and purification of the compounds, it was performed the evaluation of their anti-proliferative activity. The effect of the synthesised compounds was compared with the parent sterols and sp^2-iminosugar, as well as a positive control (5-FU), in cell lines of prostate and breast cancer, and normal skin cells. In this evaluation was applied the colorimetric MTT method.

5.3.2.1. Cell Cultures

The cell lines used in this study were from human mammary gland carcinoma (T-47D) and a lipmph node of prostate carcinoma (LNCaP), as well as were non-carcinogenic human dermal fibroblasts (NHDF), all acquired to American Type Culture Collection (ATCC; Manassas, VA, USA). The chemicals (analytical grade), assay reagents, culture mediums and supplements were all obtained from Sigma-Aldrich.

All the cell lines were cultured in 75 or 175 cm^2 culture flasks and maintained at 37 °C in a humidified atmosphere incubator with 5% CO_2. LNCaP and T-47D cells were cultured in RPMI 1640 medium with 10% FBS and 1% of the antibiotic mixture of 10,000 U/mL penicillin G and 100 mg/mL of streptomycin. NHDF cells have grown in RPMI 1640 medium supplemented with 10% FBS, 2 mM *L*-glutamine, 10 mM HEPES, 1 mM sodium pyruvate and 1% antibiotic/antimycotic (10,000 U/mL penicillin G, 100 mg/mL streptomycin and 25 µg/mL anfothericin B. For all cell types, the medium was renewed every 2–3 days until cells reach confluence. The cells used in the experiments were used in passages 20 to 24, 10 to 13 and 10 to 12 for LNCaP, T-47D and NHDF, respectively. When cells reached approximately 80–90% of confluence, they were detached by gentle trypsinization and,

before the experiments, viable cells were counted and adequately diluted in complete culture medium.

5.3.2.2. Preparation of compounds solutions

The studied compounds were all dissolved in dimethyl sulfoxide (DMSO) in a concentration of 10 mM and stored at 4 °C. From this mother-solution, the various solutions of the compounds in different concentrations were prepared by adequate dilutions in the complete culture medium before each experiment. The maximum DMSO concentration in the studies was ≤1%, a concentration without significant effect on cell viability (data not shown).

5.3.2.3. MTT cell proliferation assay

Cells treatment with compounds

Thereafter trypsinization and counting, a 100 µL suspension of cells in medium with an initial density of 2×10^4 cells/mL was seeded in 96-well culture plates (Nunc, Apogent, Denmark) and left to adhere for 48 h. Then, the medium was replaced by the several solutions of the compounds in study (10 and 50 µM for preliminary studies and 0.01, 0.1, 1, 10, 50 and 100 µM for concentration-response studies) in the appropriate medium for approximately 72 h, and untreated cells were used as negative control.

MTT assay

The *in vitro* antiproliferative effects were evaluated by the MTT (3-(4,5-dimethylthiazol-2-yl)-2,5-diphenyltetrazolium bromide) assay, by measuring the extent of reduction of MTT. After the incubation period (72 h) the medium was removed, 100 µL of phosphate buffer saline (NaCl 137 mM; KCl 2.7 mM, Na_2HPO_4 10 mM and KH_2PO_4 1.8 mM in distilled water and pH adjusted to 7.4) were used to wash the cells and then 100 µL of the MTT solution (5 mg/mL), prepared in the appropriate serum-free medium, was added to each well, followed by incubation for 4 h at 37 °C. Then, the MTT containing medium was removed and the formazan crystals were dissolved in DMSO. The absorbance was measured at 570 nm using Bio-Rad xMark™ microplate spectrophotometer. The extent of cell death was expressed as percentages of cell viability relatively to the cells used as negative control.

5.3.2.4. Flow Cytometry

To analyse cell viability, it was performed flow cytometry studies after staining dead cells with propidium iodide (PI). At first, 1 mL of LNCaP cells (density of 5 x10^4 cells/mL) in complete medium was seeded in each well of a 12-well culture plate and were incubated at 37ºC, 5% of CO_2. After 48h cells were treated with positive control (5-FU), diosgenin (for comparison) and compound **23** at concentration of 50 µM, and incubated once more. Untreated cells were also maintained to serve as negative control. 24h later, an initial evaluation of the effects of the compounds on cell morphology was performed through an optic microscope (Olympus CKX41) coupled to a digital camera (Olympus SP-500UZ) and several relevant photographs were taken (Zoom: 100 x). Thereafter, supernatant of each well were collected and pooled with the cells (harvested by trypsin treatment) in distinct tubes. The resulting cell suspension was kept on ice and pelleted by centrifugation. Subsequently, cells were resuspended with 400 µL with complete medium.

Afterwards, 395 µL of the cell suspension was transferred to a FASC tube containing 5 µL of a solution at 1 mg/mL of PI (Invitrogen) and then, a minimum of 20 000 events were acquired using a FACSCalibur flow cytometer using FSC, SSC and FL3 (Pi) channels. Acquisition and analysis was performed with CellQuest™ Pro software. To analyse the results a region (R4) was created (not shown) on the SSC/FSC contour plot to exclude part of the debris. Accurately, in the FSC/FL3 contour plot gated on R4, three regions were created: R1, corresponding to viable cells, R2 which correspond to dead cells and R3, corresponding to an intermediate population. Lastly, the percentage of events was calculated relating the number of events in each region with the total number of events on R1, R2 and R3.

5.3.2.5. Statistics

In MTT assays each experiment was performed in quadruplicate and independently repeated at least two times and flow cytometry studies were performed in duplicate or triplicate and independently repeated two times. The results of those assays were expressed as average±standard deviation (SD). *t*-Student test was applied to determine statistical significance ($p < 0,05$) in cell proliferation results. These calculations were performed using the Microsoft Excell 2010 software. The half-medium inhibitory concentration (IC_{50}) values were calculated from the concentration-response curve by sigmoid fitting (confidence interval of 95%). In flow cytometry studies cell viability in regions R1, R2 e R3 (%) were calculated with confidence interval of 95%.

5.4. Molecular Docking

The molecular docking study was performed between the synthesized compounds **18-23** plus compounds for method validation and the enzyme AcCHE, on its active site.

The two dimensional structures of all ligands were drawn using the software ChemDraw Pro version 12.0.2, and the minimization of structure energy in 3D was accomplished using MarvinSketch version 15.11.9 software (ChemAxon, Budapest, Hungary).

The human AcCHE structure crystallized with the inhibitor TB (code: 4M0F) was obtain from Protein Data Bank[122]. The protein and the ligand **TB** were isolated with the Chimera 1.9rc software. To prepare the molecules to docking, define some parameters and analyze the results was used the program AutoDock Tools 1.5.6. Therefore, docking simulations were carried out using AutoDock 4.0 package with AutoGrid4 and AutoDock4. AutoGrid4 defines the grid maps, where the docking process and makes all the needed calculations, and AutoDock4 that processes the docking itself.

The AcCHE protein was prepared by the addition of Gasteiger charges, emerging of non-polar hydrogens and removing the water molecules. The rigid roots of each compound were defined automatically. Ligands parameters were maintained as default.

For the grid maps generation, the box was centered on residue TRP286, in the AcCHE active site. The calculations were made with a spacing between two grid points of 0,2 Å. The size of the box was relatively maintained for each ligand. All the other parameters were the standard except the number of conformations generated. To obtain more feasible results, was generated 50 conformations instead of 10. The docking search method used was the Lamarckian genetic algorithm, a combination a genetic algorithm with a local search method to perform energy minimization[126].

6. References

1. Buckingham, J. *Dictionary of Natural Products. Version 9.2 on CD-ROM*. (CRC Press, 1993).

2. Davis, B. G. & Fairbanks, A. J. *Carbohydrate Chemistry*. (Oxford University Press, 2002).

3. Solomons, T. W. G. & Fryhle, C. B. *Organic Chemistry*. (John Wiley & Sons, Inc, 2011).

4. Nelson, D. L. & Cox, M. M. *Lehninger, Principles of Biochemistry*. (Ed.Freeman, 2005).

5. Crucho, C. I. C., Correia-da-Silva, Petrova, K. T. & Barros, M. T. Recent progress in the field of glyconjugates. *Carbohydr. Res.* **402,** 124–132 (2015).

6. Grynkiewicz, G. & Boryski, J. Synthetic analogs of natural glycosides in drug discovery and development. *Drug Res.* **65,** 655–676 (2008).

7. Lee, H. J., Park, J.S., *Yoon, Y.P., Shin, Y.J., Lee, S.K., Kim, Y. S., Hong, J. H., Son, K. S.* & Lee, S. K. Dioscin and methylprotodioscin isolated from the root of Asparagus cochinchinensis suppressed the gene expression and production of airway MUC5AC mucin induced by phorbol ester and growth factor. *Phytomedicine* **22,** 568–572 (2015).

8. Liu, J., Li, C.J., Ni, L., Yang, J. Z., Li, L., Zang, C., Bao, X., Zhang, D. & Zhang, D., Anti-inflammatory alkaloid glycoside and quinoline alkaloid derivates from the stems of Clausena lansium. *RSC Adv.* **5,** 80553–80560 (2015).

9. Suárez, A. I., Mancebo, M., Monache, F. D., Tirri, M. M., Sojo, F., Arvelo, F. & Tillett, S. A new indole-alkaloid and a new phenolic-glycoside with cytotoxic activity from *Strychnos fendleri*. *Nat. Prod. Res.* **30,** 399–405 (2016).

10. Galan, M. C., Benito-Alifonso, D. & Watt, G. Carbohydrate chemistry in drug discovery. *Org. Biomol. Chem.* **9,** 3598–3610 (2011).

11. Magnani, J. L. Glycomimetic Drugs - A New Source of Therapeutic Opportunities. *Discov. Med.* **8,** 247–252 (2009).

12. Klysov, A. A. in *Glycobiology and Drug Design* (ed. Klysov, A. A.) 3–22 (ACS Symposium Series, 2012).

13. Pelissier, H. The glycosylation of steroids. *Tetrahedron* **60,** 5123–5162 (2004).

14. Lew, W., Chen, X. & Kim, C. Discovery and development of GS 4104 (oseltamivir): an orally active influenza neuraminidase inhibitor. *Curr. Med. Chem.* **7,** 663–672 (2000).

15. Mota, A. H. A Review of Medicinal Plants Used in Therapy of Cardiovascular Diseases. *Int. J. Pharmacogn. Phytochem. Res.* **8,** 572–591 (2016).

16. Aubel-Sadron, G. & Londos-Gagliardi, D. Daunorubicin and doxorubicin, anthracycline

antibiotics, a physicochemical and biological review. *Biochimie* **66,** 333–352 (1984).

17. Dube, D. H. & Bertozzi, C. R. Glycans in cancer and inflammation--potential for therapeutics and diagnostics. *Nat. Rev. Drug Discov.* **4,** 477–488 (2005).

18. Wrodnigg, T. M., Steiner, A. J. & Ueberbacher, B. J. Natural and Synthetic Iminosugars as Carbohydrate Processing Enzyme Inhibitors for Cancer Therapy. *Anti-Cancer Agents Med. Chem.* **8,** 77–85 (2008).

19. Nash, R. J., Kato, A., Chu-Yi, Y. & Fleet, G. W. J. Iminosugars as therapeutic agents: recent advances and promising trends. *Future Med. Chem.* **3,** 1513–1521 (2011).

20. Bra□s, N. F., Fernandes, P. a, Ramos, M. J. & Cerqueira, N. M. in *Carbohydrates - Comprehensive Studies on Glycobiology and Glycotechnology* 117–134 (2012).

21. Chang, J., Block, T. M. & Guo, J. T. Antiviral therapies targeting host ER alpha-glucosidases: Current status and future directions. *Antiviral Res.* **99,** 251–260 (2013).

22. Tadera, K., Minami, Y., Takamatsu, K. & Matsuoka, T. Inhibition of alpha-glucosidase and alpha-amylase by flavonoids. *J. Nutr. Sci. Vitaminol.* **52,** 149–153 (2006).

23. Sánchez-Fernández, E. M., Rísquez-Cuadro, R., Chasseraud, M., Ahidouch, A., Ortiz Mellet, C., Ouadid-Ahidouch, H. & García Fernández, J. M. Synthesis of N-, S-, and C-glycoside castanospermine analogues with selective neutral alpha-glucosidase inhibitory activity as antitumour agents. *Chem. Commun.* **46,** 5328–5330 (2010).

24. Gossan, D. P. A., Alabdul Magid, A., Kouassi-Yao, P. A., Behr, J. B., Ahibo, A. C., Djakouré, L. A, Harakat, D. & Voutquenne-Nazabadioko, L. Glycosidase inhibitors from the roots of Glyphaea brevis. *Phytochemistry* **109,** 76–83 (2015).

25. Viuff, A. H., Besenbacher, L. M., Kamori, A., Jensen, M. T., Kilian, M., Kato, A. & Jensen, H. H. Stable Analogues of Nojirimycin – Synthesis and Biological Evaluation of Nojiristegine and manno-Nojiristegine. *Org. Biomol. Chem.* **13,** 9637–9658 (2015).

26. Chang, J., Guo, J.-T., Du, Y. & Block, T. Imino sugar glucosidase inhibitors as broadly active anti-filovirus agents. *Emerg. Microbes Infect.* **2,** e77 (2013).

27. Li, Y. X. Shimada, Y., Sato, K.,Kato, A., Zhang, W., Jia, Y. M., Fleet, G. W. J., Xiao, M. & Yu, C. Y. Synthesis and glycosidase inhibition of Australine and its fluorinated derivatives. *Org. Lett.* **17,** 716–719 (2015).

28. Takai, T. Higaki, K., Aguilar-Moncayo, M., Mena-Barragán, T., Hirano, Y., Yura, K., Yu, L., Ninomiya, H., García-Moreno, M. I., Sakakibara, Y., Ohno, K., Nanba, E., Ortiz Mellet, C., García Fernández, J. M. & Suzuki, Y. A bicyclic 1-deoxygalactonojirimycin derivative as a novel pharmacological chaperone for GM1 gangliosidosis. *Mol. Ther.* **21,** 526–532 (2013).

29. Cendret, V., *Legigan, T., Mingot, A., Thibaudeau, S., Adachi, I., Forcella, M., Parenti, P.,*

Bertrand, J., Becq, F., Norez, C., Désiré, J., Kato, A. & *Blériot, Y.* Synthetic deoxynojirimycin derivatives bearing a thiolated, fluorinated or unsaturated N-alkyl chain: identification of potent α-glucosidase and trehalase inhibitors as well as F508del-CFTR correctors. *Org. Biomol. Chem.* **13,** 10734–10744 (2015).

30. Brumshtein, B. Aguilar-Moncayo, M., García-Moreno, M. I., Ortiz Mellet, C., García-Fernández, J. M., Silman, I., Shaaltiel, Y., Aviezer, D., Sussman, J. L. & Futerman, A. H. Synthesis , Biological Evaluation , and Crystal Structure in Complex with Acid b-Glucosidase. *ChemBioChem* **10,** 1480 – 1485 (2009).

31. Pérez, V. M. D., García, M. I. M., Ortiz Mellet, C., Fuentes, J., Arribas, J. C. D., Cañada, F J. & García Fernández, J. M. Generalized Anomeric Effect in Action : Synthesis and Evaluation of Stable Reducing Indolizidine Glycomimetics as Glycosidase. *J. Org. Chem.* **12,** 136–143 (2000).

32. Silva, S., Sánchez-Fernández, E. M., Ortiz Mellet, C., Tatibout, A., Pilar Rauter, A. & Rollin, P. N-Thiocarbonyl iminosugars: Synthesis and evaluation of castanospermine analogues bearing oxazole-2(3H)-thione moieties. *European J. Org. Chem.* **2,** 7941–7951 (2013).

33. Riaz, S., Khan, Islam U., Bajda, M., Ashraf, M., Qurat-Ul-Ain, Shaukat, A., Rehman, T. U., Mutahir, S., Hussain, S., Mustafa, G. & Yar, M. Pyridine sulfonamide as a small key organic molecule for the potential treatment of type-II diabetes mellitus and Alzheimer's disease: In vitro studies against yeast α-glucosidase, acetylcholinesterase and butyrylcholinesterase. *Bioorg. Chem.* **63,** 64–71 (2015).

34. Sridhar, G. R., Ramachandra, Thota, H., Allam, A. R., Suresh Babu, C., Siva Prasad, A. & Divakar, C. Alzheimer's disease and type 2 diabetes mellitus: the cholinesterase connection.*Lipids Health Dis.* **5,** 28 (2006).

35. Pospieszny, T. *Steroidal Conjugates : Synthesis , Spectroscopic , and Biological Studies*. *Studies in Natural Products Chemistry* **46,** (Elsevier B.V., 2015).

36. Radwan, A. A. Targeting cancer using cholesterol conjugates. *Saudi Pharm. J.* **22,** 3–16 (2014).

37. Lemke, T. L. & Williams, D. A. *Foye's Principles of Medicinal Chemistry*. (Lippincott Williams & Wilkins, 2013).

38. Morzycki, J. W. Recent advances in cholesterol chemistry. *Steroids* **83,** 62–79 (2014).

39. Brown, A. J., Ikonen, E. & Olkkonen, V. M. Cholesterol precursors : more than mere markers of biosynthesis. *Curr. Opin. Lipidol.* **25,** 133–139 (2014).

40. Seyama, Y. Cholestanol Metabolism, Molecular Pathology, and Nutritional Implications. *J. Med. Food* **6,** 217–224 (2003).

41. Panzenboeck, U., Andersson, U., Hansson, M., Sattler, W., Meaney, S. & Björkhem, I. On the mechanism of cerebral accumulation of cholestanol in patients with cerebrotendinous xanthomatosis. *J. Lipid Res.* **48,** 1167–74 (2007).

42. Valayil, J. M., Kuriakose, G. C. & Jayabaskaran, C. Modulating the biosynthesis of a bioactive steroidal saponin, cholestanol glucoside by Lasiosiodoplodia Theobromae using abiotic stress factors. *Innovare Acad. Sci.* **7,** 40–43 (2015).

43. Choudhary, M. I., Alam, M. S., Yousuf, S., Wu, Y., Lin, A. & Shaheen, F. Pregnenolone derivatives as potential anticancer agents. *Steroids* **76,** 1554–1559 (2011).

44. Vallée, M. Neurosteroids and potential therapeutics : Focus on pregnenolone. *J. Steroid Biochem. Mol. Biol.* **160,** 78–87 (2016).

45. Chen, H. Han, C., Wu, J., Liu, X., Zhan, Y., Chen, J., Chen, Y., Gu, R., Zhang, L., Chen, S.,

Jia, J., Zhen, X., Zheng, L. T. & Jiang, B. Accessible Method for the Development of Novel Sterol Analogues with Dipeptide-like Side Chains That Act as Neuroinflammation Inhibitors. *ACS Chem. Neurosci.* **7,** 305–315 (2016).

46. Silva-Ortiz, A. V., Bratoeff, E., Ramírez-Apan, T., Heuze, Y., Sánchez, A., Soriano, J. & Cabeza, M. Synthesis and activity of novel 16-dehydropregnenolone acetate derivatives as inhibitors of type 1 5 a -reductase and on cancer cell. *Bioorg. Med. Chem.* **23,** 7535–7542 (2015).

47. Ohlsson, C., Vandenput, L. & Tivesten. DHEA and mortality: What is the nature of the association? *J. Steroid Biochem. Mol. Biol.* **145,** 248–253 (2014).

48. Maggio, M., Vita, F., Fisichella, A., Colizzi, E., Provenzano, S., Lauretani, F., Luci, M., Ceresini, G., Dall, E., Caffarra, P., Valenti, G. & Paolo, G. DHEA and cognitive function in the elderly. *J. Steroid Biochem. Mol. Biol.* **145,** 281–292 (2015).

49. Stárka, L., Dusková, M. & Hill, M. Dehydroepiandrosterone: A neuroactive steroid. *J. Steroid Biochem. Mol. Biol.* **145,** 254–260 (2015).

50. Hill, M., Dusková, M. & Stárka, L. Dehydroepiandrosterone, its metabolites and ion channels. *J. Steroid Biochem. Mol. Biol.* **145,** 293–314 (2014).

51. Kihel, L. El. Oxidative metabolism of dehydroepiandrosterone (DHEA) and biologically active oxygenated metabolites of DHEA and epiandrosterone (EpiA) - Recent reports. *Steroids* **77,** 10–26 (2012).

52. Cui, H.-W., Pengb, S., Gu, X.-Z., Chen, H., He, Y., Gao, W., Lv, F., Wang, J.-H., Wang, Y., Xie, J., Liu, M.-Y. & Yi, Z. Synthesis and biological evaluation of of D-ring fused 1,2,3-thiadiazole dehydroepiandrosterone derivatives as antitumor agents. *Eur. J. Med. Chem.* **111,** 126–137 (2016).

53. Vosooghi, M., Yahyavi, H., Divsalar, K., Shamsa, H., Kheirollahi, A., Safavi, M., Ardestani, S. K., Sadeghi-Neshat, S., Mohammadhosseini, N., Edraki, N., Khoshneviszadeh, M., Shafiee, A. & Foroumadi, A. Synthesis and In vitro cytotoxic activity evaluation of (E)-16-(substituted benzylidene) derivatives of dehydroepiandrosterone. *Daru* **21,** 34 (2013).

54. Ke, S., Wei, Y., Shi, L., Yang, Q. & Yang, Z. Synthesis of Novel Steroid Derivatives Derived from Dehydroepiandrosterone as Potential Anticancer Agents. *Anticancer. Agents Med. Chem.* **13,** 1291–1298 (2013).

55. Kaur, N., Chaudhary, J., Jain, A. & Kishore, L. Stigmasterol: A comprehensive review. *Int. J. Phamaceutical Sci. Res.* **2,** 2259–2265 (2011).

56. Piironen, V., Lindsay, D. G., Miettinen, T. A., Toivo, J. & Lampi, A. Review Plant sterols : biosynthesis , biological function and their importance to human nutrition. **966,** (2000).

57. Ibrahim, S. R. M., Elkhayat, E. S., Mohamed, G. A., Khedr, A. I. M., Fouad, M. A., Kotb, M. H. R. & Ross, S. A. Aspernolides F and G, new butyrolactones from the endophytic fungus Aspergillus terreus. *Phytochem. Lett.* **14,** 84–90 (2015).

58. Petrera, E., Níttolo, A. G. & Alché, L. E. Antiviral Action of Synthetic Stigmasterol Derivatives on Herpes Simplex Virus Replication in Nervous Cells in Vitro. *Biomed Res. Int.* **2014,** 1–9 (2014).

59. Patel, K., Gadewar, M., Tahilyani, V. & Patel, D. K. A review on pharmacological and analytical aspects of diosgenin: a concise report. *Nat. Prod. Bioprespective* **2,** 46–52 (2012).

60. Singh, M. Hamid, A., Maurya, A., Prakash, O., Khan, F., Kumar, A., Aiyelaagbe, O. O., Negi, A. S. & Bawankule, D. U. Synthesis of diosgenin analogues as potential anti-inflammatory agents. *J. Steroid Biochem. Mol. Biol.* **143,** 323–333 (2014).

61. Wei, G., Jun, X., Gao, Y., Jia, Y. & Ming, J. New polyhydroxylated metabolite derived from biotransformation of diosgenin by the white-rot fungus Coriolus versicolor. *Chinese Chem. Lett.* **21,** 446–448 (2010).

62. Rees, M. & Medicine, R. Best Practice & Research Clinical Obstetrics and Gynaecology Alternative treatments for the menopause. *Best Pract. Res. Clin. Obstet. Gynaecol.* **23,** 151–161 (2009).

63. Meagher, L. P., Smith, B. L. & Wilkins, A. L. Metabolism of diosgenin-derived saponins: implications for hepatogenous photosensitization diseases in ruminants. *Anim. Feed Sci. Technol.* **91,** 157–170 (2001).

64. Hamid, A. A., Hasanain, M., Singh, A., Bhukya, B., Omprakash, Vasudev, P. G., Sarkar, J., Chanda, D., Khan, F., Aiyelaagbe, O. O. & Negi, A. S. Synthesis of novel anticancer agents through opening of spiroacetal ring of diosgenin. *Steroids* **87,** 108–118 (2014).

65. Lu, X.-F. Yang, Z., Huang, N.-Y., He, H.-B., Deng, W.-Q. & Zou, K. Synthesis and cytotoxic activities of 2-substituted (25R)-spirostan-1,4,6-triene-3-ones via ring-opening/elimination and 'click' strategy. *Bioorg. Med. Chem. Lett.* **25,** 3726–9 (2015).

66. Montiel-Smith, S., Romero-Hern, L. L., Vega-Báez, J. L.. Abasolo, I., Schwartz Jr., S., Lopez, Ó. & Fernández-Bolaños, J. G. Diosgenin-based thio (seleno) ureas and triazolyl

glycoconjugates as hybrid drugs . Antioxidant and antiproliferative pro fi le. *Eur. J. Med. Chem.* **99,** 67–81 (2015).

67. Chang, L. C., Bhat, K. P. L., Pisha, E., Kennelly, E. J., Fong, H. H. S. & Pezzuto, J. M. Activity-Guided Isolation of Steroidal Alkaloid Antiestrogen-Binding Site Inhibitors from Pachysandra procumbens. *J. Nat. Prod.* **61,** 1257–1262 (1998).

68. Ke, S., Shi, L. & Yang, Z. Discovery of novel isatin–dehydroepiandrosterone conjugates as potential anticancer agents. *Bioorg. Med. Chem. Lett.* **25,** 4628–4631 (2015).

69. Zu, L., Zhao, Y. & Gu, G. Recent Development in the Synthesis of Natural Saponins and Their Derivatives Recent Development in the Synthesis of Natural Saponins and Their Derivatives. **8303,** (2015).

70. Newman, D. J. & Cragg, G. M. Natural Products as Sources of New Drugs from 1981 to 2014. *J. Nat. Prod.* **79,** 629–661 (2016).

71. Man, S., Gao, W., Zhang, Y., Huang, L. & Liu, C. Chemical study and medical application of saponins as anti-cancer agents. *Fitoterapia* **81,** 703–714 (2010).

72. Podolak, I., Galanty, A. & Sobolewska, D. Saponins as cytotoxic agents : a review. *Phytochem. Rev.* **9,** 425–474 (2010).

73. Fernández-Herrera, M. A., López-muñoz, H., Hernández-Vázquez, J. M. V., Sánchez-Sánchez, L., Escobar-Sánchez, M. L., Pinto, B. M. & Sandoval-Ramírez, J., Synthesis and selective anticancer activity of steroidal glycoconjugates. *Eur. J. Med. Chem.* **54,** 721–727 (2012).

74. Siu, F., Cheung, Y., Lok, C., Yan, K., Yang, Z., Yang, M., Xu, S., Ko, B. C., He, Q. & Che, C. Proteomic and transcriptomic study on the action of a cytotoxic saponin (Polyphyllin D): Induction of endoplasmic reticulum stress and mitochondria- mediated apoptotic pathways. *Proteomics* **8,** 3105–3117 (2008).

75. Rong-Tsun, W., Chiang, H., Fu, W., Chien, K., Chung, Y. & Horng, L. Formosanin-C, an immunomodulator with antitumour activity. *Int. Soc. J. Immunopharmacol.* **12,** 777–786 (1990).

76. Cai, J., Liu, M., Wang, Z. & Ju, Y. Apoptosis Induced by Dioscin in Hela Cells. *Biol. Pharm. Bull.* **25,** 193–196 (2002).

77. Hu, K., Dong, A., Yao, X., Kobayashi, H. & Iwasaki, S. Antineoplastic Agents II. Four Furostanol Glycosides from Rhyzomes of Discorea collettii var. hypoglauca. *Planta Med.* **63,** 161–165 (1997).

78. Song, G., Yang, S., Zhang, W. & Cao, Y. Discovery of the First Series of Small Molecule H5N1 Entry Inhibitors. *J. Med. Chem.* **52,** 7368–7371 (2009).

79. Cui, J.-M. *Kang, L.-P., Zhao, Y., Zhao, J.-Y., Zhang, J., Pang, X., Yu, H.-S., Jia, D.-X., Liu,*

C., Yu, L.-Y. & *Ma, B.-P.* Steroidal Saponins from the Rhizomes of Aspidistra typica. *PLoS One* **11,** 1–15 (2016).

80. Arthan, D. *Svasti, J., Kittakoop, P., Pittayakhachonwut, D., Tanticharoen, M.* & *Thebtaranonth, Y.* Antiviral isoflavonoid sulfate and steroidal glycosides from the fruits of Solanum torvum. *Phytochemistry* **59,** 459–463 (2002).

81. Sadeghi, M., Zolfaghari, B., Senatore, M. & Lanzotti, V. Spirostane, furostane and cholestane saponins from Persian leek with antifungal activity. *Food Chem.* **141,** 1512–1521 (2013).

82. Lunga, I., Bassarello, C., Kintia, P., Shvets, S., Piacente, S. & Pizza, C. Steroidal glycosides from the seeds of Hyoscyamus niger L. *Nat. Prod. Commun.* **3,** 731–734 (2008).

83. Walczewska, A. *Grzywacz, D., Bednarczyk, D., Nowacki, A., Kamysz, W., Liberek, B.* & *Myszka, H.* N -Alkyl derivatives of diosgenyl 2-amino-2-deoxy- ß -D-gluco- pyranoside ; synthesis and antimicrobial activity. *J. Org. Chem.* **11,** 869–874 (2015).

84. Xiang, L., Wang, Y., Yi, X., Feng, J. & He, X. Furospirostanol and spirostanol saponins from the rhizome of Tupistra chinensis and their cytotoxic and anti-inflammatory activities. *Tetrahedron* **72,** 134–141 (2016).

85. Wang, W. & Meng, H. Cytotoxic, anti-inflammatory and hemostatic spirostane-steroidal saponins from the ethanol extract of the roots of Bletilla striata. *Fitoterapia* **101,** 12–18 (2015).

86. Pérez-Labrada, K., Brouard, I., Estévez, S., Marrero, M. T., Estévez, F., Bermejo, J. & Rivera, D. G. New insights into the structure-cytotoxicity relationship of spirostan saponins and related glycosides. *Bioorganic Med. Chem.* **20,** 2690–2700 (2012).

87. Zhang, Y., Li, Y., Guo, T., Guan, H. & Shi, J. Syntheses of chlorogenin 6α- O -acyl-3- O -ß-chacotriosides and their antitumor activities. **340,** 1453–1459 (2005).

88. Lahmann, M., Gyba, H., Garegg, P. J. & Oscarson, S. A facile approach to diosgenin and furostan type saponins bearing a 3ß-chacotriose moiety. **337,** 2153–2159 (2002).

89. Chen, P., Wang, P., Song, N. & Li, M. Convergent synthesis and cytotoxic activities of 26-thio- and selenodioscin. *Steroids* **78,** 959–966 (2013).

90. Zan, X., Gao, J., Gu, G., Liu, S., Sun, B., Liu, L. & Lou, H. Synthesis and cytotoxic effect of pseudodiosgenyl saponins with thio-ring F. *Bioorg. Med. Chem. Lett.* **24,** 1600–1604 (2014).

91. Pérez-labrada, K., Zan, X., Gao, J., Gu, G., Liu, S., Sun, B., Liu, L. & Lou, H. Effect of C-ring modifications on the cytotoxicity of spirostan saponins and related glycosides. Bioorg. Med. Chem. **20,** 4522–4531 (2012).

92. Chun, J., Han, L. & Ying, M. The induction of apoptosis by a newly synthesized diosgenyl saponin through the suppression of estrogen receptor- a in MCF-7 human breast cancer cells.

Arch. Pharm. Res. **37,** 1477–1486 (2014).

93. Wang, B., *Chun, J., Liu, Y., Han, L., Wang, Y.S., Joo, E.-J., Kim, Y.-S.* & *Cheng, M.-S.* Synthesis of novel diosgenyl saponin analogues and apoptosis-inducing activity on A549 human lung adenocarcinoma. *Org. Biomol. Chem.* **10,** 8822 (2012).

94. Raju, J., Patlolla, J. M. R., Swamy, M. V & Rao, C. V. Diosgenin , a Steroid Saponin of Trigonella foenum graecum (Fenugreek), Inhibits Azoxymethane-Induced Aberrant Crypt Foci Formation in F344 Rats and Induces Apoptosis in HT-29 Human Colon Cancer Cells. **13,** 1392–1399 (2004).

95. Kuroda, M., Kubo, S., Matsuo, Y., Atou, T., Satoh, J., Fujino, T., Hayakawa, M. & Mimaki, Y. New Cardenolide Glycosides from the Seeds of Digitalis purpurea and Their Cytotoxic Activity. *Biosci Biotechnol Biochem* **77,** 1186–1192 (2013).

96. Morzycki, J. W. & Wojtkielewicz, A. Synthesis of a highly potent antitumor saponin OSW-1 and its analogues. *Phytochem. Rev.* **4,** 259–277 (2005).

97. Mohamed, N. H., Liu, M., Abdel-Mageed, W. M., Alwahibi, L. H., Dai, H., Ismail, M. A., Badr, G., Quinn, R. J., Liu, X., Zhang, L. & Shoreit, A. A. M. Cytotoxic cardenolides from the latex of Calotropis procera. *Bioorganic Med. Chem. Lett.* **25,** 4615–4620 (2015).

98. Fujino, T., Kuroda, M., Matsuo, Y., Kubo, S., Tamura, C., Sakamoto, N., Mimaki, Y. & Hayakawa, M. Cardenolide glycosides from the seeds of Digitalis purpurea exhibit carcinoma-specific cytotoxicity toward renal adenocarcinoma and hepatocellular carcinoma cells. *Biosci. Biotechnol. Biochem.* **8451,** 1–8 (2014).

99. Zhang, M., Rao, L. L., Xiang, C., Li, B. C. & Li, P. C21 steroidal glycosides from the roots of Cynanchum saccatum. *Steroids* **101,** 28–36 (2015).

100. Komarnytsky, S., Esposito, D., Poulev, A. & Raskin, I. Pregnane glycosides interfere with steroidogenic enzymes to down-regulate corticosteroid production in human adrenocortical H295R cells. *J. Cell. Physiol.* **228,** 1120–1126 (2013).

101. Zheng, D. Guan, Y., Chen, X., Xu, Y., Chen, X. & Lei, P. Synthesis of cholestane saponins as mimics of OSW-1 and their cytotoxic activities. *Bioorg. Med. Chem. Lett.* **21,** 3257–3260 (2011).

102. Morzycki, J. W. & Wojtkielewicz, A. Synthesis of a cholestane glycoside OSW-1 with potent cytostatic activity. *Carbohydr. Res.* **337,** 1269–1274 (2002).

103. Sakurai, K., Takeshita, T., Hiraizumi, M. & Yamada, R. Synthesis of OSW-1 derivatives by site-selective acylation and their biological evaluation. *Org. Lett.* **16,** 6318–6321 (2014).

104. Ma, X., Yu, B., Hui, Y., Xiao, D. & Ding, J. Synthesis of glycosides bearing the disaccharide of OSW-1 or its 1 " 4-linked analogue and their antitumor activities. **329,** 495–505 (2000).

105. Tang, Y., Li, N., Duan, J. A. & Tao, W. Structure, bioactivity, and chemical synthesis of OSW-

1 and other steroidal glycosides in the genus ornithogalum. *Chem. Rev.* **113,** 5480–5514 (2013).

106. Kim, K. Maharjan, S., Lim, C., Kim, N., Agrawal, V., Taek, Y., Lee, S., An, H., Yun, H., Choi, H., Kwon, Y. & Suh, Y. Glucal-conjugated sterols as novel vascular leakage blocker : Structure e activity relationship focusing on the C 17 -side chain. *Eur. J. Med. Chem.* **75,** 184–194 (2014).

107. Maslov, M. A., Morozova, N. G., Chizhik, E. I., Rapoport, D. A., Ryabchikova, E. I., Zenkova, M. A. & Serebrennikova, G. A. Synthesis and delivery activity of new cationic cholesteryl glucosides. *Carbohydr. Res.* **345,** 2438–2449 (2010).

108. Pelin, M., Della, R., Tubaro, A. & Sosa, S. Phytochemistry Steroids with anti-inflammatory activity from Vernonia nigritiana Oliv . &. *Phytochemistry* **96,** 288–298 (2013).

109. Guevara, A. P., Lim-Sylianco, C., Dayrit, F. & Finch, P. Antimutagens from Momordica charantia. *Mutat. Res. Mol. Mech. Mutagen.* **230,** 121–126 (1990).

110. Khabazian, I., Bains, J. S., Williams, D. E., Cheung, J., Wilson, J. M. B., Pasqualotto, B. A., Pelech, S. L., Andersen, R. J., Wang, Y., Liu, L., Nagai, A., Kim, S. U., Craig, U.-K. & Shaw, C. A. Isolation of various forms of sterol β - *D* -glucoside from the seed of Cycas circinalis : neurotoxicity and implications for ALS-parkinsonism dementia complex. *J. Neurochem.* **82,** 516–528 (2002).

111. Richmond, V., Santos, G. A. G., Murray, A. P. & Maier, M. S. Synthesis and acetylcholinesterase inhibitory activity of 2β,3α-disulfoxy-5α-cholestan-6-one. *Steroids* **76,** 1160–1165 (2011).

112. Sartori, G., Ballini, R., Bigi, F., Bosica, G., Maggi, R. & Righi, P. Protection (and Deprotection) of Functional Groups in Organic Synthesis by Heterogeneous Catalysis. *Chem. Rev.* **104,** 199–250 (2004).

113. Sánchez-Fernández, E. M., Rísquez-Cuadro, R., Ortiz Mellet, C., García Fernández, J. M., Nieto, P. M. & Angulo, J. sp^2-Iminosugar O-, S-, and N-glycosides as conformational mimics of α-linked disaccharides; implications for glycosidase inhibition. *Chem. Eur.J.* **18,** 8527–8539 (2012).

114. Dax, K., Gaigg, B., Grassberger, V., Kölblinger, B. & Stütz, A. E. Einfache Synthesen von 1.5-didesoxy-1.5-imino-*D*-glucit (1-desoxynojirimycin) und 1,6-didesoxy-1,6-imino-*D*-glucit aus *D*-glucofuranurono-6.3-lacton. *J. Carbohydr. Chem.* **9,** 479–499 (1990).

115. Pavia, D. L., Lampman, G. M. & Kriz, G. S. *Introduction to Spectroscopy- A Guide for Students of Organic Chemistry*. (Saunders College Publishing, 1996).

116. Jagadeesan, J., Langeswaran, K. & Gowthamkumar, S. Diosgenin exhibits beneficial efficiency on human mammary carcinoma cell line MCF-7 and against N-nitroso-N-methylurea (NMU) induced experimental mammary carcinoma. *Biomed. Prev. Nutr.* **3,** 381–388 (2013).

117. Seidl, K. & Zinkernagel, A. S. The MTT assay is a rapid and reliable quantitative method to assess Staphylococcus aureus induced endothelial cell damage. *J. Microbiol. Methods* **92,** 307–

309 (2013).

118. Liederer, B. M. & Borchardt, R. T. Enzymes involved in the bioconversion of ester-based prodrugs. *Journal of Pharmaceutical Sciences* **95,** 1177–1195 (2006).

119. Jozwik, K. M. & Carroll, J. S. Pioneer factors in hormone-dependent cancers. *Nat. Rev. Cancer* **12,** 381–385 (2012).

120. Henry, C. M., Hollville, E. & Martin, S. J. Measuring apoptosis by microscopy and flow cytometry. *Methods* **61,** 90–97 (2013).

121. Santos, A., Sarmento-Ribeiro, A. B., Pedroso De Lima, M. C., Simões, S. & Moreira, J. N. Simultaneous evaluation of viability and Bcl-2 in small-cell lung cancer. *Cytom. Part A* **73,** 1165–1172 (2008).

122. Berman, H. M., *Westbrook, J., Feng, Z., Gilliland, G., Bhat, T.N., Weissig, H., Shindyalov, I.N.* & *Bourne, P.E.* The Protein Data Bank. *Nucleic Acids Res.* **28,** 235–242 (2000).

123. Eslami, M., Hashemianzadeh, S. M., Bagherzadeh, K. & Seyed Sajadi, S. A. Molecular perception of interactions between bis(7)tacrine and cystamine-tacrine dimer with cholinesterases as the promising proposed agents for the treatment of Alzheimer's disease. *J. Biomol. Struct. Dyn.* **1102,** 1–15 (2015).

124. Cheenpracha, S., Jitonnom, J., Komek, M., Ritthiwigrom, T. & Laphookhieo, S. Acetylcholinesterase inhibitory activity and molecular docking study of steroidal alkaloids from Holarrhena pubescens barks. *Steroids* **108,** 92–98 (2016).

125. Cheung, J., Gary, E. N., Shiomi, K. & Rosenberry, T. L. Structures of human acetylcholinesterase bound to dihydrotanshinone i and territrem B show peripheral site flexibility. *ACS Med. Chem. Lett.* **4,** 1091–1096 (2013).

126. Mannu, J., Jenardhanan, P. & Mathur, P. P. A computational study of CYP3A4 mediated drug interaction profiles for anti-HIV drugs. *J. Mol. Model.* **17,** 1847–1854 (2011).

7. Attachments

Attachment 1 - ^{13}C and ^{1}H RMN Spectra

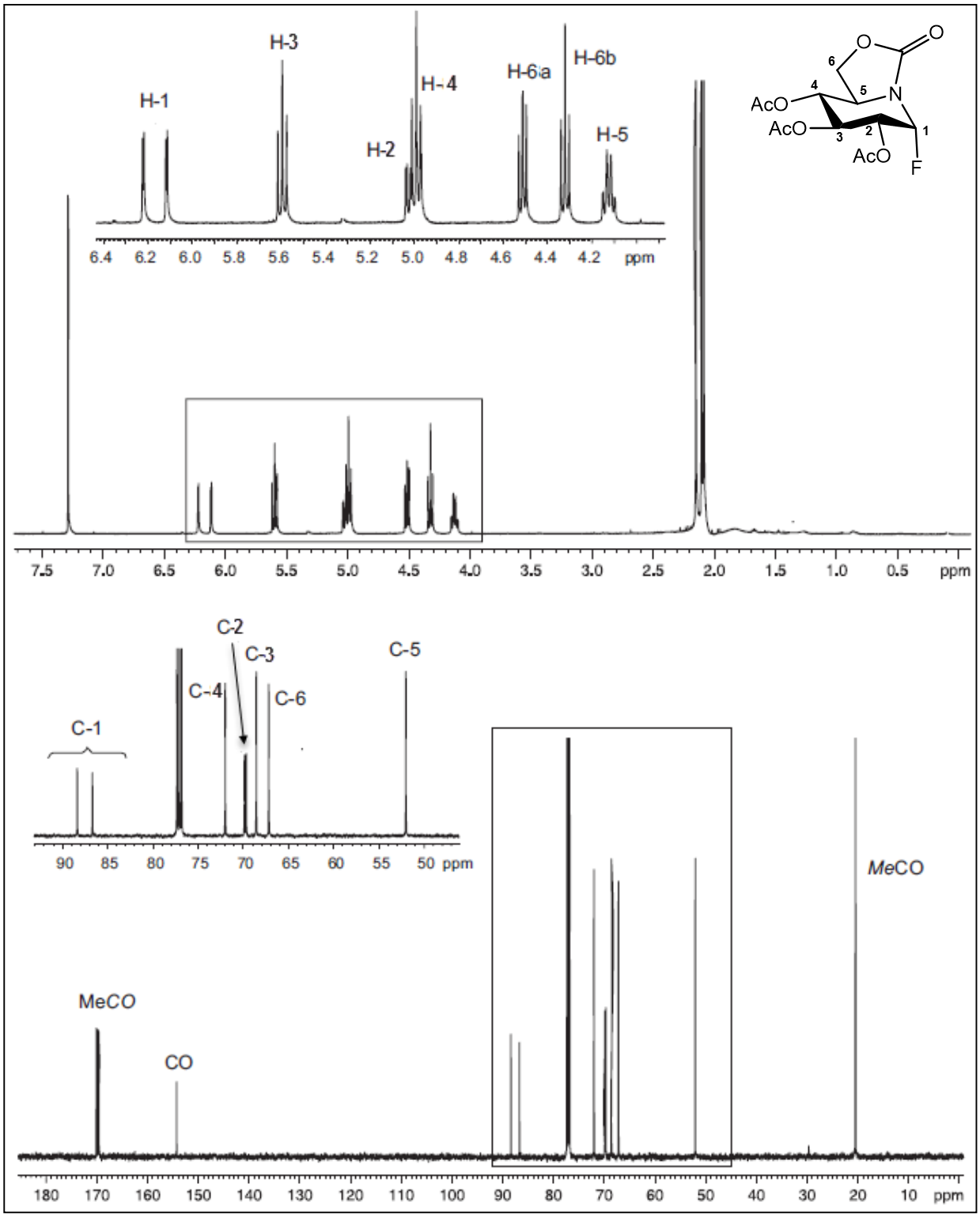

^{1}H and ^{13}C NMR spectra (500 MHz and 125.7 MHz, $CDCl_3$) of 11.

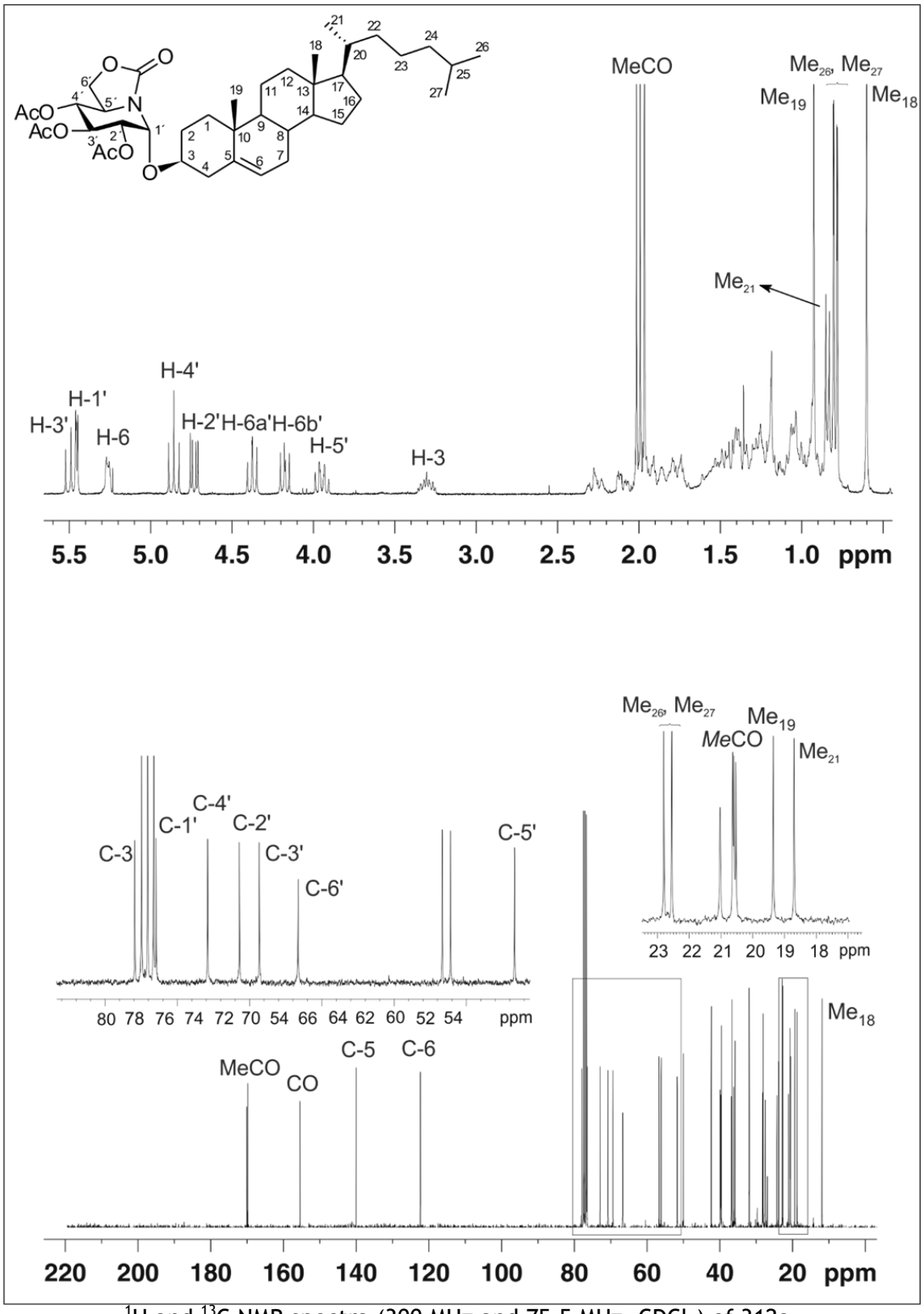

^{1}H and ^{13}C NMR spectra (300 MHz and 75.5 MHz, $CDCl_3$) of 312a.

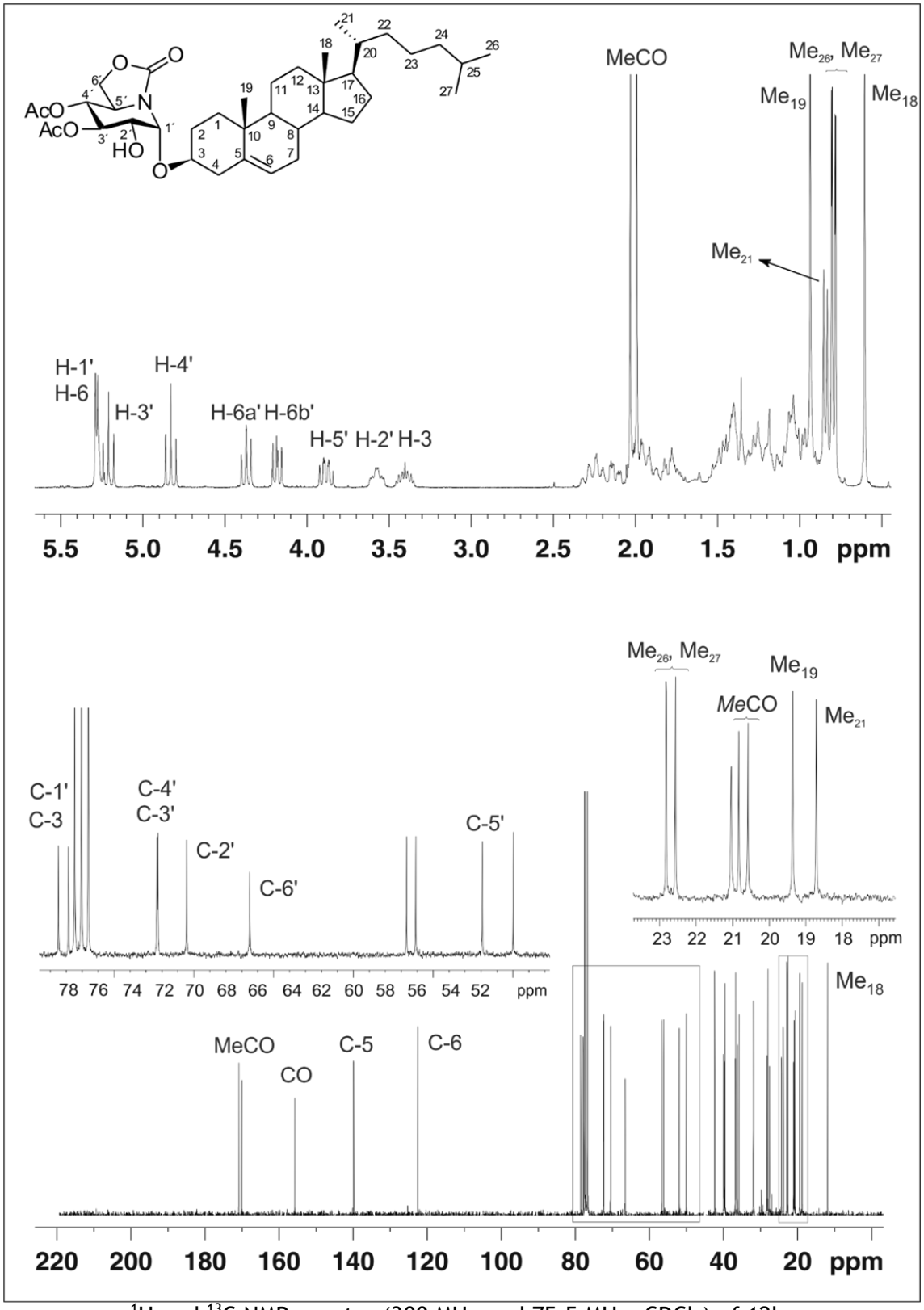

^{1}H and ^{13}C NMR spectra (300 MHz and 75.5 MHz, $CDCl_3$) of 12b.

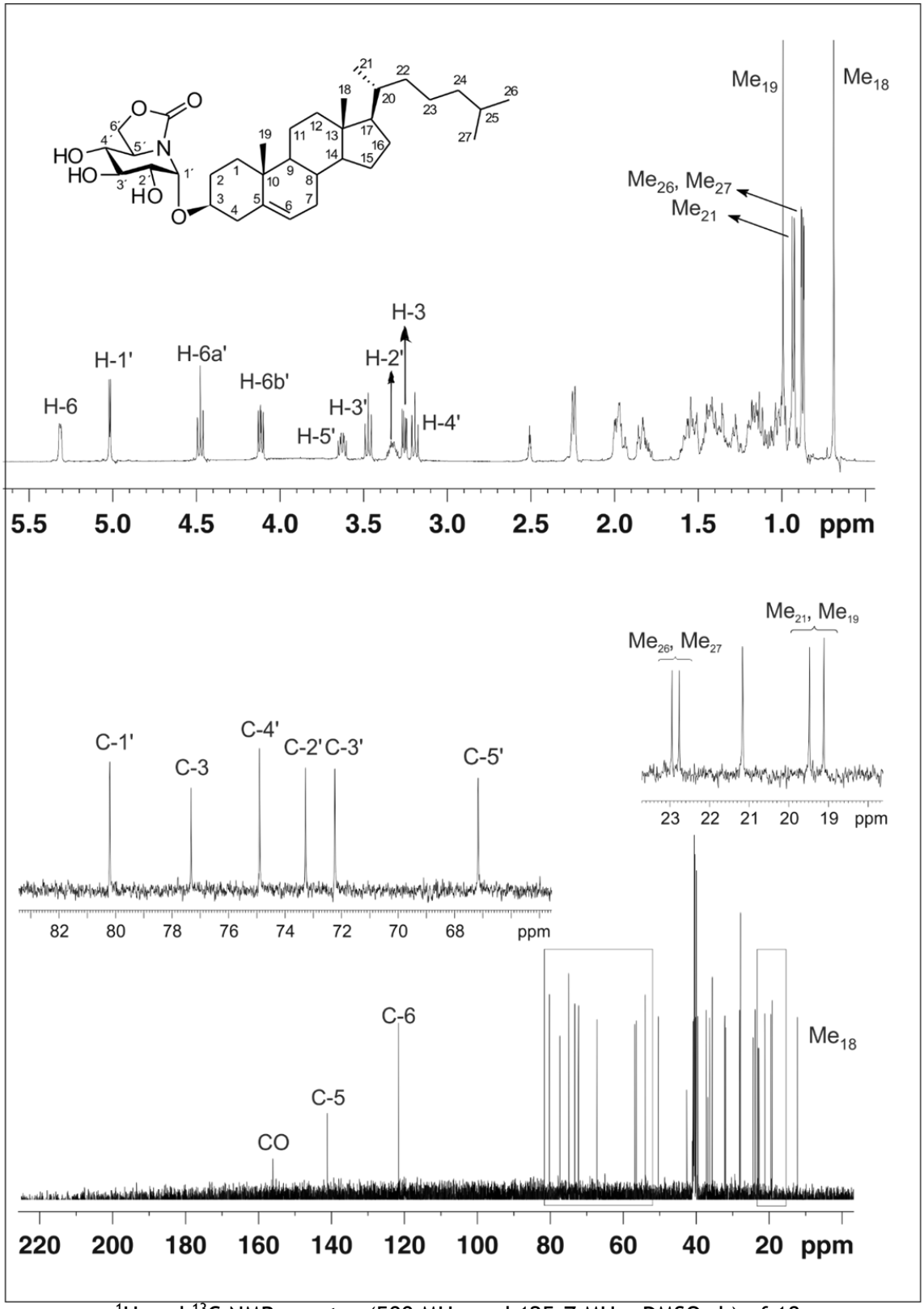

^{1}H and ^{13}C NMR spectra (500 MHz and 125.7 MHz, DMSO-d_6) of 18.

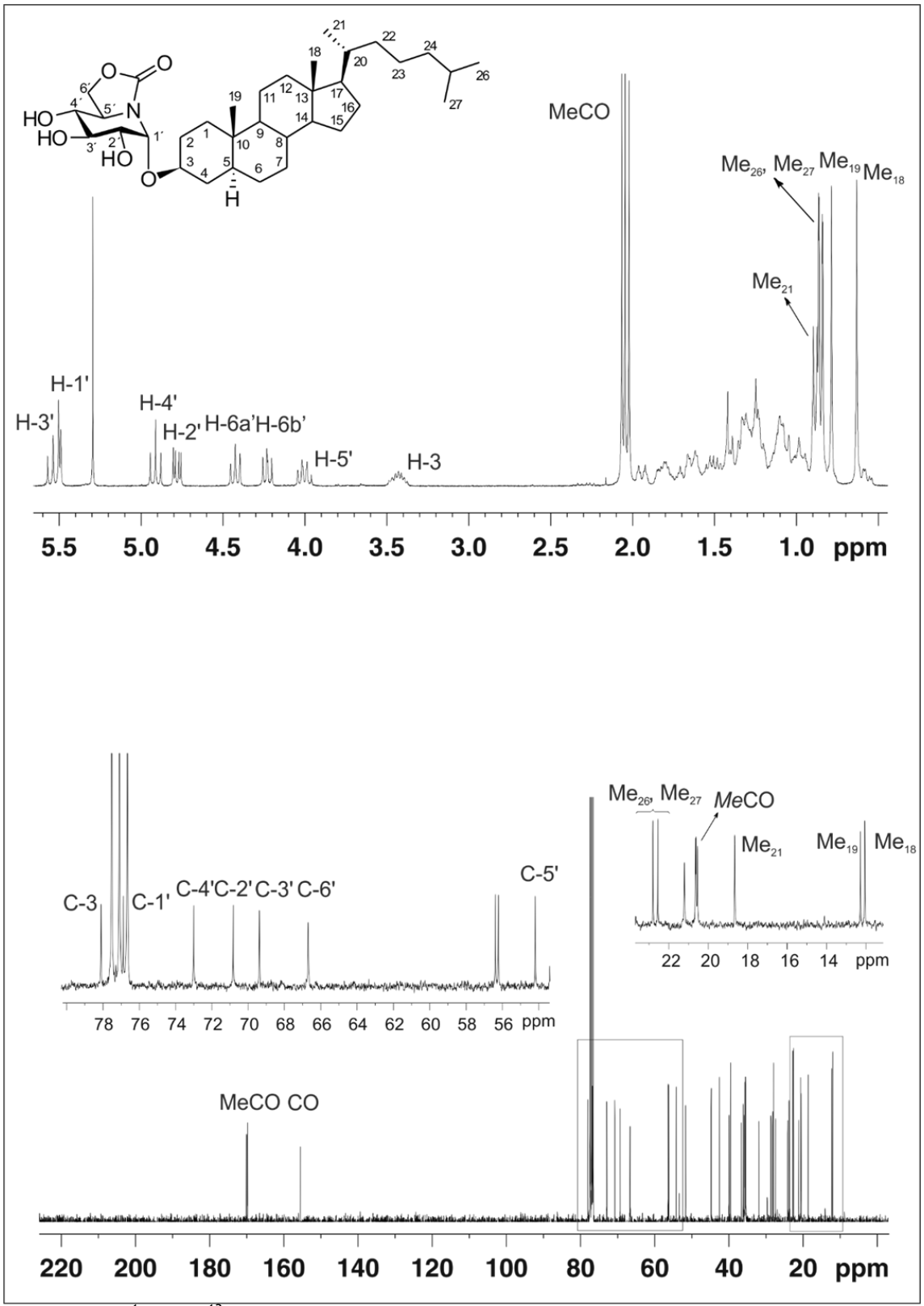

^{1}H and ^{13}C NMR spectra (300 MHz and 75.5 MHz, $CDCl_3$) of 13a.

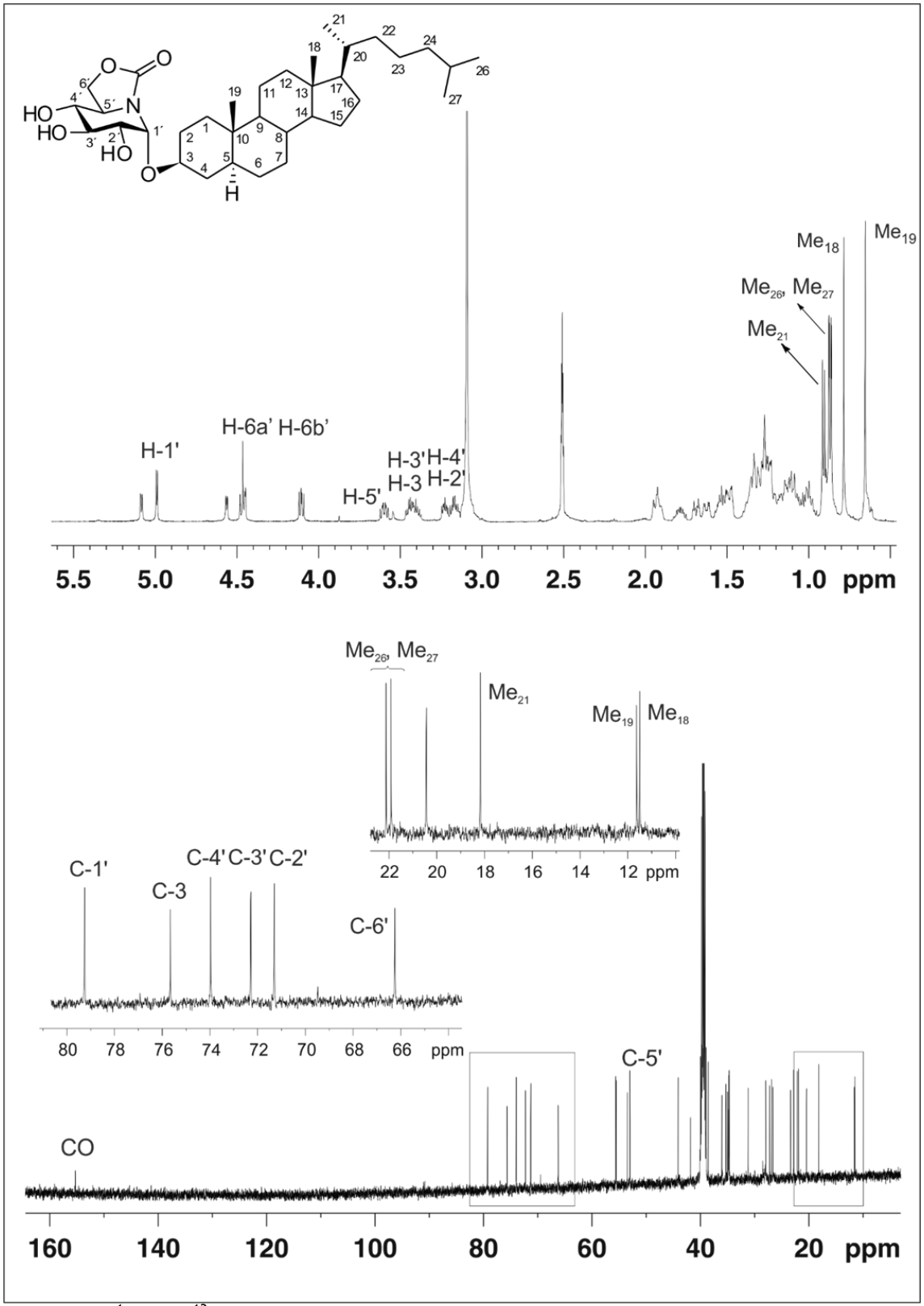

^{1}H and ^{13}C NMR spectra (500 MHz and 125.7 MHz, DMSO-d_6) of 19.

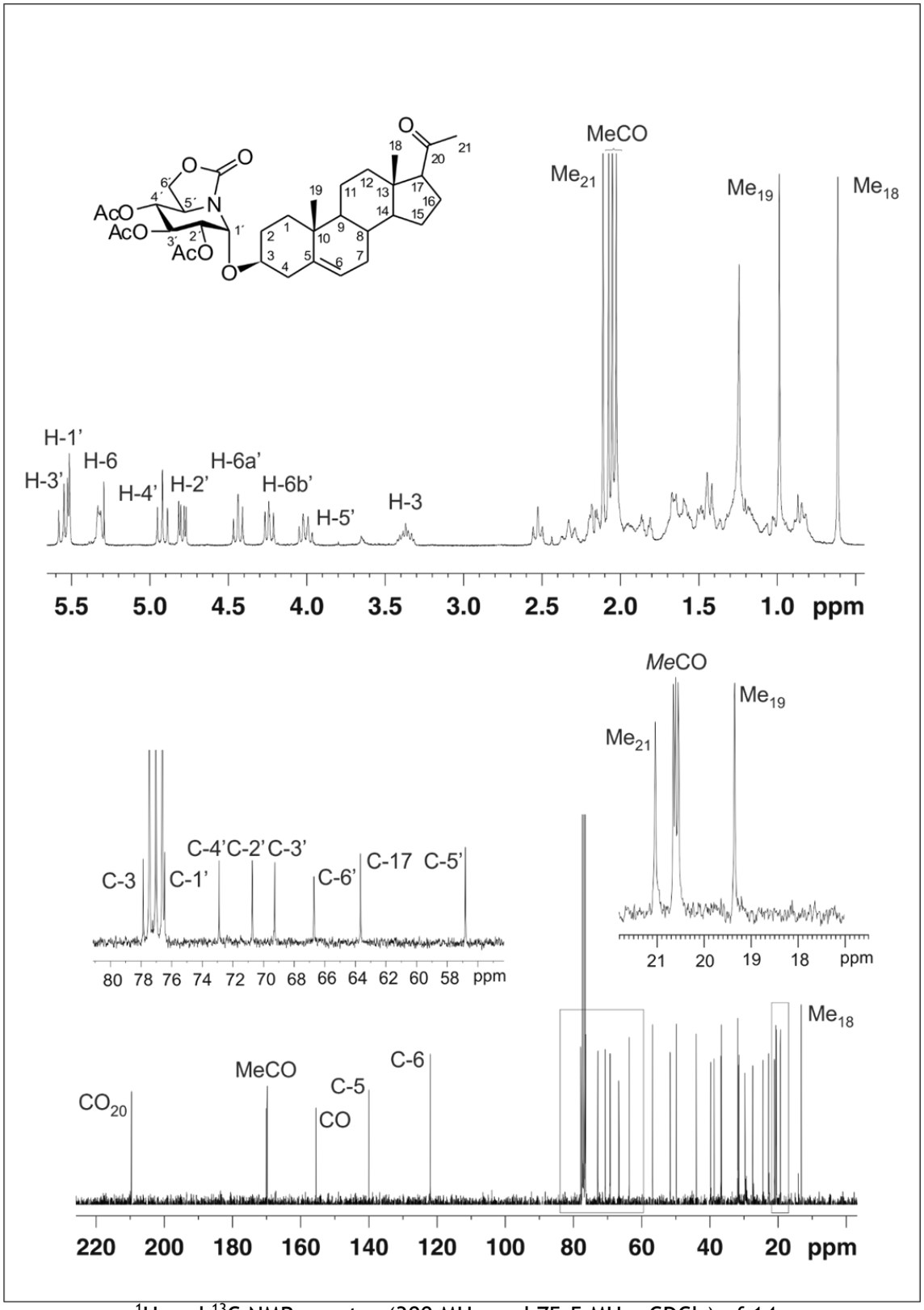

^{1}H and ^{13}C NMR spectra (300 MHz and 75.5 MHz, $CDCl_3$) of 14a

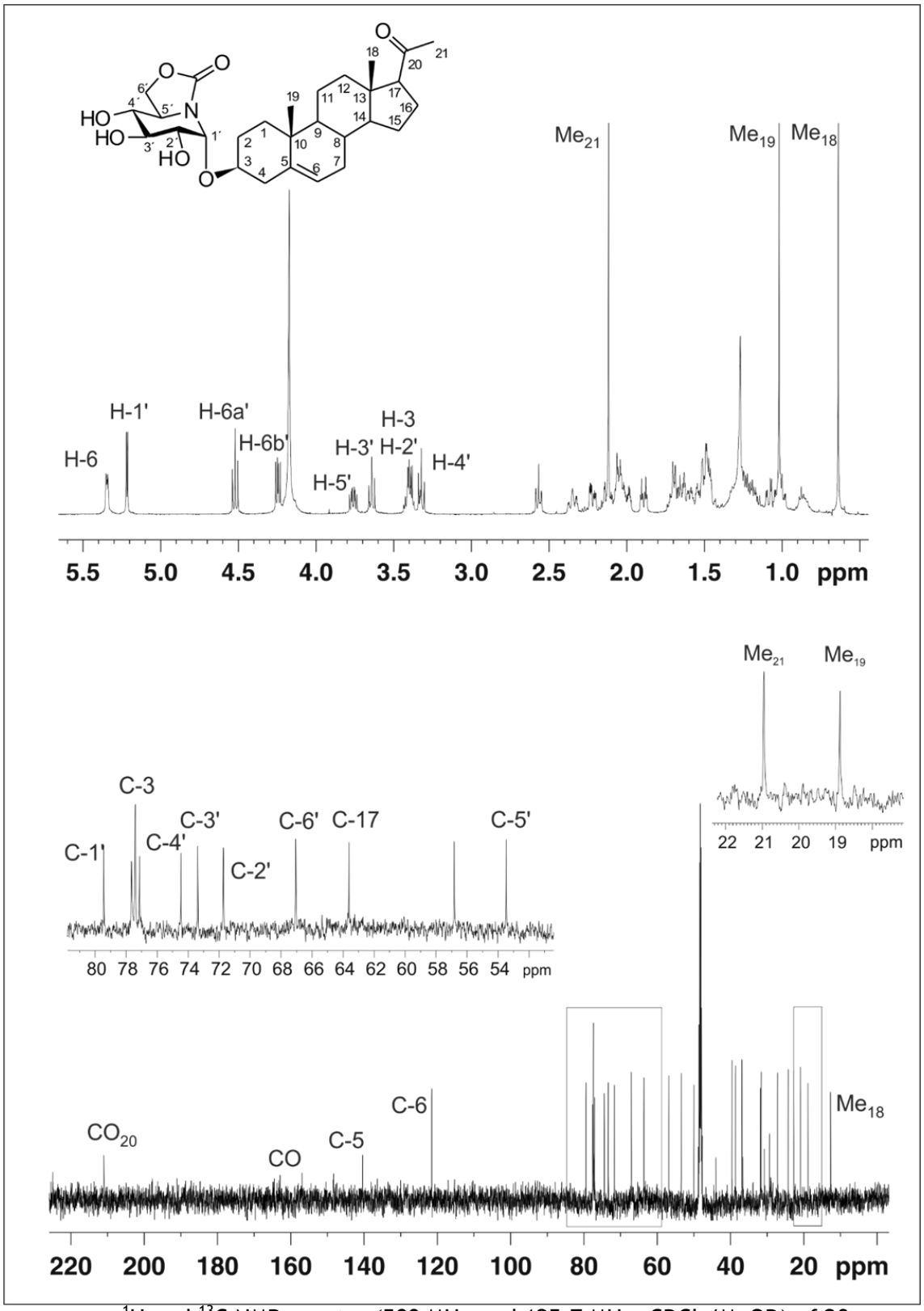

^{1}H and ^{13}C NMR spectra (500 MHz and 125.7 MHz, $CDCl_3$/MeOD) of 20.

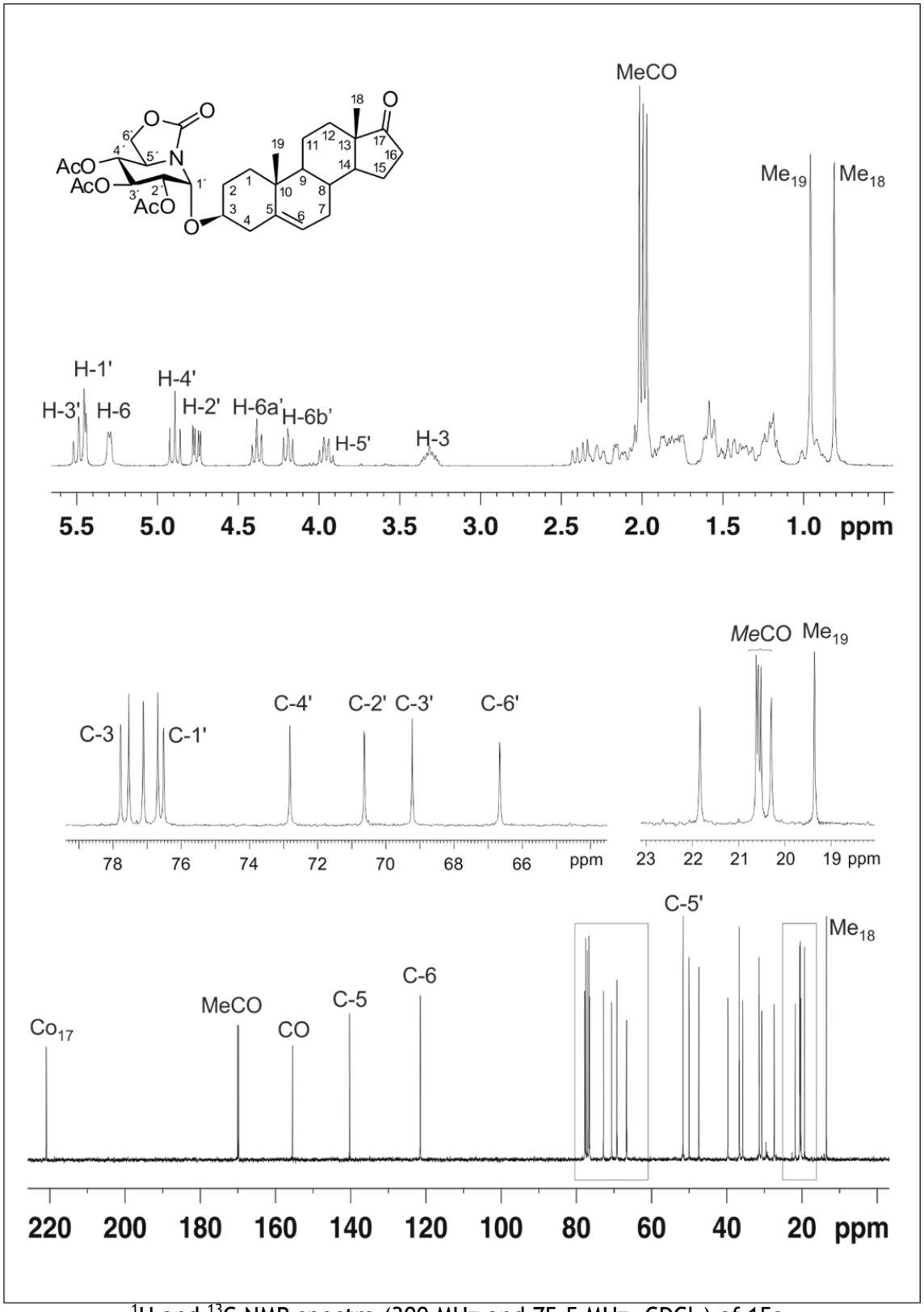

^{1}H and ^{13}C NMR spectra (300 MHz and 75.5 MHz, $CDCl_3$) of 15a.

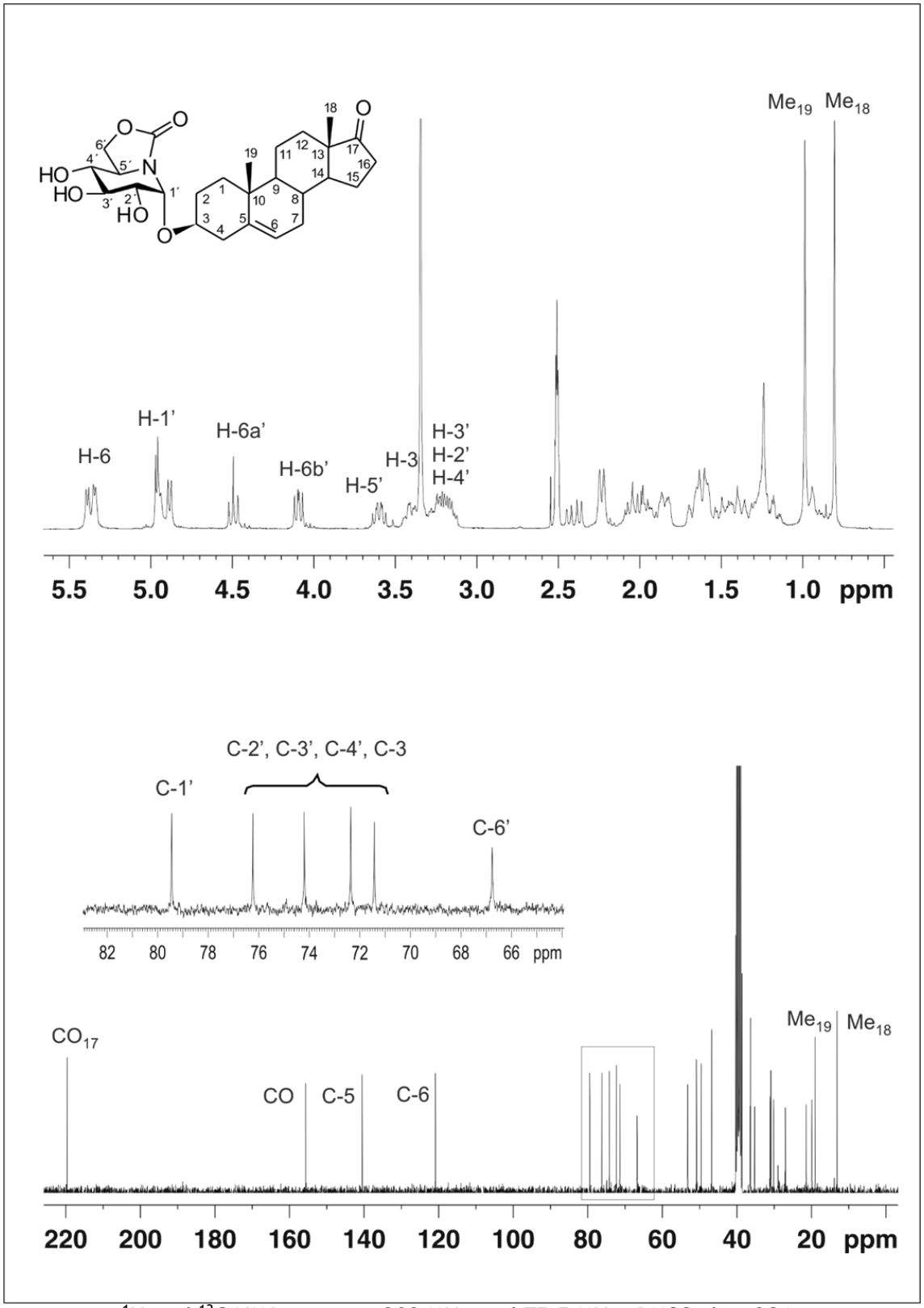

^{1}H and ^{13}C NMR spectra (300 MHz and 75.5 MHz, DMSO-d_6) of 21.

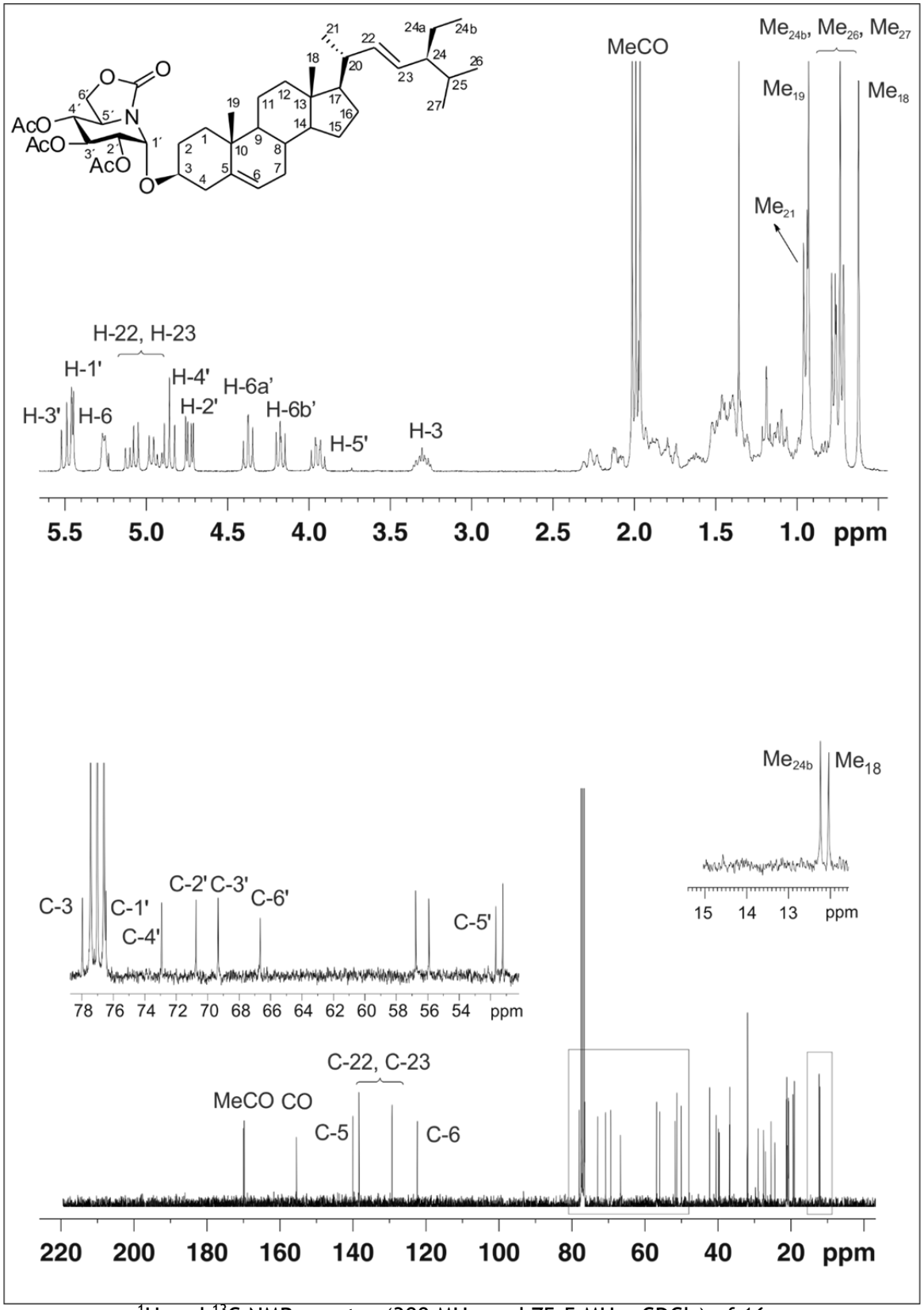

^{1}H and ^{13}C NMR spectra (300 MHz and 75.5 MHz, $CDCl_3$) of 16a.

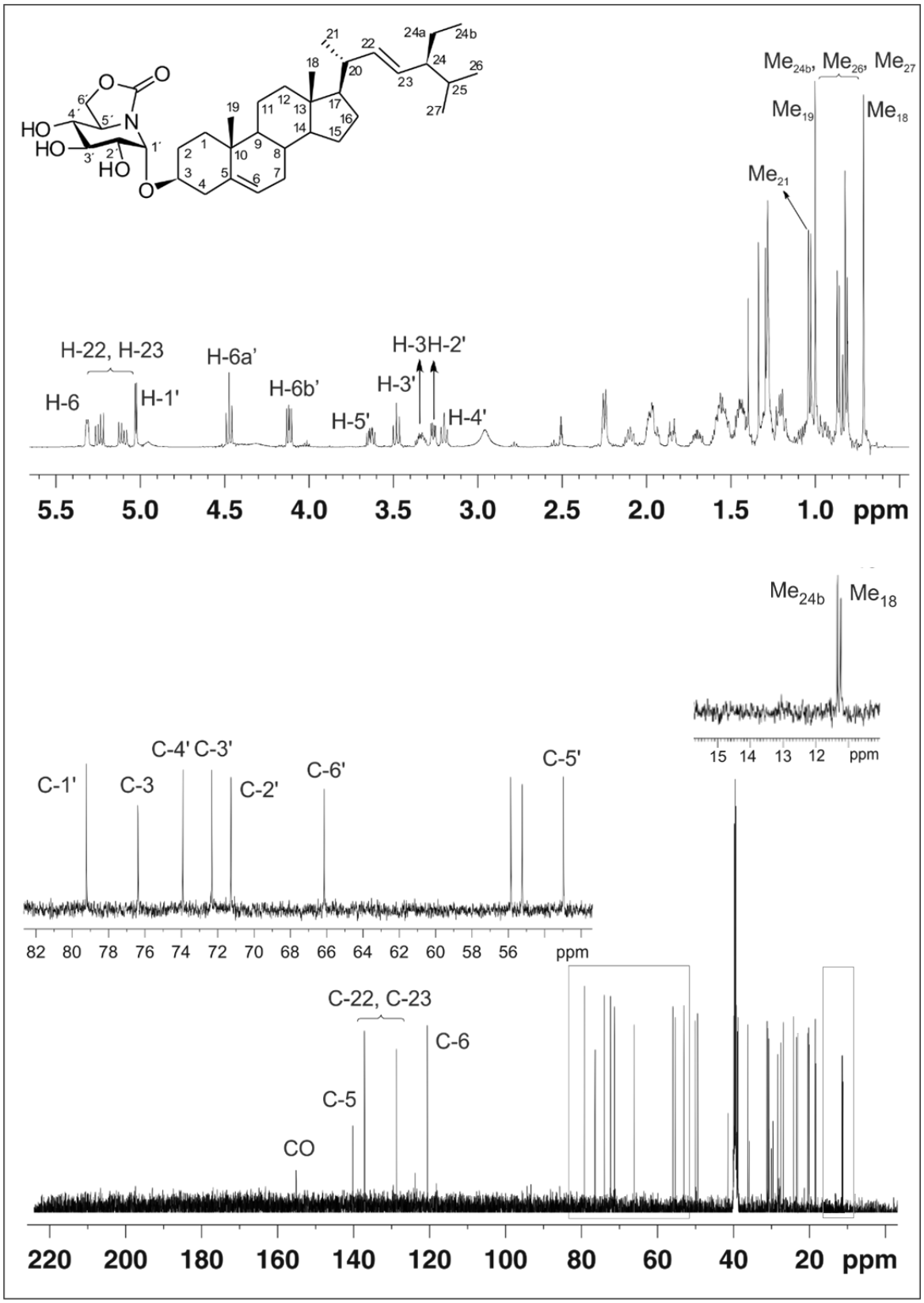

^{1}H and ^{13}C NMR spectra (500 MHz and 125.7 MHz, DMSO-d_6) of 22.

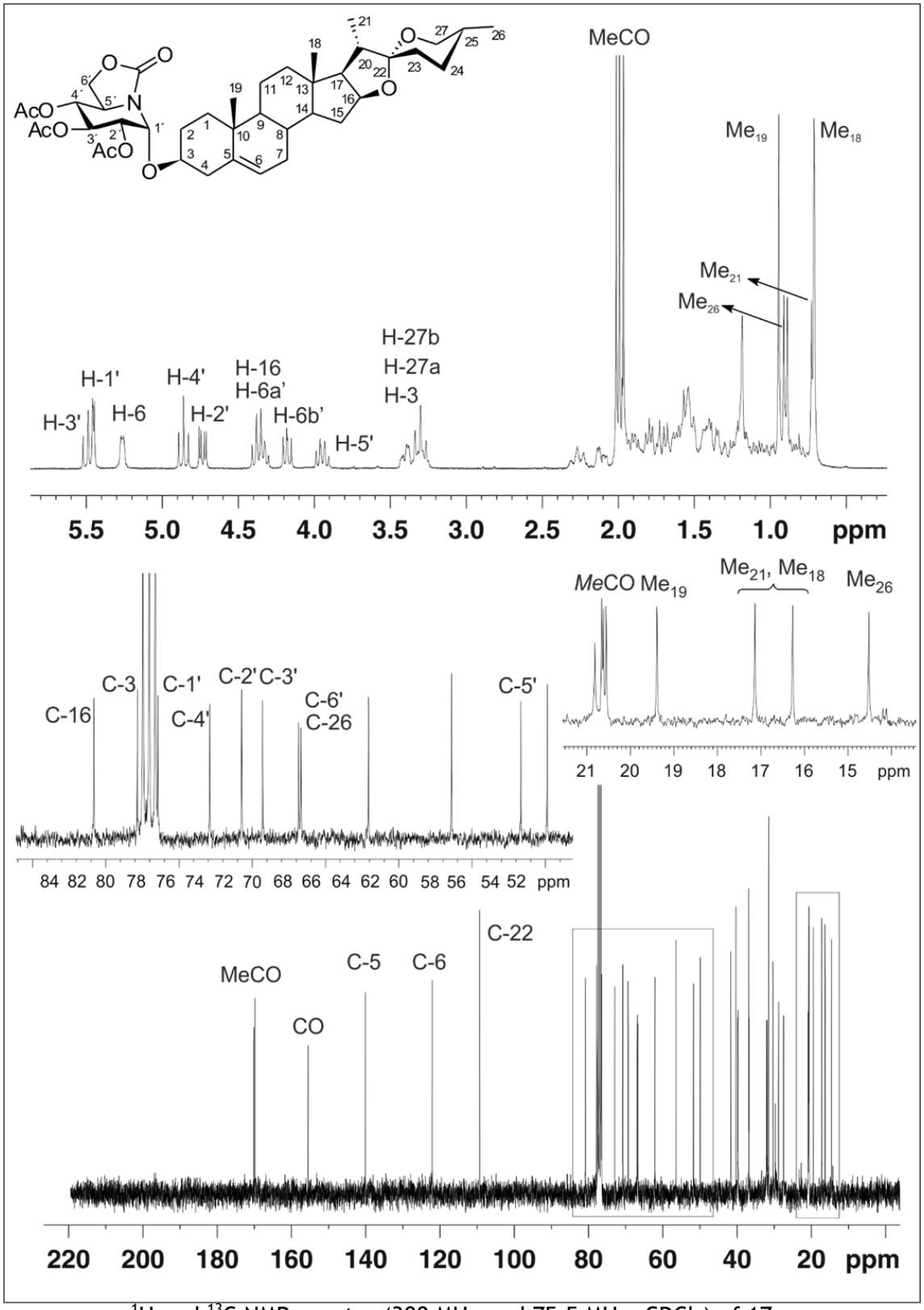

^{1}H and ^{13}C NMR spectra (300 MHz and 75.5 MHz, $CDCl_3$) of 17a.

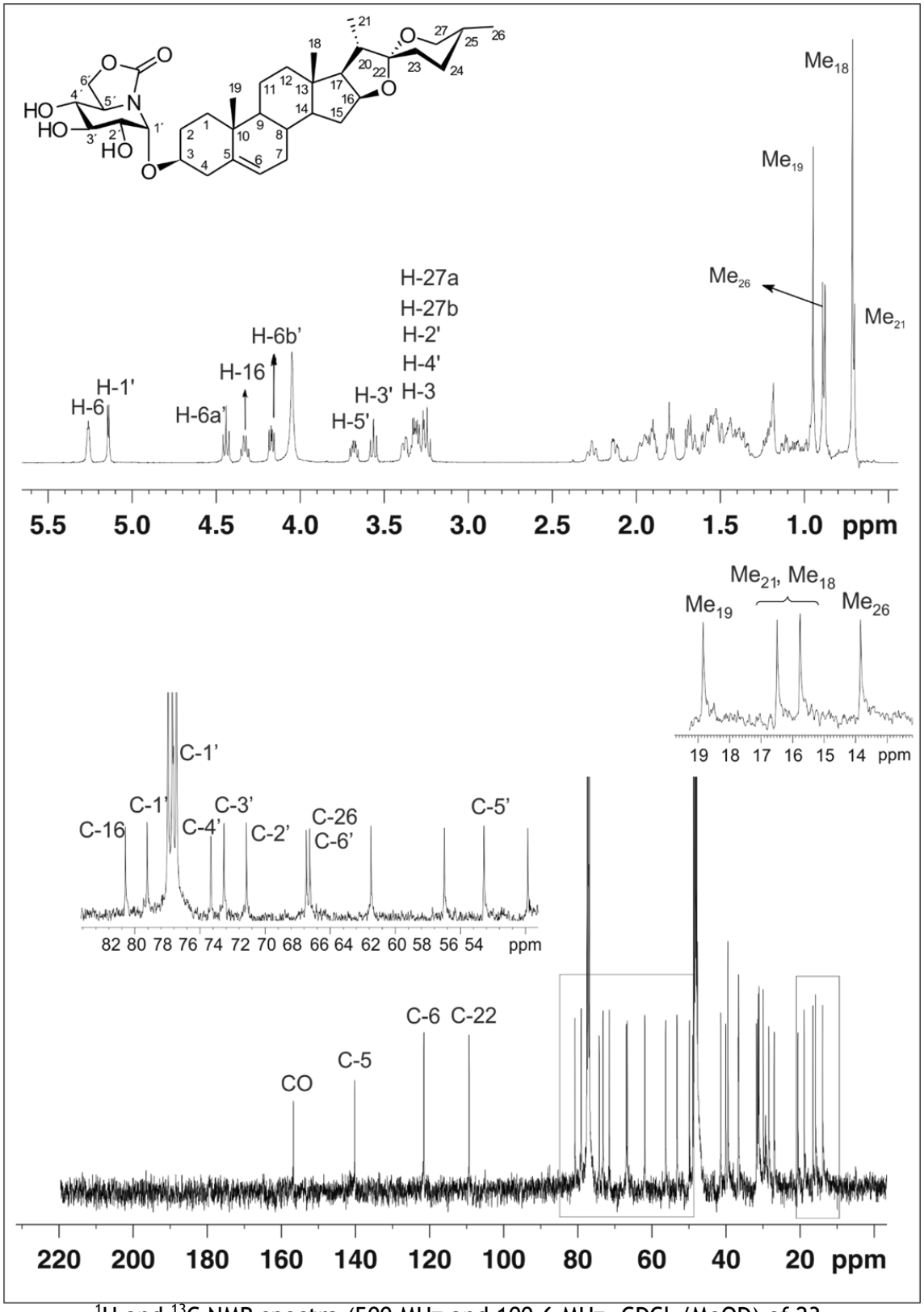

^{1}H and ^{13}C NMR spectra (500 MHz and 100.6 MHz, $CDCl_3$/MeOD) of 23.

Attachment 2 – X-Ray diffraction results

Table 1A | Atomic coordinates (x 10^4) and equivalent isotropic displacement parameters ($Å^2$x 10^3) for 23. U(eq) is defined as one third of the trace of the orthogonalized U^{ij} tensor.

	x	y	z	U(eq)
O(1)	6820(2)	4572(5)	6762(1)	26(1)
O(2)	5492(2)	7125(5)	5736(2)	37(1)
O(3)	6222(2)	4974(5)	4531(1)	35(1)
O(4)	8080(3)	1825(6)	4909(2)	50(1)
O(5)	10231(2)	6361(6)	6262(2)	46(1)
O(6)	9376(2)	9013(6)	6827(2)	44(1)
O(7)	7449(3)	-297(6)	12861(2)	42(1)
N(1)	8457(2)	5814(6)	6367(2)	25(1)
C(1)	7305(3)	6360(7)	6441(2)	24(1)
C(2)	6631(3)	6628(7)	5696(2)	27(1)
C(3)	6751(3)	4571(7)	5244(2)	26(1)
C(4)	7974(3)	3975(8)	5212(2)	32(1)
C(5)	8680(3)	3889(7)	5946(2)	28(1)
C(6)	9961(3)	4176(9)	5957(2)	42(1)
C(7)	9341(3)	7244(8)	6516(2)	31(1)
C(8)	6556(3)	5132(6)	8694(2)	25(1)
C(9)	6227(3)	5375(7)	7893(2)	27(1)
C(10)	7154(3)	4437(7)	7520(2)	26(1)
C(11)	7365(3)	1987(7)	7711(2)	25(1)
C(12)	7644(3)	1643(7)	8507(2)	21(1)
C(13)	8536(3)	460(7)	8784(2)	22(1)
C(14)	8888(3)	10(7)	9561(2)	23(1)
C(15)	7983(3)	639(6)	10014(2)	19(1)
C(16)	7395(3)	2839(6)	9745(2)	20(1)
C(17)	6835(3)	2706(6)	8955(2)	20(1)
C(18)	6578(3)	3665(7)	10240(2)	27(1)
C(19)	7088(3)	3752(6)	11027(2)	23(1)
C(20)	7622(3)	1508(7)	11274(2)	20(1)
C(21)	8501(3)	937(6)	10791(2)	19(1)
C(22)	9207(3)	-950(7)	11179(2)	26(1)
C(23)	9176(3)	-513(9)	11972(2)	37(1)
C(24)	8396(3)	1522(7)	12013(2)	25(1)

C(25)	6713(3)	-291(7)	11263(2)	27(1)
C(26)	5753(3)	1274(7)	8861(2)	24(1)
C(27)	7730(3)	1469(8)	12627(2)	30(1)
C(28)	7421(4)	3669(9)	12914(2)	46(1)
O(8)	3794(3)	4382(6)	6014(2)	44(1)

Table 2A. Bond lengths [Å] and angles [°] for 23.

O(1)-C(1)	1.394(4)	C(8)-H(8A)	0.9900
O(1)-C(10)	1.437(4)	C(8)-H(8B)	0.9900
O(2)-C(2)	1.410(4)	C(9)-C(10)	1.514(5)
O(2)-H(2)	0.8400	C(9)-H(9A)	0.9900
O(3)-C(3)	1.424(4)	C(9)-H(9B)	0.9900
O(3)-H(3)	0.8400	C(10)-C(11)	1.508(6)
O(4)-C(4)	1.412(5)	C(10)-H(10)	1.0000
O(4)-H(4)	0.8400	C(11)-C(12)	1.512(5)
O(5)-C(7)	1.345(5)	C(11)-H(11A)	0.9900
O(5)-C(6)	1.435(6)	C(11)-H(11B)	0.9900
O(6)-C(7)	1.201(5)	C(12)-C(13)	1.317(5)
O(7)-C(27)	1.206(5)	C(12)-C(17)	1.524(5)
N(1)-C(7)	1.351(5)	C(13)-C(14)	1.496(5)
N(1)-C(5)	1.443(5)	C(13)-H(13)	0.9500
N(1)-C(1)	1.445(4)	C(14)-C(15)	1.532(4)
C(1)-C(2)	1.526(5)	C(14)-H(14A)	0.9900
C(1)-H(1)	1.0000	C(14)-H(14B)	0.9900
C(2)-C(3)	1.512(6)	C(15)-C(21)	1.523(5)
C(2)-H(2A)	1.0000	C(15)-C(16)	1.532(5)
C(3)-C(4)	1.518(5)	C(15)-H(15)	1.0000
C(3)-H(3A)	1.0000	C(16)-C(18)	1.540(5)
C(4)-C(5)	1.517(5)	C(16)-C(17)	1.548(5)
C(4)-H(4A)	1.0000	C(16)-H(16)	1.0000
C(5)-C(6)	1.541(5)	C(17)-C(26)	1.536(5)
C(5)-H(5)	1.0000	C(18)-C(19)	1.527(5)
C(6)-H(6A)	0.9900	C(18)-H(18A)	0.9900
C(6)-H(6B)	0.9900	C(18)-H(18B)	0.9900
C(8)-C(9)	1.521(5)	C(19)-C(20)	1.519(5)
C(8)-C(17)	1.541(5)	C(19)-H(19A)	0.9900

C(19)-H(19B)	0.9900	O(1)-C(1)-H(1)	110.7
C(20)-C(25)	1.522(5)	N(1)-C(1)-H(1)	110.7
C(20)-C(21)	1.539(4)	C(2)-C(1)-H(1)	110.7
C(20)-C(24)	1.558(5)	O(2)-C(2)-C(3)	112.2(3)
C(21)-C(22)	1.522(5)	O(2)-C(2)-C(1)	110.4(3)
C(21)-H(21)	1.0000	C(3)-C(2)-C(1)	111.2(3)
C(22)-C(23)	1.536(5)	O(2)-C(2)-H(2A)	107.6
C(22)-H(22A)	0.9900	C(3)-C(2)-H(2A)	107.6
C(22)-H(22B)	0.9900	C(1)-C(2)-H(2A)	107.6
C(23)-C(24)	1.535(6)	O(3)-C(3)-C(2)	109.8(3)
C(23)-H(23A)	0.9900	O(3)-C(3)-C(4)	106.8(3)
C(23)-H(23B)	0.9900	C(2)-C(3)-C(4)	112.9(3)
C(24)-C(27)	1.514(5)	O(3)-C(3)-H(3A)	109.1
C(24)-H(24)	1.0000	C(2)-C(3)-H(3A)	109.1
C(25)-H(25A)	0.9800	C(4)-C(3)-H(3A)	109.1
C(25)-H(25B)	0.9800	O(4)-C(4)-C(3)	112.1(3)
C(25)-H(25C)	0.9800	O(4)-C(4)-C(5)	105.8(4)
C(26)-H(26A)	0.9800	C(3)-C(4)-C(5)	112.0(3)
C(26)-H(26B)	0.9800	O(4)-C(4)-H(4A)	109.0
C(26)-H(26C)	0.9800	C(3)-C(4)-H(4A)	109.0
C(27)-C(28)	1.483(6)	C(5)-C(4)-H(4A)	109.0
C(28)-H(28A)	0.9800	N(1)-C(5)-C(4)	111.1(3)
C(28)-H(28B)	0.9800	N(1)-C(5)-C(6)	100.1(3)
C(28)-H(28C)	0.9800	C(4)-C(5)-C(6)	114.9(3)
O(8)-H(1O)	0.885(19)	N(1)-C(5)-H(5)	110.1
O(8)-H(2O)	0.90(2)	C(4)-C(5)-H(5)	110.1
		C(6)-C(5)-H(5)	110.1
C(1)-O(1)-C(10)	114.3(3)	O(5)-C(6)-C(5)	105.4(3)
C(2)-O(2)-H(2)	109.5	O(5)-C(6)-H(6A)	110.7
C(3)-O(3)-H(3)	109.5	C(5)-C(6)-H(6A)	110.7
C(4)-O(4)-H(4)	109.5	O(5)-C(6)-H(6B)	110.7
C(7)-O(5)-C(6)	110.8(3)	C(5)-C(6)-H(6B)	110.7
C(7)-N(1)-C(5)	113.9(3)	H(6A)-C(6)-H(6B)	108.8
C(7)-N(1)-C(1)	124.6(3)	O(6)-C(7)-O(5)	123.2(4)
C(5)-N(1)-C(1)	119.6(3)	O(6)-C(7)-N(1)	128.2(4)
O(1)-C(1)-N(1)	110.0(3)	O(5)-C(7)-N(1)	108.7(4)
O(1)-C(1)-C(2)	106.8(3)	C(9)-C(8)-C(17)	114.9(3)
N(1)-C(1)-C(2)	107.9(3)	C(9)-C(8)-H(8A)	108.5

C(17)-C(8)-H(8A)	108.5	C(16)-C(15)-H(15)	108.9
C(9)-C(8)-H(8B)	108.5	C(14)-C(15)-H(15)	108.9
C(17)-C(8)-H(8B)	108.5	C(15)-C(16)-C(18)	111.7(3)
H(8A)-C(8)-H(8B)	107.5	C(15)-C(16)-C(17)	112.8(3)
C(10)-C(9)-C(8)	109.9(3)	C(18)-C(16)-C(17)	112.9(3)
C(10)-C(9)-H(9A)	109.7	C(15)-C(16)-H(16)	106.3
C(8)-C(9)-H(9A)	109.7	C(18)-C(16)-H(16)	106.3
C(10)-C(9)-H(9B)	109.7	C(17)-C(16)-H(16)	106.3
C(8)-C(9)-H(9B)	109.7	C(12)-C(17)-C(26)	107.8(3)
H(9A)-C(9)-H(9B)	108.2	C(12)-C(17)-C(8)	109.3(3)
O(1)-C(10)-C(11)	107.8(3)	C(26)-C(17)-C(8)	110.0(3)
O(1)-C(10)-C(9)	109.8(3)	C(12)-C(17)-C(16)	110.3(3)
C(11)-C(10)-C(9)	110.4(3)	C(26)-C(17)-C(16)	111.8(3)
O(1)-C(10)-H(10)	109.6	C(8)-C(17)-C(16)	107.7(3)
C(11)-C(10)-H(10)	109.6	C(19)-C(18)-C(16)	114.5(3)
C(9)-C(10)-H(10)	109.6	C(19)-C(18)-H(18A)	108.6
C(10)-C(11)-C(12)	111.9(3)	C(16)-C(18)-H(18A)	108.6
C(10)-C(11)-H(11A)	109.2	C(19)-C(18)-H(18B)	108.6
C(12)-C(11)-H(11A)	109.2	C(16)-C(18)-H(18B)	108.6
C(10)-C(11)-H(11B)	109.2	H(18A)-C(18)-H(18B)	107.6
C(12)-C(11)-H(11B)	109.2	C(20)-C(19)-C(18)	111.1(3)
H(11A)-C(11)-H(11B)	107.9	C(20)-C(19)-H(19A)	109.4
C(13)-C(12)-C(11)	120.8(3)	C(18)-C(19)-H(19A)	109.4
C(13)-C(12)-C(17)	122.9(3)	C(20)-C(19)-H(19B)	109.4
C(11)-C(12)-C(17)	116.4(3)	C(18)-C(19)-H(19B)	109.4
C(12)-C(13)-C(14)	125.2(3)	H(19A)-C(19)-H(19B)	108.0
C(12)-C(13)-H(13)	117.4	C(19)-C(20)-C(25)	110.0(3)
C(14)-C(13)-H(13)	117.4	C(19)-C(20)-C(21)	107.6(3)
C(13)-C(14)-C(15)	113.4(3)	C(25)-C(20)-C(21)	113.1(3)
C(13)-C(14)-H(14A)	108.9	C(19)-C(20)-C(24)	116.0(3)
C(15)-C(14)-H(14A)	108.9	C(25)-C(20)-C(24)	109.9(3)
C(13)-C(14)-H(14B)	108.9	C(21)-C(20)-C(24)	100.0(3)
C(15)-C(14)-H(14B)	108.9	C(15)-C(21)-C(22)	119.8(3)
H(14A)-C(14)-H(14B)	107.7	C(15)-C(21)-C(20)	113.1(3)
C(21)-C(15)-C(16)	108.8(3)	C(22)-C(21)-C(20)	104.6(3)
C(21)-C(15)-C(14)	111.0(3)	C(15)-C(21)-H(21)	106.1
C(16)-C(15)-C(14)	110.4(3)	C(22)-C(21)-H(21)	106.1
C(21)-C(15)-H(15)	108.9	C(20)-C(21)-H(21)	106.1

C(21)-C(22)-C(23)	104.8(3)	C(21)-C(22)-H(22A)	110.8
C(23)-C(22)-H(22A)	110.8		
C(21)-C(22)-H(22B)	110.8		
C(23)-C(22)-H(22B)	110.8	H(25A)-C(25)-H(25C)	109.5
H(22A)-C(22)-H(22B)	108.9	H(25B)-C(25)-H(25C)	109.5
C(24)-C(23)-C(22)	106.9(3)	C(17)-C(26)-H(26A)	109.5
C(24)-C(23)-H(23A)	110.3	C(17)-C(26)-H(26B)	109.5
C(22)-C(23)-H(23A)	110.3	H(26A)-C(26)-H(26B)	109.5
C(24)-C(23)-H(23B)	110.3	C(17)-C(26)-H(26C)	109.5
C(22)-C(23)-H(23B)	110.3	H(26A)-C(26)-H(26C)	109.5
H(23A)-C(23)-H(23B)	108.6	H(26B)-C(26)-H(26C)	109.5
C(27)-C(24)-C(23)	114.9(3)	O(7)-C(27)-C(28)	121.8(3)
C(27)-C(24)-C(20)	112.7(3)	O(7)-C(27)-C(24)	121.0(4)
C(23)-C(24)-C(20)	103.3(3)	C(28)-C(27)-C(24)	117.3(4)
C(27)-C(24)-H(24)	108.6	C(27)-C(28)-H(28A)	109.5
C(23)-C(24)-H(24)	108.6	C(27)-C(28)-H(28B)	109.5
C(20)-C(24)-H(24)	108.6	H(28A)-C(28)-H(28B)	109.5
C(20)-C(25)-H(25A)	109.5	C(27)-C(28)-H(28C)	109.5
C(20)-C(25)-H(25B)	109.5	H(28A)-C(28)-H(28C)	109.5
H(25A)-C(25)-H(25B)	109.5	H(28B)-C(28)-H(28C)	109.5
C(20)-C(25)-H(25C)	109.5	H(1O)-O(8)-H(2O)	107(3)

Table 3A. Anisotropic displacement parameters ($Å^2 x\ 10^3$) for 23. The anisotropic displacement factor exponent takes the form: $-2\pi^2[h^2 a^{*2} U^{11} + ... + 2 h k a^* b^* U^{12}]$

	U^{11}	U^{22}	U^{33}	U^{23}	U^{13}	U^{12}
O(1)	25(1)	32(2)	22(1)	2(1)	5(1)	-5(1)
O(2)	24(1)	39(2)	48(2)	12(1)	6(1)	5(1)
O(3)	35(2)	42(2)	26(1)	6(1)	-4(1)	-12(1)
O(4)	44(2)	59(2)	45(2)	-26(2)	-2(1)	11(2)
O(5)	21(1)	53(2)	65(2)	-9(2)	11(1)	-5(2)
O(6)	34(2)	35(2)	63(2)	-8(2)	2(1)	-6(2)
O(7)	49(2)	43(2)	37(2)	6(2)	20(1)	-1(2)
N(1)	20(1)	30(2)	25(2)	-2(1)	4(1)	-2(1)
C(1)	21(2)	26(2)	27(2)	-2(2)	10(1)	-1(2)
C(2)	22(2)	29(2)	30(2)	7(2)	6(2)	-1(2)
C(3)	25(2)	30(2)	24(2)	3(2)	3(1)	-6(2)
C(4)	32(2)	40(3)	25(2)	-3(2)	9(2)	-1(2)
C(5)	25(2)	34(2)	27(2)	-3(2)	8(2)	3(2)
C(6)	26(2)	55(3)	45(2)	-9(2)	5(2)	5(2)
C(7)	22(2)	38(3)	33(2)	4(2)	-1(2)	-1(2)
C(8)	27(2)	18(2)	31(2)	0(2)	11(2)	1(2)
C(9)	31(2)	23(2)	28(2)	3(2)	7(2)	3(2)
C(10)	25(2)	32(2)	22(2)	0(2)	7(1)	-6(2)
C(11)	24(2)	28(2)	24(2)	-5(2)	8(1)	2(2)
C(12)	17(2)	21(2)	27(2)	-4(2)	6(1)	-5(2)
C(13)	18(2)	24(2)	26(2)	-6(2)	10(1)	-1(2)
C(14)	17(2)	23(2)	30(2)	0(2)	8(1)	3(2)
C(15)	15(2)	17(2)	26(2)	-2(2)	7(1)	1(2)
C(16)	19(2)	17(2)	26(2)	-3(2)	8(1)	-2(2)
C(17)	19(2)	19(2)	23(2)	-1(2)	5(1)	1(2)
C(18)	29(2)	25(2)	29(2)	-1(2)	9(2)	12(2)
C(19)	27(2)	19(2)	27(2)	-3(2)	12(2)	5(2)
C(20)	17(2)	18(2)	26(2)	-1(2)	6(1)	1(2)
C(21)	15(2)	18(2)	26(2)	-1(2)	6(1)	-2(2)
C(22)	17(2)	32(2)	31(2)	1(2)	8(1)	5(2)
C(23)	27(2)	49(3)	34(2)	4(2)	7(2)	16(2)
C(24)	21(2)	33(2)	23(2)	-2(2)	4(1)	0(2)

C(25)	22(2)	27(2)	34(2)	-3(2)	11(2)	-2(2)
C(26)	18(2)	23(2)	32(2)	-1(2)	6(1)	1(2)
C(27)	22(2)	41(3)	26(2)	4(2)	3(2)	6(2)
C(28)	59(3)	47(3)	34(2)	-1(2)	14(2)	16(3)
O(8)	52(2)	43(2)	43(2)	-9(2)	24(1)	-8(2)

Table 4A. Hydrogen coordinates (x 10^4) and isotropic displacement parameters (Å^{2}x 10^3) for 23.

	x	y	z	U(eq)
H(2)	5204	6048	5933	55
H(3)	5592	4320	4459	53
H(4)	7571	1654	4556	75
H(1)	7278	7778	6723	29
H(2A)	6952	7945	5467	32
H(3A)	6375	3257	5440	32
H(4A)	8299	5133	4919	38
H(5)	8526	2461	6193	34
H(6A)	10386	2983	6250	51
H(6B)	10148	4096	5469	51
H(8A)	5928	5706	8926	29
H(8B)	7223	6097	8851	29
H(9A)	5514	4551	7734	32
H(9B)	6102	6987	7768	32
H(10)	7865	5321	7663	31
H(11A)	7999	1424	7483	30
H(11B)	6685	1095	7524	30
H(13)	8992	-157	8465	26
H(14A)	9584	877	9731	28
H(14B)	9069	-1613	9628	28
H(15)	7408	-595	9977	23
H(16)	8002	4007	9768	24
H(18A)	6309	5194	10087	32
H(18B)	5912	2654	10183	32
H(19A)	7668	4955	11103	28
H(19B)	6490	4128	11312	28
H(21)	9011	2278	10808	23
H(22A)	9993	-895	11078	31
H(22B)	8879	-2443	11034	31
H(23A)	8880	-1853	12193	44
H(23B)	9944	-183	12225	44
H(24)	8864	2927	12051	30

H(25A)	6329	-505	10773	40
H(25B)	6163	190	11563	40
H(25C)	7061	-1715	11444	40
H(26A)	5927	-235	9059	36
H(26B)	5450	1148	8354	36
H(26C)	5191	1995	9111	36
H(28A)	6904	3418	13258	69
H(28B)	7049	4614	12524	69
H(28C)	8104	4428	13151	69
H(1O)	3520(40)	4420(80)	6418(15)	53
H(2O)	3840(40)	2920(40)	5900(20)	53

Table 5A. Torsion angles [°] for jm00116a.

C(10)-O(1)-C(1)-N(1)	78.1(3)
C(10)-O(1)-C(1)-C(2)	-165.0(3)
C(7)-N(1)-C(1)-O(1)	-136.0(4)
C(5)-N(1)-C(1)-O(1)	60.7(4)
C(7)-N(1)-C(1)-C(2)	107.8(4)
C(5)-N(1)-C(1)-C(2)	-55.5(4)
O(1)-C(1)-C(2)-O(2)	60.7(4)
N(1)-C(1)-C(2)-O(2)	179.0(3)
O(1)-C(1)-C(2)-C(3)	-64.5(3)
N(1)-C(1)-C(2)-C(3)	53.8(4)
O(2)-C(2)-C(3)-O(3)	62.5(4)
C(1)-C(2)-C(3)-O(3)	-173.3(3)
O(2)-C(2)-C(3)-C(4)	-178.4(3)
C(1)-C(2)-C(3)-C(4)	-54.2(4)
O(3)-C(3)-C(4)-O(4)	-70.9(4)
C(2)-C(3)-C(4)-O(4)	168.3(3)
O(3)-C(3)-C(4)-C(5)	170.4(4)
C(2)-C(3)-C(4)-C(5)	49.6(5)
C(7)-N(1)-C(5)-C(4)	-113.0(4)
C(1)-N(1)-C(5)-C(4)	52.0(4)
C(7)-N(1)-C(5)-C(6)	8.8(4)
C(1)-N(1)-C(5)-C(6)	173.8(3)
O(4)-C(4)-C(5)-N(1)	-168.0(3)
C(3)-C(4)-C(5)-N(1)	-45.6(5)
O(4)-C(4)-C(5)-C(6)	79.3(5)
C(3)-C(4)-C(5)-C(6)	-158.4(4)
C(7)-O(5)-C(6)-C(5)	8.4(5)
N(1)-C(5)-C(6)-O(5)	-9.8(4)
C(4)-C(5)-C(6)-O(5)	109.3(4)
C(6)-O(5)-C(7)-O(6)	176.4(4)
C(6)-O(5)-C(7)-N(1)	-3.1(5)
C(5)-N(1)-C(7)-O(6)	176.4(4)
C(1)-N(1)-C(7)-O(6)	12.2(6)
C(5)-N(1)-C(7)-O(5)	-4.2(5)
C(1)-N(1)-C(7)-O(5)	-168.4(3)
C(17)-C(8)-C(9)-C(10)	-56.3(4)

C(1)-O(1)-C(10)-C(11)	-138.1(3)
C(1)-O(1)-C(10)-C(9)	101.7(3)
C(8)-C(9)-C(10)-O(1)	177.4(3)
C(8)-C(9)-C(10)-C(11)	58.7(4)
O(1)-C(10)-C(11)-C(12)	-176.0(3)
C(9)-C(10)-C(11)-C(12)	-56.1(4)
C(10)-C(11)-C(12)-C(13)	-130.0(4)
C(10)-C(11)-C(12)-C(17)	50.7(4)
C(11)-C(12)-C(13)-C(14)	-179.8(4)
C(17)-C(12)-C(13)-C(14)	-0.6(6)
C(12)-C(13)-C(14)-C(15)	11.9(5)
C(13)-C(14)-C(15)-C(21)	-160.2(3)
C(13)-C(14)-C(15)-C(16)	-39.5(4)
C(21)-C(15)-C(16)-C(18)	-51.4(4)
C(14)-C(15)-C(16)-C(18)	-173.4(3)
C(21)-C(15)-C(16)-C(17)	-179.8(3)
C(14)-C(15)-C(16)-C(17)	58.2(4)
C(13)-C(12)-C(17)-C(26)	-104.8(4)
C(11)-C(12)-C(17)-C(26)	74.4(4)
C(13)-C(12)-C(17)-C(8)	135.8(4)
C(11)-C(12)-C(17)-C(8)	-45.0(4)
C(13)-C(12)-C(17)-C(16)	17.5(5)
C(11)-C(12)-C(17)-C(16)	-163.2(3)
C(9)-C(8)-C(17)-C(12)	48.0(4)
C(9)-C(8)-C(17)-C(26)	-70.1(4)
C(9)-C(8)-C(17)-C(16)	167.9(3)
C(15)-C(16)-C(17)-C(12)	-46.1(4)
C(18)-C(16)-C(17)-C(12)	-173.9(3)
C(15)-C(16)-C(17)-C(26)	73.8(4)
C(18)-C(16)-C(17)-C(26)	-54.0(4)
C(15)-C(16)-C(17)-C(8)	-165.3(3)
C(18)-C(16)-C(17)-C(8)	66.9(4)
C(15)-C(16)-C(18)-C(19)	49.9(4)
C(17)-C(16)-C(18)-C(19)	178.2(3)
C(16)-C(18)-C(19)-C(20)	-52.7(4)
C(18)-C(19)-C(20)-C(25)	-67.4(4)
C(18)-C(19)-C(20)-C(21)	56.2(4)
C(18)-C(19)-C(20)-C(24)	167.1(3)

C(16)-C(15)-C(21)-C(22)	-175.9(3)
C(14)-C(15)-C(21)-C(22)	-54.3(4)
C(16)-C(15)-C(21)-C(20)	59.9(4)
C(14)-C(15)-C(21)-C(20)	-178.4(3)
C(19)-C(20)-C(21)-C(15)	-62.4(4)
C(25)-C(20)-C(21)-C(15)	59.3(4)
C(24)-C(20)-C(21)-C(15)	176.2(3)
C(19)-C(20)-C(21)-C(22)	165.5(3)
C(25)-C(20)-C(21)-C(22)	-72.8(4)
C(24)-C(20)-C(21)-C(22)	44.1(4)
C(15)-C(21)-C(22)-C(23)	-158.0(3)
C(20)-C(21)-C(22)-C(23)	-29.9(4)
C(21)-C(22)-C(23)-C(24)	3.3(4)
C(22)-C(23)-C(24)-C(27)	147.0(3)
C(22)-C(23)-C(24)-C(20)	23.9(4)
C(19)-C(20)-C(24)-C(27)	79.0(4)
C(25)-C(20)-C(24)-C(27)	-46.6(5)
C(21)-C(20)-C(24)-C(27)	-165.7(4)
C(19)-C(20)-C(24)-C(23)	-156.4(3)
C(25)-C(20)-C(24)-C(23)	78.0(3)
C(21)-C(20)-C(24)-C(23)	-41.1(4)
C(23)-C(24)-C(27)-O(7)	-30.3(5)
C(20)-C(24)-C(27)-O(7)	87.7(5)
C(23)-C(24)-C(27)-C(28)	151.1(4)
C(20)-C(24)-C(27)-C(28)	-90.9(5)

Table 6A. Hydrogen bonds for 23 [Å and °].

D-H...A	d(D-H)	d(H...A)	d(D...A)	<(DHA)
O(8)-H(2O)...O(3)#1	0.90(2)	1.92(2)	2.809(5)	169(5)
O(8)-H(1O)...O(7)#2	0.885(19)	1.93(2)	2.798(4)	165(4)
O(4)-H(4)...O(8)#1	0.84	2.26	2.998(5)	146.7
O(3)-H(3)...O(2)#1	0.84	1.83	2.645(4)	161.7
O(2)-H(2)...O(8)	0.84	1.98	2.718(4)	145.7

Symmetry transformations used to generate equivalent atoms:

#1 -x+1,y-1/2,-z+1 #2 -x+1,y+1/2,-z+2